THE UNIVERSITY OF WARWICK

Model Based Analysis of Power Plant Integrated with a Post Combustion Carbon Capture Process

Thesis submitted in accordance with the requirements of the University of Warwick for the degree of Doctor of Philosophy

in

Engineering School

By

Shen Guo

B.Eng., M.Phil.

July 2015

to my parents

Acknowledgements

First and foremost, I would like to express my sincere appreciation to my supervisor, Professor Jihong Wang, for her support, guidance and patience during my PhD study. Her scientific belief and her persistent efforts constitute the essential part of the project, and her passion and knowledge in science exceptionally inspire and enrich my growth as a student, a researcher and an engineer want to be.

I would also be very grateful to Prof. Qirui Gao, Dr. Yali Xue and Dr. Jianlin Wei for sharing their invaluable knowledge in the thermodynamics, control and programing. Their important advices and critical comments gave me great experiences throughout the work. Many thanks to Prof. Junfu Lv and Dr. Nan Jia for the valuable experiences from both academia and industry.

It has been a great pleasure to work with and I also want to give my thanks to my colleagues Dr. Xing Luo, Dr. Hao Sun, Mr. Yue Wang, Dr. Jacek Wojcik and Dr. Mihai Draganescu in the research group. Many shining ideas in the project has come from the cooperation and discussions with them.

Finally and mostly, I would like to give my special appreciates to my family and my friends. None of this would have been possible without their encouragement, support and understanding.

Abstract

It is well recognised that there are two main options for reducing CO_2 emissions from fossil-fuelled power generation, namely, improvement of energy efficiency and Carbon Capture and Storage (CCS). Efficient power generation leads to lower fuel consumption, in turn, lower CO_2 emission. Post combustion carbon capture as it can be introduced to existing power plants by retrofitting to the plant, which has attracted a lot of academic and industrial attention. A lot of research activities have been carried out to study this capture technology but most of this research focused on the steady state and the balance of the chemical reaction. As the initial investigation on the power plant response with carbon capture is a very important process before the plant is built, the dynamic simulation study can be helpful to provide the necessary guidance for the design of the plant and control system. This thesis reports the modelling and impact analysis of the supercritical power plant with integration of post combustion carbon capture. The work described in this thesis contributes to three aspects: model based dynamic study of capture plant, model based flue gas estimation and the analysis of power plant response caused by the carbon capture.

A dynamic modular model of the capture plant has been built based on the mass and thermal balance for the study of plant dynamics. In this model, the methodology based on the average enthalpy has been introduced to solve the relationship between the specific enthalpy and the temperature of amine-water

mixture under different conditions. A model based real-time estimation algorithm for the steam required to satisfy the heat duty is also developed in the work presented in this thesis.

An accurate flow rate of the flue gas can greatly support the study of the absorption process simulation. An improved coal mill model which provides the estimation of mill status in the normal milling progress is developed in this project. The information provided by this coal mill model can further estimate the flow rate of the flue gas. In addition to supporting the study of carbon capture process, OPC based on-line implementation algorithms are proposed to enhance the mill operation.

The heat duty to maintain the reaction temperature in the regeneration process is satisfied by the steam from the power plant in this thesis. Several modification plans have been tested in the simulator to study the different dynamic responses to the power plant caused by the steam extraction, and an approach that is able to meet the heat demand with least impact to the plant dynamics is proposed. As coal fired power plants are obliged to balance their output in response to the changing power demand from the grid, this thesis also provides a control strategy to overcome this power penalty by adding the equivalent power to the power demand.

CONTENTS

LIST OF FIGURES

LIST OF TABLES

Chapter 1.

INTRODUCTION

1.1 BACKGROUND

One of the most important environment challenges faced nowadays is Global Warming. In December 2010, the UN Framework Convention on Climate Change (UNFCCC) committed to control the temperature rise no more than 2 ℃ compared with the pre-industrial level and will work to achieve lower temperature rise , less than 1.5 ℃ in the near future to prevent the most severe impacts of climate change (Symon, 2013). It has been widely accepted that the greenhouse effect is one of the main causes for climate chang. Actually, the greenhouse gases (GHG), in which Carbon Dioxide (CO_2) is the main constituent, are considered to have made the major contribution to the temperature rise. From the reported studies, it is known that the global

temperature increase per decade from 1957 to 2007 was almost twice of that from 1907 to 1957 (IPCC, 2007), while the CO_2 concentration in the atmosphere has increased by 19% between 1975 and 2012 (NOOA, 2013). Therefore, the emission reduction is capable to play a very important role in control of climate change.

The Department of Energy & Climate Change (DECC, UK) announced the goal of "Reducing the UK's greenhouse gas emissions by 80% by 2050" in 2008, which has been clearly stated in the governments legislation document (Anon, 2008). In January 2014, the European Commission published their target to reduce 80-95% of the GHG emissions based on the data in 1990 by 2050 to reach the EU's long term climate objective (European Commission, 2014). The United States has different policies in different states but the White House also showed their ambitions in 2009 to reduce the GHG emission by more than 17% to 20% of the 2005 level before 2020 and more than 83% GHG emissions reduction by 2050 (Anon, 2010).

Data from Carbon Dioxide Information Analysis Center (CDIAC) shows that there were 29.888 million metric tons of CO_2 generated in the year 2009 (CDIAC, n.d.), in which more than 40% of world CO_2 emission was from electricity and heat generation, 22% was from transportation, 21% was other industrial activities (Figure 1.1).

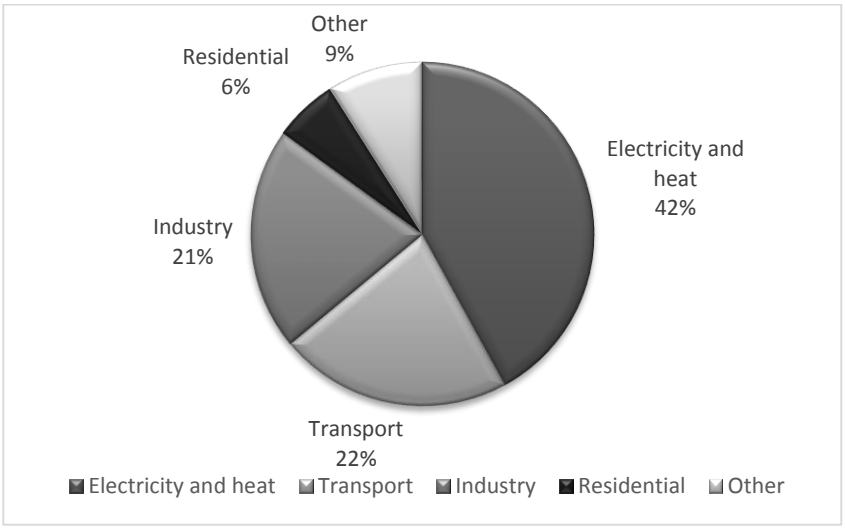

Figure 1-1: World CO_2 emissions by sector 2011 (IEA, 2013a)

Targeting of transportation for world CO_2 emission reduction is not enough as it is technically not realistic to remove the CO_2 from the exhaust of vehicles. As a result, the potential to reduce the emission from power generation is becoming increasingly important in achieving the CO_2 reduction target.

It is reported that the world electricity generation has been increased by over 80% in the past decade as shown in Table 1.1 and Figure 1.2 (IEA, 2013b, OECD, 2013). The world net electricity demand is predicted to reach 39000 TWh by the year 2040 from 21431.5 TWh in 2010 (EIA, 2013), which indicates an increase of over 80% in the next 30 years. Table 1-1 shows that although many new technologies have been developed and applied in power generation, the share of the world electricity generated from fossil fuel has never dropped below 62% (total) and 36% (coal) of the world electricity generation, and reached to 67% (coal 40%) in Year 2010 (OECD, 2013).

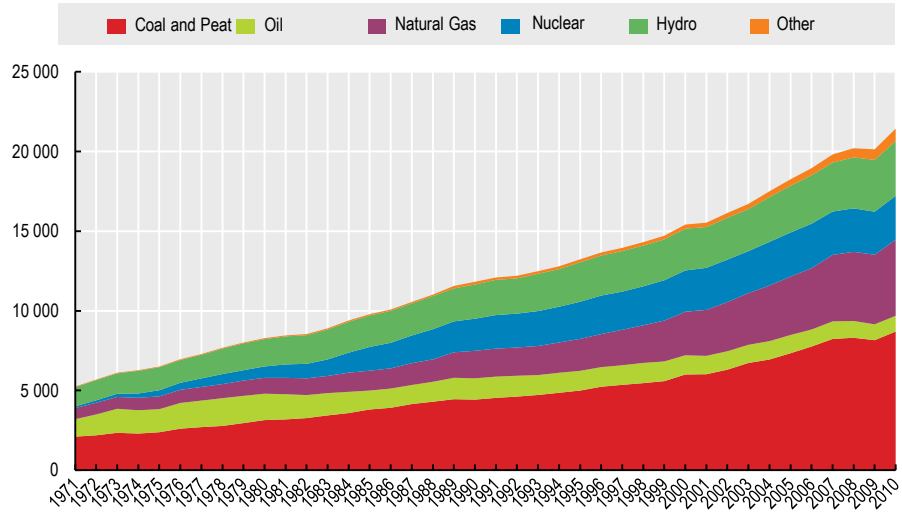

Figure 1-2: World electricity generation by source of energy (OECD, 2013)

Table 1-1: World electricity generation by source of energy in Terawatt hours (TWh) (OECD, 2013)

	1980	1990	1995	2000	2005	2008	2010
Coal and Peat	3,140.74	4,425.97	4,995.10	6,001.41	7,335.40	8,307.89	8,697.51
Oil	1,655.62	1,336.42	1,237.12	1,206.72	1,144.70	1,053.72	989.26
Natural Gas	996.78	1,727.12	2,002.40	2,732.42	3,665.11	4,336.50	4,768.08
Nuclear	713.38	2,012.90	2,331.95	2,590.62	2,767.95	2,731.02	2,756.29
Hydro	1,716.86	2,143.53	2,480.24	2,622.58	2,930.64	3,199.21	3,437.48
Other	58.58	173.05	182.87	256.74	406.56	573.04	782.85
Total	8281.95	11819	13229.7	15410.5	18250.4	20201.4	21431.5

Other generation technologies, such as nuclear, bio-mass and especially renewables, can be helpful to reduce the CO_2 emission. However replacing all the conventional power generation with renewables is not a short term project. Nuclear is a well-developed clean power generation technology but the safety concerns has led to re-assessment of its deployment after the catastrophic failure at the Fukushima Nuclear Power Plant (Glaser, 2011, Srinivasan and Gopi Rethinaraj, 2013). There have already been some attempts of bio-mass/coal co-

firing power generation but this technology is not convincing due to its complications brought to power plants. Renewable energy is also unable to replace all the coal-fired power generation unless they can have some milestone progress (Wang, 2011). As coal has a relatively abundant reserve on the earth (BP, 2014), it is currently occupying the biggest share of the electricity generation market and this domination will continue for a long time. Without removing coal fired power generation from the market, reducing or removing the CO_2 emission from coal-fired power plants becomes a more realistic way forward. There are two main approaches referred to reducing CO_2 emissions associated with coal-fired power generation: to improve the generation efficiency and to capture and deposit the CO_2 to a safe place to prevent the emission to the atmosphere.

Improving the efficiency of coal-fired power plants provides the possibility to achieve the same power output by consuming less coal, in turn, resulting in less emissions. A very established technology which is already implemented in many countries is the supercritical power plant, which is able to increase the thermal efficiency from 30%-38% of the normal subcritical power plant to 46% (Vocke, 2007).

Capturing the flue gas and transporting it into a sealed space can reduce CO_2 emission dramatically. But CO_2 only has a smaller proportion of the flue gas in normal coal fired power stations and the majority is nitrogen from the primary and secondary air. It makes no sense to waste the limited space to store the nitrogen which is totally harmless to the environment. The Carbon dioxide

Capture is to separate the waste CO_2 from the flue gas generated in a coal-fired power station so it can be stored into a hermetical area instead of being emitted into the atmosphere. The complete process, including CO_2 capture, compression, transportation, storage, is summarized as Carbon Capture and Storage (CCS). Although CCS is able to reduce the emission significantly and can achieve zero emissions for coal-fired power generations, the implementation of the CO_2 capture costs 10% - 40% of the energy generated no matter what kind of carbon capture technology is employed in a power station (Beér, 2007). This energy penalty usually includes the capture and compression of CO_2, but excludes the cost in the transportation and storage stage. So there is a debate between the benefit and the energy penalty and no convincing conclusion is agreed (Rochon, 2008). The project is set to conduct the system modelling and simulation study to investigate the feasible capture process and the impact on the power plant dynamics brought onto by CCS. With consideration of the current advanced and future technology, the more efficient supercritical power plant is chosen in the study.

1.2 Overview of Carbon Capture Technologies

Data from IEA shows that four large-scale CCS projects have been completed and have captured and stored 55Mt CO_2 in total; nine more large-scale CCS projects are expected to be finished by 2016, with an additional annual CO_2 capture capacity of 14Mt and fifteen more are in the planning stage (IEA, 2014).

Carbon capture can be classified into three different technologies: Pre combustion capture, oxy-fuel combustion and post combustion capture.

1.2.1 PRE COMBUSTION CAPTURE

Pre combustion capture refers to a technology that captures the CO_2 before combustion. This technology is not available to pulverized coal (PC) power plants that comprise most of the existing capacity. This technology is ideally designed for the integrated coal gasification combined cycle (IGCC) plants. In the IGCC plants, coal is first mixed with water and blends into coal slurry. The coal slurry is then pumped to the top of the gasifier vessel to react with liquid oxygen which comes from the air separation unit in an incomplete combustion reaction at 1300°C and 60 bar (g) pressure. The product mixture is quenched at the bottom section of the gasifier where slag is removed and cooled saturated syngas leaves. The syngas, which is mainly a mixture of carbon monoxide and hydrogen, is then piped to the water-gas shift (WGS) where the CO further reacts with steam to form CO_2 and more H_2 (Higman and Van der Burgt, 2008, Herzog *et al*., 2009, Karmarkar, 2006). The CO_2 then can be removed while the H_2 can be used in gas turbines for power generation or can be used by fuel cells. The Pre combustion capture will be a very attractive choice in future because it is potentially cheaper than post combustion capture, and IGCC power plants with pre combustion carbon capture also have higher efficiency than PC power plants. However, the cost of building IGCC plants remains high and it has been reported that the estimated generation cost per megawatt had been increased by 65% from the year 2007 to 2011(IEA, 2012, Russell, 2011). The direct consequence is that

only very few IGCC plants are currently under construction or to be built in a plan (IEA, 2012). Additionally the blades in the gas turbine need a very precise manufacturing process that limits the development of the IGCC plant.

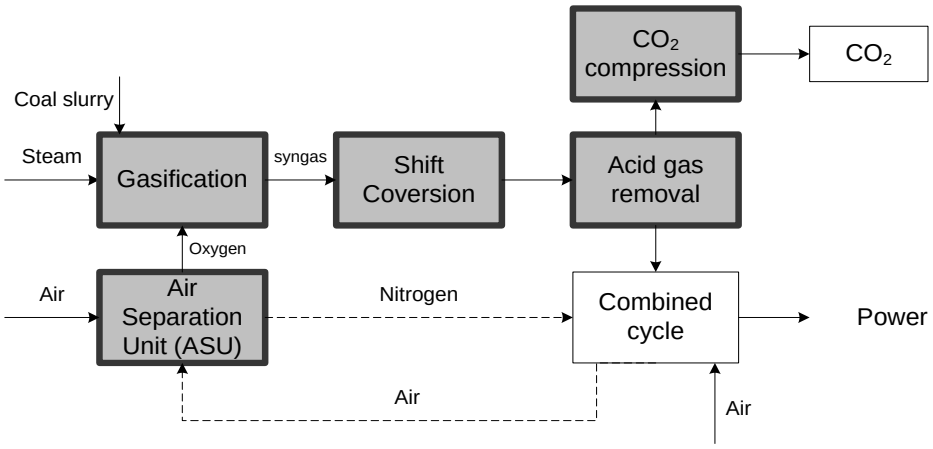

Figure 1-3: Pre-combustion Capture

1.2.2 CARBON CAPTURES ON CONVENTIONAL POWER GENERATION

In a conventional coal-fired power plant, the coal is fed into the furnace by the primary air where the combustion takes place. The flue gas, which is usually refers to the exhaust gas from the combustion, normally consist of mostly nitrogen (typically more than two thirds) derived from the combustion air, carbon dioxide (CO_2), water vapour and excess oxygen (also derived from the combustion air) as well as some other gases like NO_x and SO_x. Both the oxy-fuel combustion and the post combustion capture can be implemented to the existing power plants.

Coal-fired power stations convert the chemical energy stored in coal to electricity. The main reaction of this process is the combustion of coal with

oxygen from the air, which produces the majority of the greenhouse gas. The idea of oxy-fuel combustion capture is to use a high purity oxygen stream (≥95%) instead of air. As the nitrogen has been removed prior to the combustion, the CO_2 capture can be greatly simplified because the exhaust flue gas stream is free of nitrogen components. The problem of the oxy-fuel combustion capture is that the air separation plant which is necessary to produce high purity oxygen stream would consume 23% - 37% of the total plant output (Yang *et al*., 2008, Herzog *et al*., 2009). Without the high efficiency of the IGCC plant, the oxy-fuel combustion is less competitive compared with the other two technologies.

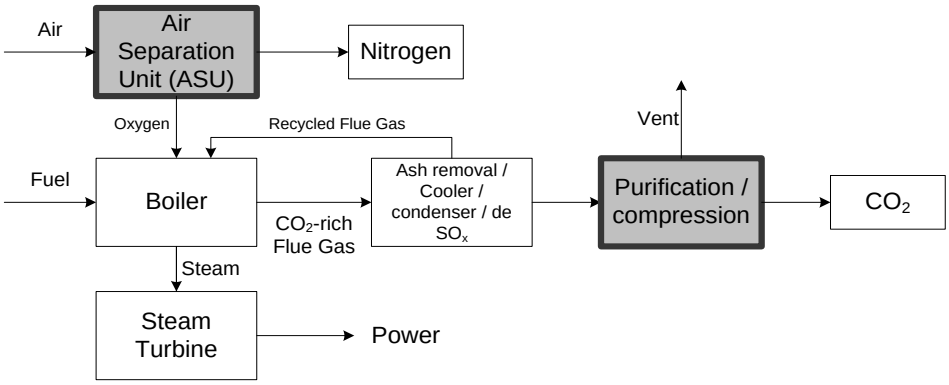

Figure 1-4: Oxy-fuel combustion

Post combustion capture represents the capture process of the carbon dioxide from the flue gas of coal-fired power plants after combustion takes place. The flue gas, which is originally leaving the power plant through the chimney, is now introduced to the capture plant where most of the CO_2 is separated from the flue gas. This capture technology is the simplest and the oldest capture method of the three. But there are three unique advantages that the pre combustion capture and oxy-fuel combustion cannot achieve: The post combustion capture can be

retrofitted to the existing PC power plants without substantial change in the combustion technology. It also provides the flexibility to stop the capture process without stopping the electricity generation. Finally it is the only candidate for the gas-fired power plants, which shares a very high percentage in some countries (Yang *et al*., 2008, Herzog *et al*., 2009). Due to these reasons, post combustion is still very competitive that attracts much industrial and academic attention.

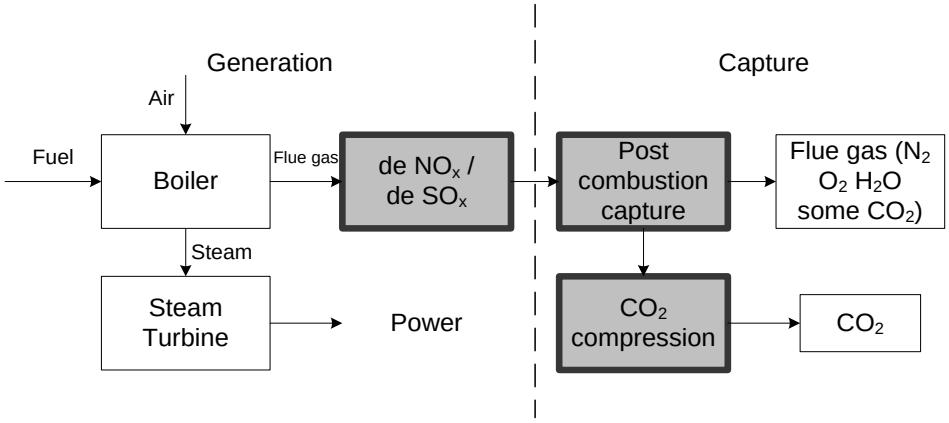

Figure 1-5: Post-combustion Capture

1.3 CO_2 STORAGE AND UTILIZATION

The CO_2 capture activity itself gives no contribution to the greenhouse emission reduction, and to the contrary, capturing without storage increases the fuel cost which means more CO_2 is generated. Therefore the carbon dioxide must be sequestered after it is captured from the power station. Various options have been considered for CO_2 permanent storage, including ocean carbon storage, mineral carbon storage and geological carbon storage.

Ocean carbon storage refers to the direct injection of CO_2 into the deep sea. As the carbon dioxide is soluble in water, the ocean is big enough to dissolve a large amount of CO_2. However it has been pointed out that ocean storage causes ocean acidification which is harmful to the marine organisms near the injection point, therefore it is not considered as a storage solution any longer (Green Facts, 2012).

The reaction of the CO_2 and magnesium or calcium minerals that occurs naturally to form stable carbonates over time. Those magnesium and calcium minerals are very abundant and the reaction products are relatively stable therefore the CO_2 can be stored. But this natural progress is very long and the storage speed is far away from the CCS needs. Mineral carbon storage is a similar solution to this naturally occurring reaction but by increasing the pressure and temperature, the process can be much faster (IPCC, 2005).

Geological carbon storage is currently the most encouraging method of carbon storage. This storage refers to the injection of CO_2 directly into underground geological formations. This option is attractive because this method is not only a storage technology. The integration of geologic CO_2 storage and enhanced oil recovery (EOR) using CO_2 flooding (CO_2-EOR) has been proved to be a very good example of the CO_2 utilization (Jiao *et al*., 2013). In fact, the first idea of carbon capture is not about the concern of climate change, rather, it gained attentions as a possible inexpensive source of CO_2. In the early stage of the petroleum industry, called 'primary' production phase, the production of oil is naturally caused by the reservoir's internal energy. However this primary production is only a very small part of the oil reservoir. After a certain depletion,

the internal energy fails to maintain the natural production and 80% to 90% more oil is still "trapped" in the pore spaces of the rock therefore artificial drive is necessary to continue the oil production (Melzer, 2012, Latin, 1980). Enhanced oil recovery (EOR), especially CO_2 flooding recovery (CO_2-EOR) is already an established technology as the artificial drive now. CO_2 is injected into oil reservoirs to increase the mobility of the oil and, thereby the productivity of the reservoir (Herzog *et al*., 2009)

The Enhanced Gas Recovery (EGR), which is similarly to the EOR, has also been demonstrated and reported as realistic recently to inject the CO_2 into gas reservoirs (Vandeweijer *et al*., 2011).

1.4 OBJECTIVES OF THE PROJECT

The project is to study post combustion carbon capture integration with supercritical power generation process. A number of post combustion capture technologies have been studied, reviewed and compared. Amine based capture, which refers to monoethanolamine in this thesis, is known as the most established technology with a long development history in all post combustion capture options. So the project will focus on the amine based capture technology and its integration with power plant. Then the impact on power plant dynamics will be investigated while the capture process is operating.

A simulator of the 600 MW supercritical power plant is available which is developed through a parallel project within Power and Control Systems

Research Laboratory, which provides a simulation platform for study of the whole system dynamics. In this project, retrofit of the post combustion capture to the supercritical power plant is implemented onto the simulator and the integrated power plant dynamics is analysed.

As the carbon dioxide is generated from the combustion of fuel with sufficient oxygen in the furnace, the coal property including the flow rate is the key factor that affects the flue gas and CO_2 flow rate, which is important to the carbon capture process. The first phase of the research work is to develop a detailed coal mill model that can deliver a more reasonable feed coal calculation than the transfer function implemented in the simulator. More accurate feed coal flow rate leads to more accurate flue gas estimation.

Then the project moves to develop a mathematical model that can represent the dynamic behaviour of the whole carbon capture process. With this model the required heat from the power plant can be estimated.

Once the mathematical model for the capture process is established, necessary changes to the simulators are implemented therefore the simulator can be connected with the capture process. Further analysis based on the simulation of the supercritical power plant with post combustion carbon capture is then carried out.

1.5 THESIS OUTLINE

The thesis is organized as seven chapters and the main contribution of the rest chapters are:

Chapter 2 reviews the thermal power generation and the post combustion capture technologies. The whole water-steam loop from the feed water to the condensed water is introduced and the efficiency analysis of thermal plants based on the temperature-entropy diagram is carried out to explain the reason that the supercritical power plants a have higher generation efficiency than conventional subcritical power plants. This chapter also introduces the existing post combustion carbon capture approaches available and chemical absorption using amine is studied in detail as it is the most established technology.

Chapter 3 gives an introduction of different simulation approaches to represent the power plant used in this project. The first principle model and the simulator based on the thermodynamics and the fluid network calculation are studied. Discussion of the advantages and drawbacks of both approaches are carried out. The simulator, which considers more inputs including the control system, is chosen as it provides more information and flexibility.

Chapter 4 provides a dynamic mathematical model of the coal mill which is very important to the fuel preparation process. Based on the working principle and enhanced by the empirical equation, the coal mill model can give a more accurate estimation of the coal flow. This model can be implemented on-line in

the power station for self-adaptive parameter update and to provide extra information to the site engineers.

Chapter 5 introduced the model development of the amine based post combustion capture plant. Different components, including the absorber, heat exchanger, regenerator and reboiler, are modelled and connected together. The validation works based on published data of a pilot scale capture plant and based on the scaled-up simulations from other literatures has been carried out showing that the model is able to represent the capture process.

Chapter 6 developed a simplified start-up procedure for an idle capture plant by which the steam demand to satisfy the heat duty can be estimated. Modification of the power plant simulators will be introduced in this Chapter and steam from the exit of intermediate pressure turbine is used to satisfy this steam demand. The dynamic response of power plant caused by this steam extraction has been analysed and pressure stabilization and penalty recovery strategy are proposed to make sure the output of the power plant is able meet the power demand.

Finally in **Chapter 7** the contributions and findings of the whole thesis are concluded and the possible research directions are recommended at the end of thesis.

1.6 PUBLICATIONS DURING THIS PERIOD

Guo, S., *et al*. (2014). "A new model-based approach for power plant Tube-ball mill condition monitoring and fault detection." *Energy Conversion and Management* **80**(0): 10-19.

Chapter 2.

COAL-FIRED POWER GENERATION AND POST COMBUSTION CAPTURE

This chapter covers the review of thermal power plant process and the main post combustion capture technologies. In the first part of this chapter, the supercritical coal-fired power generation process is described as the research conducted technology which has a higher energy conversion efficiency compared with the conventional subcritical power plants. Then the technologies for post combustion carbon dioxide capture are reviewed and the amine based capture technology is described in detail as it has been identified as the most feasible technology for post combustion carbon dioxide capture.

2.1 THERMAL POWER PLANT PROCESS

Thermal power plants generate electricity from high temperature high pressure steam. Classified by the prime power source of the generation there are different types of thermal power plants, including fossil fuel, nuclear, geothermal, solar power generations. Fossil fuel power generations, especially coal-fired, has the biggest share in the electricity generation market now.

2.1.1 THE GENERATION PROCESS OF COAL-FIRED POWER PLANT

In a coal-fired power plant, coal is first transported to the plant site and stored in bunkers in the plant. It is delivered to the coal mill by the feeder when needed where it is crushed into powder by hundreds of steel balls in a spinning drum (for tube-ball mills). The pulverized coal is brought out by the primary air and is conveyed to the boiler.

As the coal enters the boiler with the primary air, it ignites with the secondary air, releasing energy and generating intense heat to change the high quantity feed water into steam in the waterwall. Ash as one of the by-products in the combustion process drops to the bottom of the furnace and is taken away by an ash hopper while the flue gas, which can be at a temperature of over 1000 ◦C rises up, passing the superheater, and reheater where the thermal energy generated in the ignition process vaporizes the feed water into main steam. The energy in the main steam is then transformed to mechanical energy via the turbine which drives a generator to produce electricity. The economizer is the

last heat exchanger that is located at the end of the furnace, which is used to preheat the feed water. (Rayaprolu, 2009).

The feed water comes from the deaerator that is used to remove the dissolved air in the feed water to reduce the corrosiveness. The purified water is then pumped to a high pressure and enters the boiler after a series of preheating heat exchangers (Ben-Abdennour *et al*., 1993). The water firstly flows through the economizer where it is further heated by the flue gas. Traditionally, the high pressure water flows to a drum and then flows down to the furnace waterwall, where the water is heated by the flame and part of the water vaporized to steam. The steam water mixture is sent to the steam drum again where the steam is separated from the unvaporized water and flows to the superheater for further heating. The water is mixed with the feed water and flows back to the furnace waterwall again for vaporization (Abdennour, 2000).

As the water is removed from the drum, the steam that enters the superheater is either saturated or superheated steam. The temperature and pressure of the steam are further elevated by the three-stage superheater at the top of the furnace (Cold Superheater, Platen Superheater and Hot Superheater) to a higher temperature and then piped to the first stage of the turbine system which transforms the thermal energy into mechanical torque.

The turbine system consists of four steam turbines that share the same shaft, high pressure turbine (HP), intermediate pressure turbine (IP) and two low pressure turbines (LP). A generator is connected to the turbine system on the same shaft

to generate electricity by the mechanical power provided by the turbine. The main steam from the superheater enters the high pressure steam turbine, releasing its pressure and thermal energy to the turbine and returns to the boiler as soon as it leaves the HP turbine. After being heated again in the two stage reheater (Cold Reheater and Hot Reheater) by the flue gas, the reheated steam is then introduced to the intermediate and low pressure turbines to generate mechanical power. Usually the exhausts of the low pressure turbines are pumped to negative relative pressure as the low pressure enables the steam temperature to drop to under 100˚C without condensing, which is the saturated temperature at 1 atm, therefore that more thermal energy can be obtained.

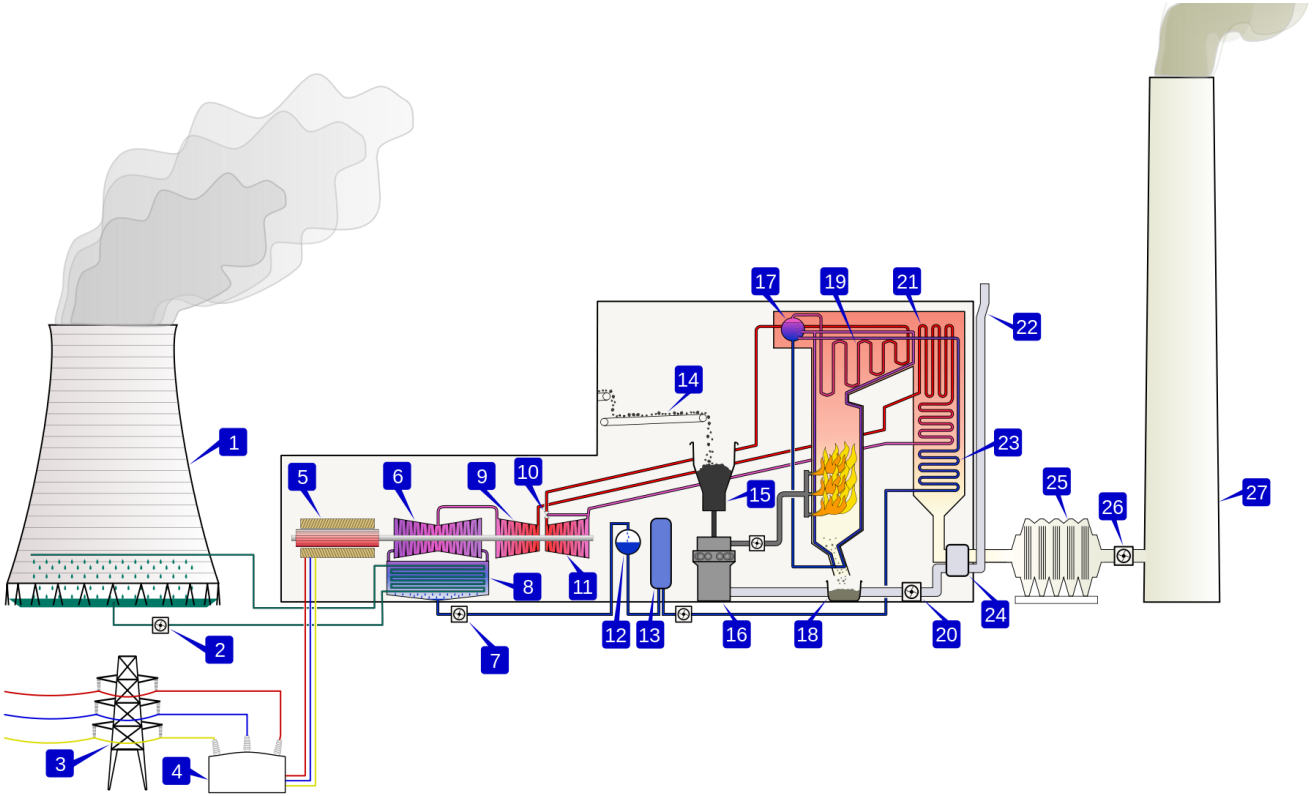

Figure 2-1: A coal-fired thermal power station (BillC, 2006)

1. Cooling tower. 2. Cooling water pump. 3. Transmission line (3-phase). 4. Unit transformer (3-phase). 5. Electric generator (3-phase). 6. Low pressure turbine. 7. Condensate extraction pump. 8. Condensor. 9. Intermediate pressure turbine. 10. Steam governor valve. 11. High pressure turbine. 12. Deaerator. 13. Feed heater. 14. Coal conveyor. 15. Coal hopper. 16. Pulverised fuel mill. 17. Boiler drum. 18. Ash hopper. 19. Superheater. 20. Forced draught fan. 21. Reheater. 22. Air intake. 23. Economiser. 24. Air preheater. 25. Precipitator. 26. Induced draught fan. 27. Chimney Stack.

The steam that leaves from the LP turbine is condensed into water in the condenser and is sent back to the deaerator after a series of heat exchangers to increase the water temperature, which is ready to be pumped for the next steam water cycle. Figure 2.1 gives a brief view of the coal-fired power generation.

2.1.2 THE RANKINE CYCLE

The Rankine cycle, which is a model that is used to predict the performance of steam-operated heat engines, represents the ideal thermodynamic cycle of the process in which heat is converted to mechanical energy. Figure 2.2 shows a typical Rankine cycle that includes a pump, a boiler and a turbine connected with a load and a condenser.

In a complete Rankine cycle, water is pumped into high pressure (1-2), and enters a boiler where it is heated to the saturation temperature and evaporated into vapour (2-3). The steam then passes through a turbine to drive a generator for generating power; the steam condenses into water in the last stage of this progress (3-4). The whole cycle ends at the condenser where the wet steam is finally condensed into water (4-1) which is then sent back to the pump as feed water for the next cycle.

The temperature - entropy diagram (T-s diagram) is usually introduced to visualize the changes of temperature and specific entropy in a thermodynamic process. A vertical line in the T-s diagram stands for an isentropic process whereas a horizontal line means an isothermal process.

Figure 2.3 is an example of T-s diagram for different Rankine cycles. In the T-s diagram of a water-steam system, the saturated curve is divided into two parts by the critical point: the curve on the left represents the saturated water, while the one on the other side is the saturated steam. The area below the saturation curve in the figure is the two phase region in which the substance is a mixture of liquid water and gaseous steam. The vaporization line (for example 3-3') which is shown as the horizontal line between the saturation curve, is related to the value of the specific latent heat of vaporization and the percentage of the position from the left side can represent how 'wet' the steam is. It also can be seen from the T-s diagram that when the pressure is high enough so that the saturation temperature reaches the critical point, there is not any heat of vaporization and the water can be vaporized into steam directly without any two phase region. This state of substance, which doesn't have a clear boundary between the liquid and gaseous phase, is defined as supercritical fluid.

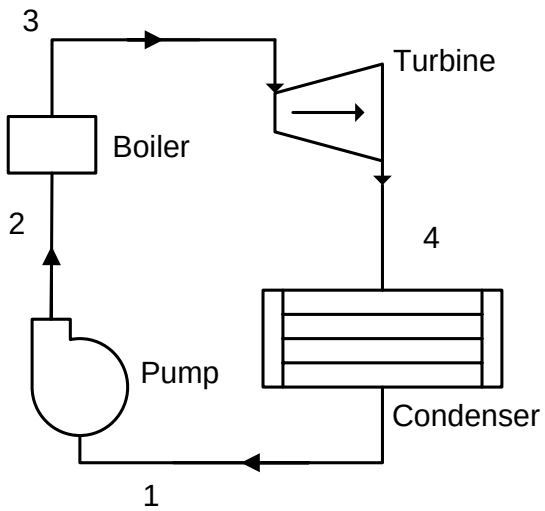

Figure 2-2: Typical Rankine cycle

It can be observed in the typical Rankine cycle (Figure 2.3, 1-2-3-3'-4-1) that part of the saturated steam will become condensed during expansion, which means the steam flow becomes wet. As too much moisture is harmful to the blade of the steam turbine, the wet steam, which is the two phase region below the saturation curve in the figure, should be controlled below 10% in the turbine. The easiest way is superheating the saturated steam (Figure 2.3, 1-2-3-3'-3''-4'-1). By heating the saturated steam into superheated steam, the expansion process can be shifted from 3'-4' to 3''-4'' in the figure so a drier steam can be produced in the turbine.

The thermal efficiency can be defined as the ratio of the work introduced to the

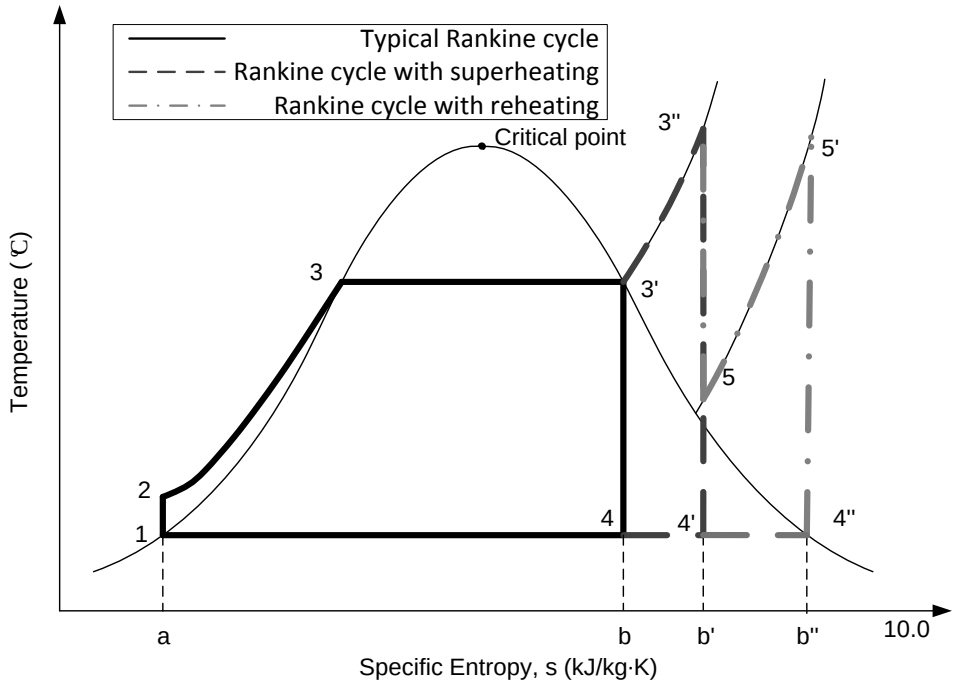

Figure 2-3: T-s diagram of typical Rankine cycle, Rankine cycle with superheating, and Rankine cycle with reheating

turbine to the total heat transferred to the working fluid. In Figure 2.3, the efficiency of the typical Rankine cycle can be described as:

$$\eta = \frac{W_{turb}}{Q_{total}} = \frac{area\ 1-2-3-3'-4-1}{area\ a-2-3-3'-b-a}$$

It can be observed that the ratio of the work to the turbine (area 3'-3"-4'-4) and the heat transferred from the boiler (area 3'-3"-b'-b) in the superheating section is higher than that of a typical Rankine cycle, therefore it can be concluded that the superheating can also contribute to the cycle efficiency of the generation.

Figure 2.3 also shows a fact that if the temperature of the superheated steam is high enough, the steam after expansion in the turbine can be completely dry. This would be the ideal case in the power generation and the temperature is not achievable at this moment due to technical difficulties. The reheating of the steam after the HP turbine can help avoid excessive moisture in the LP turbine by increasing the steam temperature. However it has been pointed out that the

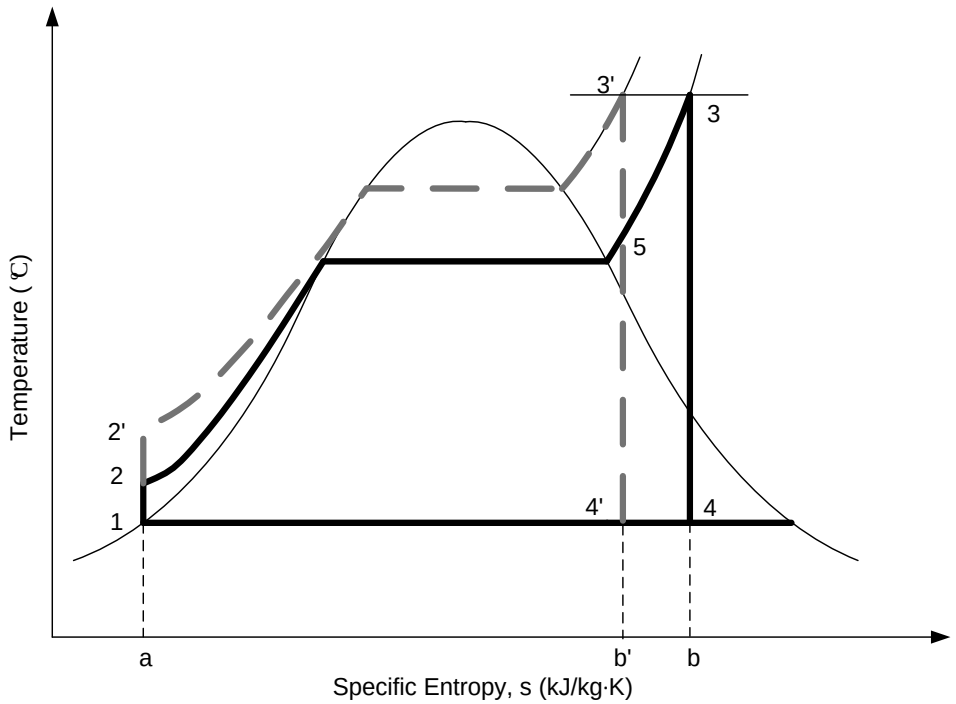

Figure 2-4: T-s diagram of a Rankine cycle with superheating with different water-steam pressure

contribution of reheating on the cycle efficiency is very little because the average temperature at which heat is supplied is not greatly changed.

Apart from the steam temperature, the pressure can also influence the cycle efficiency of a Rankine cycle. Figure 2.4 is a temperature-entropy diagram that represents the Rankine cycle with different water-steam pressures.

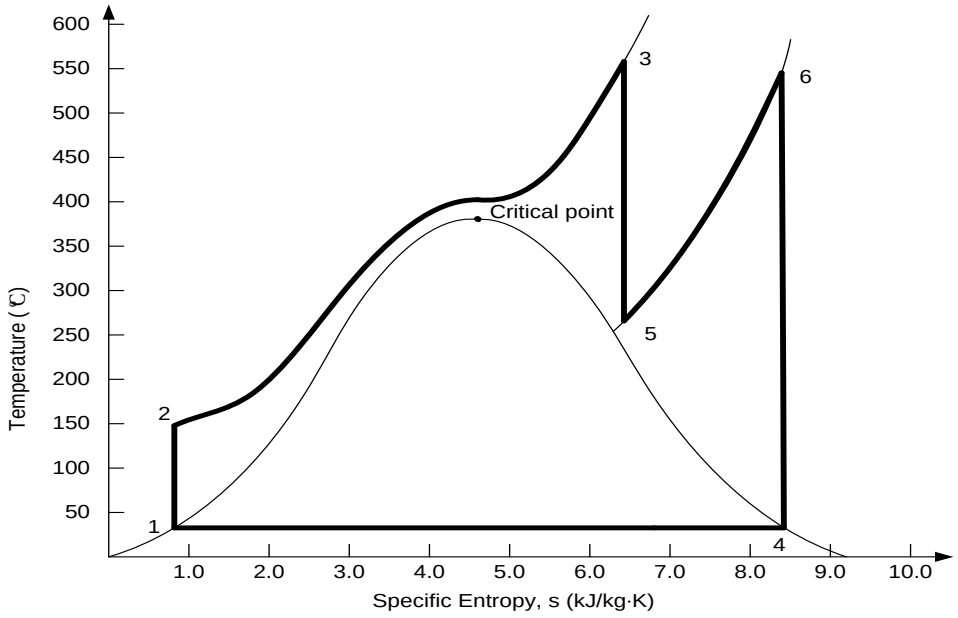

Figure 2-5: T-s diagram of an ideal supercritical power generation

With the same superheating temperature and the exhaust pressure, increasing the water-steam pressure reshapes the cycle from 1-2-3-4-1 to 1-2'-3'-4'-1 in Figure 2.4. The network delivered to the turbine is increased by area 2-2'-3'-5 and decreased by area 5-3-4-4', which almost remains the same level. But the heat rejected decreases by area 4'-4-b-b' hence the overall efficiency of the Rankine cycle is increased. (Wylen *et al*., 1994, Borgnakke and Sonntag, 2009)

2.1.3 SUPERCRITICAL POWER GENERATION

As increasing the pressure can increase the cycle efficiency, the supercritical fluid can be employed for power generation for higher efficiency. Supercritical boilers were first developed in U.S. in the 1950s and with the development of materials and components, which are better fitted nowadays to withstand high pressure/temperature conditions, they are today reliable and operationally flexible. It has been reported that there are more than 400 supercritical power plants in operation worldwide in the year 2002 (Mitsui Babcock Ltd). The traditional power plant that works under the critical point can be denoted subcritical power, referring to the supercritical power plant using supercritical fluid.

Compared with the efficiency between 33% and 39% in the subcritical power plants, the power generation with supercritical fluid has a higher efficiency of up to 48%, which is around 10% above the traditional plants (Vocke, 2007, Wang and Guo, 2009). Figure 2.5 gives an example of the cycle of the ideal supercritical power generation in the T-s diagram.

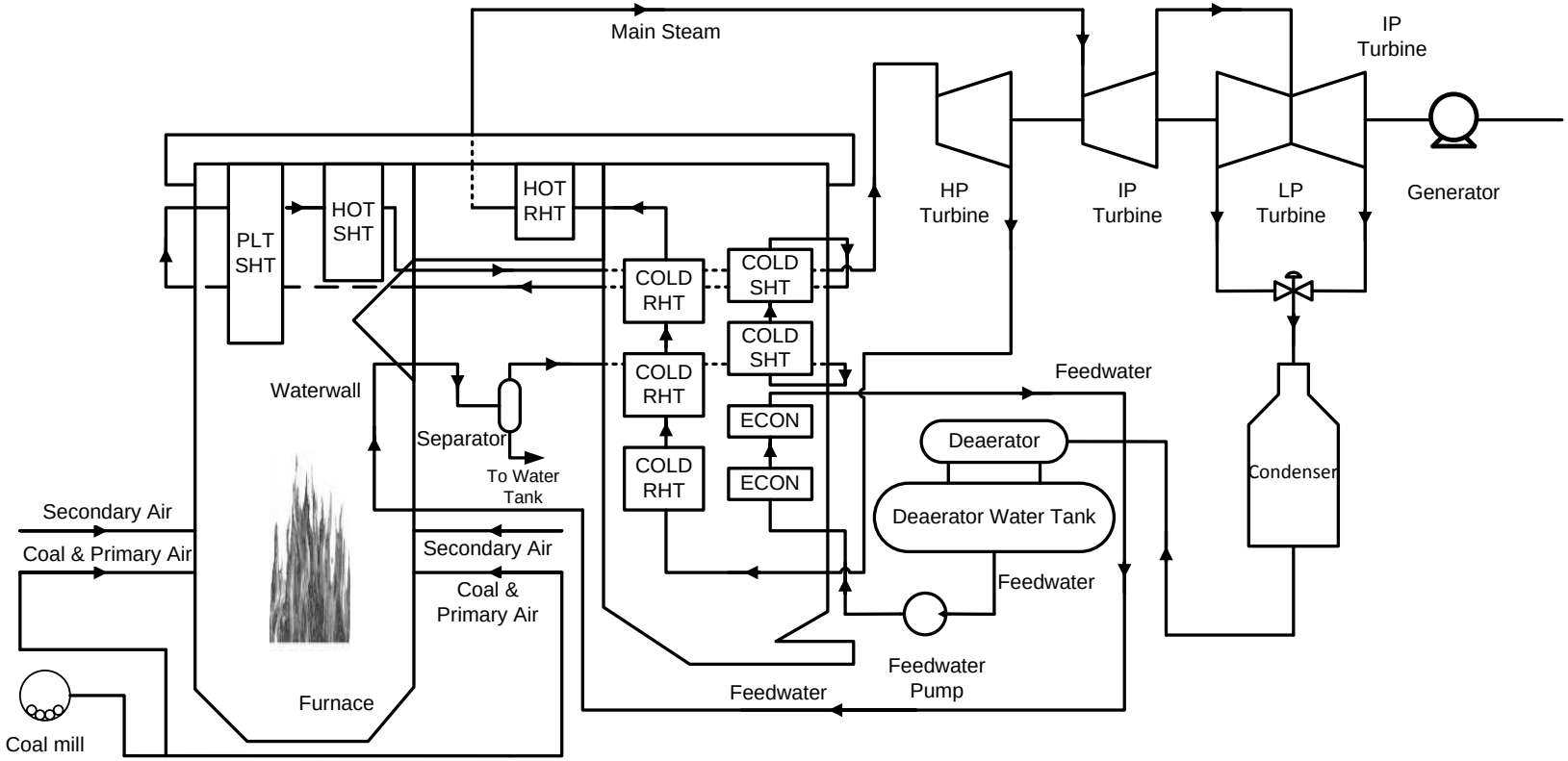

Figure 2-6: Schematic diagram of a supercritical boiler

As there is not a clear boundary of water and steam in the supercritical fluid, one significant design difference of the supercritical power plant, which is also called once-through boiler, is that the flow at the exit of the waterwall is dry steam in supercritical condition therefore the drum is not necessary in the generation in most of the conditions (Chaibakhsh *et al*., 2007, Ghaffari *et al*., 2007). Therefore the drum is removed from the boiler and steam water separators, which are smaller than conventional drums in a drum boiler of the same rated power, are employed to act as the drum's role in the consideration of low load generation especially the system is starting up (Eitelberg and Boje, 2004).

2.2 POST COMBUSTION CAPTURES

There are over 100 post combustion CO_2 capture technologies (Herzog *et al*., 2009). All the capture process use one or more of the following technologies: absorbent, adsorbent and membrane, converts CO_2 to a mineral or employs bio-fixation. Chemical absorption based on aqueous amines is a major capture method in industry. As the objective of this study is to investigate the dynamical responses or interactions of the capture process engagement to a power plant, making the best choice of technologies is not the project focus. In this project the most mature capture technology based on aqueous amines absorption is chosen (Bhown and Freeman, 2011).

2.2.1 CHEMICAL ABSORPTION

Absorption refers to an absorption/regeneration process to capture the CO_2 from the flue gas. The flue gas transfers into the bulk phase of another material, for

example amine solution. This technology has been commercialized and used in natural gas industry for 60 around years and is regarded as the most mature process. (Bhown and Freeman, 2011, Yang *et al*., 2008)

The basic principle of the absorption capture is that the carbon dioxide can react with the absorbent at flue gas temperature (40 – 60 ˚C) while the other species of the flue gas (majorly nitrogen) cannot. The "tower" in which the flue gas contacts the absorbent is called "Absorber". Most of the CO_2 can be removed from the flue gas in this absorber so the emission of "greenhouse gas" can be controlled. Rich CO_2 solvent is then directed to a "regeneration unit", which is called stripper or regenerator, where it is heated to reverse the reaction and to release CO_2 by increasing the temperature (Wang *et al*., 2011, Bhown and Freeman, 2011, Herzog *et al*., 2009). The CO_2 released from the solvent is then captured and compressed so it is ready for transportation. The lean CO_2 solvent with high temperature can be used to heat the rich CO_2 solvent from absorber in a cross heat exchanger and then pumped back to the absorber. For efficiency concern, most absorption units use the steam from the generation unit to heat the solution in the stripper.

2.2.1.1 Amine

Amines are water soluble organic chemicals that contain reactive nitrogen atoms (Herzog *et al*., April 2009). Monoethanolamine (MEA, C_2H_7NO) is studied and used for post combustion captures in various pilot plants (Notz *et al*., 2012, Artanto *et al*., 2012, Kittel *et al*., 2009, Moser *et al*., 2011) and it has also been

adopted in the majority of post combustion capture process simulations (Ahn *et al*., 2013, Mores *et al*., 2011, Zhang *et al*., 2011, Liu *et al*., 1999, Harun *et al*., 2012). Rapid, selective and reversible reaction with CO_2, relatively non-volatile and inexpensive makes MEA a very good absorbent. However there are also problems including its corrosiveness, the degradation by SO_2, NO_2, and oxygen which exist in the flue gas, and it also requires considerable amounts of thermal energy for the CO_2 regeneration (Fauth *et al*., 2005, Resnik *et al*., 2004, Yeh *et al*., 2005). The main reaction mechanism for the MEA-CO2 absorption can be described as the following formation and the maximum load capacity for the MEA is 0.5 mol CO_2 /mol amine based on the formation.

$$CO_2 + 2\cdot(C_2H_4OH)NH_2 \longleftrightarrow (C_2H_4OH)HNCOO^- + (C_2H_4OH)NH_3^+$$

Mixed amines are also used in amine capture and reported to be a possible solution. By mixing MEA with either diethanolamine (DEA, $C_4H_{11}NO_2$) or methyldiethanolamine (MDEA, $CH_3N(C_2H_4OH)_2$), the regeneration cost can be reduced but the circulation rate will also drop (Yang *et al*., 2008, Herzog *et al*., 2009). Results from Idem *et al*. (2006) shows that huge heat duty reduction can be achieved by using a mixed MEA/MDEA solution instead of a single MEA solution in an industrial environment of a CO_2 capture plant, although this benefit depends on whether the chemical stability of the solvent can be maintained (Yang *et al*., 2008, Idem *et al*., 2006).

As monoethanolamine is the majority of post combustion capture process simulation, and also for the consideration of reducing the system complexity, all

the CO_2 contact and amine capture in this report will be referred to the monoethanolamine.

2.2.1.2 Ammonia

Ammonia based solution, which uses aqueous ammonia as absorbent, can offer an absorption process with more stable solvents and less corrosive. The CO_2 uptake capacity of ammonia is estimated to be 3 times that of the MEA (Yeh and Bai, 1999). Furthermore the steam required for regeneration is 1/3 of that required with MEA (Resnik *et al*., 2004). It is estimated that the operating and capital costs with ammonia are 15%-20% less than with MEA (Yang *et al*., 2008). Two of the major by-products (ammonium sulphate and ammonium nitrate) from this process are fertilizers while the other one, ammonium bicarbonate, can be thermally decomposed to recycle ammonium (Yang *et al*., 2008, Herzog *et al*., 2009).

Ammonia based capture has a very significant disadvantage, that is, ammonia is a toxic gas. Therefore the capture and recycle of toxic ammonia vapour generated in the regenerator is a necessity. In the meantime this technology is not yet ready because research activities are still being carried out to reduce evaporative ammonia losses without sacrificing CO_2 capture performance (Herzog *et al*., 2009).

2.2.2 ADSORPTION

Activated carbon and charcoal are two effective sorbents due to their high porosities. They have high CO_2 capture capacities of 10% - 15% by weight.

However because of their low CO_2/N_2 selectivity, they can only be fitted in carbon capture processes with high purity of CO_2, for example the pre combustion carbon capture, and it is obvious that post combustion capture is not that kind of process. Zeolites, which offer 10 – 15 times greater CO_2/N_2 selectivity than activated carbon or charcoal, are able to separate the CO_2 from the flue gas so it can be used in post combustion capture. However, their CO_2 capacity is much lower, which is only about 1/3 to 1/2 of the carbonaceous materials, and the performance will be worse when water vapour exists. As a result, the solid sorbents are not good candidates unless they have greater selectivity, capacity and less sensitivity to steam (Konduru *et al*., 2007).

The chemical adsorption process is based on the alkali metal based sorbents. The development of adsorption processes for CO_2 capture would require development of both adsorbent materials and corresponding processes.

Limestone (CaCO3), which has a long history in industrial processes, releases CO_2 at 850 ˚C and transforms to calcium oxide (CaO), which recombines with CO_2 at 650 ˚C. This $CaO/CaCO_3$ system has a high CO_2 capture capacity, but the high temperature to release CO_2 makes it far from the possible capture solution. Porous sodium based sorbents work efficiently at the same temperature range as amines, but with considerably lower CO_2 capture capacity, while Lithium based sorbents can offer greater CO_2 capture capacity but work at a temperature of 400-500˚C (Yang *et al*., 2008).

Other investigations of alternative sophisticated materials as solid sorbent are still in early stages and none of the new materials have advanced beyond the lab scale testing. In addition, it is still not clear whether they are sufficient to offset their high cost (Herzog *et al*., April 2009).

2.2.3 MEMBRANE BASED SEPARATIONS

Another important capture technology uses a "filter" to separate the CO_2, called membrane based separation. The membranes are made up of thin polymeric films, and the different permeation rates of the film, caused by the relative size of the permeating molecules or the solubility coefficients in the membrane material, result the selectivity of the polymeric membrane.

The membrane separation is well established and mature technology, but there are problems unsolved. As the membrane permeation is generally pressure driven, the main challenge comparing to the absorption or adsorption capture is the low pressure of flue gas (Herzog *et al*., April 2009). In addition, the CO_2/N_2 selectivity of most available polymers is between 50 and 60, which is far away from 200 competing with amine based absorption.

There are a large number of other exploratory approaches under development, including ionic liquid (Chen *et al*., 2013, Zhao *et al*., 2012, Ramdin *et al*., 2012) and biological mechanisms like carbonic anhydrase (Bond *et al*., 2001, Dilmore *et al*., 2009) and microalgae systems (Cheng *et al*., 2006, Skjånes *et al*., 2007). But these approaches are far away from realistic as they're still in lab scale.

2.3 AMINE BASED CAPTURE PROCESS

A standard design of the capture plant that has been widely accepted is composed of at least four parts: the absorber, the regenerator, the reboiler and the main heat exchanger, to complete the whole capture and regeneration process. Figure 2.7 is a process diagram for post combustion capture with aqueous amines.

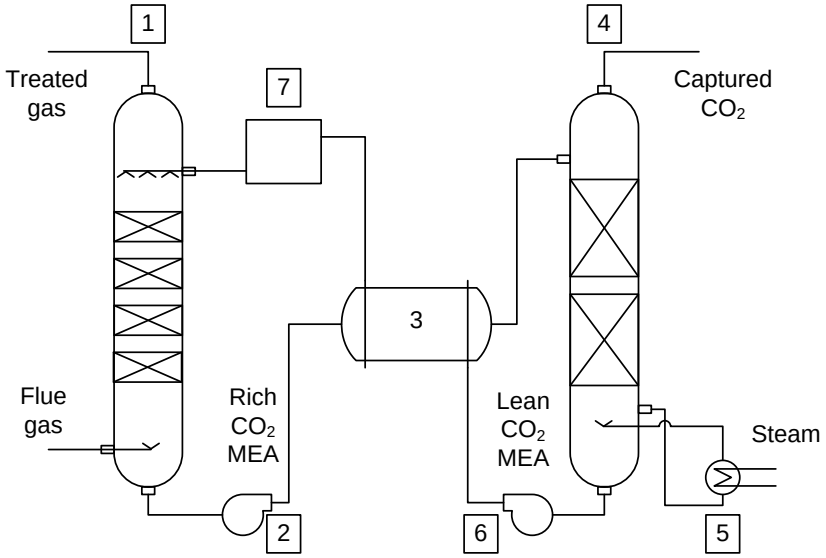

Figure 2-7: Post combustion capture with aqueous amines

1. Absorber. 2. Rich amine pump. 3. Heat exchanger. 4. Regenerator. 5. Reboiler. 6. Lean amine pump. 7. Lean amine Storage tank.

The absorber is the vessel where the flue gas from the coal-fired power plant contacts with the amine based sorbent. They are basically mass transfer columns with either tray or packed columns to improve the contact between gases and liquid in a chemical process, however, most of them are the structured packed tower systems with lower pressure drop and larger interfacial area (Mersmann *et al.*, 2011, Rao, 2002, Seader and Henley, 2006)

The flue gas enters the absorber from the bottom when the amine flows in from the top of the absorber by a liquid distributer. Most of the carbon dioxide is selected from the flue gas and dissolved into the solvent by chemical reaction in the packing area. Other gases come from the flue which exits the absorber from the top and is emitted to atmosphere. The CO_2 rich amine exits the bottom of the absorber and is pumped to the heat exchanger.

The Shell and Tube Heat Exchanger is the best established heat exchanger that dominates over 90% of the industry market (Chisholm, 1980). This heat exchanger design consists of a large pressure vessel with a bundle of tubes inside, and two fluids flow through the shell and the tube separately. Heat transfer takes place from the hotter fluid to the colder through the tube walls so that waste heat can be recovered. In the post combustion capture, the rich CO_2 amine enters the tube side of the heat exchanger and is heated by the hot lean CO_2 amine from the bottom of the reboiler. The preheated amine is directed to the top of the regenerator for the CO_2 regeneration.

The regenerator and the reboiler are interconnected facilities that are used to provide enough heat for the amine to reach the temperature needed in the reverse reaction of absorption. The regenerator is a packed tower system similar to the absorber while the reboiler is basically a heat exchanger. Low pressure but high temperature steam extracted from the turbine of the power plant is introduced to the reboiler to vaporize the water that acts as solvent in the amine solution. The steam ascends to the regenerator while the rest of the amine solution drops down to the bottom and is pumped to the heat exchanger to preheat the rich CO_2 amine.

Rich CO_2 amine is heated to around 120 ˚C by the direct contact with the vaporized steam in the regenerator, releasing CO_2 that leaves the column from the top for compression and storage, and flows to the reboiler afterwards.

2.4 SIMULATION OF AMINE BASED CAPTURE

Simulation can be very helpful at the early stage development of a technology in design and optimization prior to the implementation. A number of simulation works on the amine based capture has been carried out. These research activities are typically based on the mass transfer in columns with two simulation methods: the equilibrium stage simulation or the rate based simulation (Browne, 2014).

An equilibrium stage is an ideal condition that the equilibrium of liquid and gas phase is established. Having a series of equilibrium stages makes it possible to simulate the steady state of a separation process. The equilibrium stage modelling is good at non-reactive systems due to its simplicity. However the equilibrium can be hardly achieved in the reactive capture therefore this method is difficult to represent the actual process (Browne, 2014). Several research works based on the equilibrium stage model have been published by Afkhamipour and Mofarahi (2013) and Mores *et al*. (2011).

The rate based simulation which considers the reaction rates, the electrolytes as well as the mass and heat transfer provides a much greater complexity than the equilibrium stage simulation. The two-film theory of mass transfer is one of the most common analysis methods of the rate based simulation. In this theory the

equilibrium is attained only at the gas-liquid interface and a thin gas film and a thin liquid film distribute on each side of the interface (Kvamsdal *et al*., 2009, Pacheco and Rochelle, 1998, Al-Baghli *et al*., 2001). Focusing on the film around the interface of the liquid and gas, this approach divided the phase into four parts based on the position: bulk gas, gas film, liquid film and bulk liquid. This feature makes the more detailed calculations achievable, including the electrolyte, the mass transfer resistances, and the reaction kinetics (Kenig *et al*., 2001).

Both the equilibrium stage simulation and the rate based simulation are steady state simulations to optimise the operation at the nominal condition where the flow rate and content of the flow gas are constant. The post combustion capture is moving to the industrial implementation, the dynamic study is of increasing importance. However, few research activities reported are focusing on the dynamic simulations at this moment. Lawal *et al*. (2009) and Kvamsdal *et al*. (2009) worked on the absorber, Ziaii *et al*. (2009) studied the regeneration column and Harun *et al*. (2012) developed a model for the whole system.

2.5 SUMMARY

The coal-fired power generation and the post combustion capture technologies have been reviewed in this chapter. The generation process of the typical coal-fired power plant is introduced in the first part of this chapter. From the basic analysis of thermodynamics it is proved that supercritical plants have a higher generation efficiency comparing with the traditional subcritical boilers. As a

result, the supercritical generation unit will be used as a reference plant for the research on the dynamic response of the post combustion capture.

The second part of this chapter introduces several different post combustion capture technologies available today. Chemical absorption based on aqueous amines, as the major capture method in industry, is focused in this thesis. A detailed study of the capture process has been studied and different modelling approaches are also reviewed in this chapter.

Chapter 3.

POWER PLANT PROCESS MODELLING AND SIMULATION STUDY

The goal of this study is to analyse and examine the plant performance while it is integrated with post combustion carbon capture process through plant dynamic simulation. So a mathematical model that is able to represent the power plant generation process is a prerequisite for simulation study. The mathematical description should provide sufficient information of the important component thermodynamics in the process and the model should be derived based on their physical principles. However, sometimes the dynamic behaviour in the actual power generation process is very difficult to be described mathematically. A very significant example is that some of the model parameters differ in a wide range when identified from different level of generation outputs. In the first principle models, this is usually solved by a look up table which hosts various

values of these parameters obtained from past experience and tests. Additionally these parameters of the model may lead to quite different model behaviours. This indicates that it is an unachievable task in the power plant simulation to represent the full range of operation conditions by one single model, especially in the cases which have not been considered in the parameter identification processes. Black-box approaches, including neural network and autoregressive moving average model, are possible options to overcome these difficulties but it is difficult for these approaches based on empirical data to convince industry as they are lack of support from physics and engineering laws.

A lot of work has been reported for the mathematical model of the coal-fired supercritical power plant (Salisbury, 1950, Thomas and Finney, 1979, Usoro *et al*., 1983, Kola *et al*., 1989, Shinohara and Koditshek, 1996, Lu, 1999, Lu and Hogg, 2000, Inoue and Amano, 2006, Gu *et al*., 2009). In this chapter, two simulation approaches for the power plant modelling will be studied: the first principle model and the power plant simulator based on thermodynamics and fluidic networks.

3.1 FIRST PRINCIPLE MODEL

Supercritical power generation process is a complex system with multi interconnection of subsystems and components. A simplified whole system dynamic model of the supercritical power plant is developed by Mohamed (2012) based on the mass and energy balance of each components from the boiler, turbine and generator.

Focusing on the generation process of the power plant, the structure of this model is divided into six subsystems: Economizer (ECON), Waterwall (WW), Superheater (SH), HP turbine (HP), Reheater (RH) and IP/LP turbine (IP/LP). The IP and LP turbines are considered as one in this model because they are connected without any heating process in between. These subsystems follow the flow direction of the water-steam except for the generator and they can be basically categorized as boiler systems (ECON, WW, SH and RH) and Turbine systems (HP, IP/LP).

3.1.1 MODEL OF THE BOILER SYSTEMS

Despite the chemical reaction in the combustion process, the main role of the boiler system is to transfer the heat from the flue gas to the water-steam. Therefore study on the heat exchange between the flue gas and the steam is an important task for the boiler modelling. These boiler subsystems where the water-steam in their tubes is heated are considered as uniform heat exchangers with different thermal coefficients.

The mathematical description of the heat exchangers is based on the calculations that start from the mass balance and energy balance, which are described as equation 3.1 and 3.2:

$$\frac{dm}{dt} = w_i - w_o \qquad \text{Eq 3.1}$$

$$\frac{dU}{dt} = \dot{Q} + w_i \cdot h_i - w_o \cdot h_o \qquad \text{Eq 3.2}$$

where m is the mass of water-steam in the heat exchanger while U is the internal energy. w and h are the flow rate and specific enthalpies of the water steam fluid that enters and leaves the heat exchanger. $\dot{Q}$ represents the heat radiation rate to the system. From the definition of enthalpy $H=U+pV$, the internal energy U in equation 3.3 can be described by the equation of enthalpy H, the pressure p and the volume V as $U = H - pV$. Considering the volume V in the heat exchangers as a constant, the equation 3.1 and 3.2 can be transformed into:

$$\frac{dm}{dt} = V \cdot \frac{d\rho}{dt} = V \cdot \left(\left.\frac{\partial \rho}{\partial p}\right|_T \cdot \frac{dp}{dt} + \left.\frac{\partial \rho}{\partial T}\right|_p \cdot \frac{dT}{dt} \right) \qquad \text{Eq 3.3}$$

$$\begin{aligned} \frac{dU}{dt} &= V \cdot \left(\frac{d(\rho \cdot h)}{dt} - \frac{dp}{dt} \right) = V \cdot \left(h \cdot \frac{d\rho}{dt} + \rho \frac{dh}{dt} - \frac{dp}{dt} \right) \\ &= V \cdot \left(h \cdot \left(\left.\frac{\partial \rho}{\partial p}\right|_T \cdot \frac{dp}{dt} + \left.\frac{\partial \rho}{\partial T}\right|_p \cdot \frac{dT}{dt} \right) + \rho \cdot \left(\left.\frac{\partial h}{\partial p}\right|_T \cdot \frac{dp}{dt} + \left.\frac{\partial h}{\partial T}\right|_p \cdot \frac{dT}{dt} \right) - \frac{dp}{dt} \right) \end{aligned}$$

Eq 3.4

where V is the internal volume of the heat exchanger, ρ is the density, p is the pressure, t is the temperature and h is the specific enthalpy of water steam fluid. Solving the equations 3.3 and 3.4 after putting these two formulas in, the pressure and the temperature can be calculated by Eqs 3.5 & 3.6.

$$\dot{p} = \frac{\dot{Q} + w_i \cdot k_i - w_o \cdot k_o}{k_c} \qquad \text{Eq 3.5}$$

$$\dot{T} = k_a \cdot (w_i - w_o) - k_b \cdot \dot{p} \qquad \text{Eq 3.6}$$

where k_i, k_o, k_a, k_b, k_c are the parameters that can be described by the density ρ, the specific enthalpy h, the pressure p and the temperature t. These parameters can be treated as constant if the load demand variations of the power plant are not significant.

For the simplification purpose, this model did not implement the thermodynamics of the coal combustion and the flue gas side, instead, energy that was provided by coal, was simplified as the product of the calorific value of the fed coal. The coal flow rate into the mill, represented by a 1st order transfer function to reflect the combustion delay effect in system dynamic responses (Eq 3.7), is provided to the model as an input, which is derived from the differential equation $\frac{d\dot{Q}}{dt} = k \cdot \left(q \cdot w_{coal} - \dot{Q} \right)$ (Mohamed *et al.*, 2011).

$$\dot{Q} = \frac{1}{1+\tau s} \cdot q \cdot w_{coal} \qquad \text{Eq 3.7}$$

where $\dot{Q}$ is the heat generated from the combustion, q is the calorific value of coal and w_{coal} is the flow rate that enters the furnace for combustion. τ is the time constant of the 1st order transfer function that represents the time required for the combustion. As this heat is serving all the boiler components, the heat absorbed by the exchangers shares this energy proportionally: as $\dot{Q}_{ECON} = k_{ECON} \cdot \dot{Q}$, $\dot{Q}_{WW} = k_{WW} \cdot \dot{Q}$, $\dot{Q}_{SH} = k_{SH} \cdot \dot{Q}$, $\dot{Q}_{RH} = k_{RH} \cdot \dot{Q}$.

3.1.2 MODEL OF THE TURBINE SYSTEM

The turbine model can be simplified to represent the energy balance because the turbine and generator response is much faster than the boiler. Considering the turbine as a non-storage device this approach assumes that the outlet mass flow rate of the turbine is equal to the inlet mass flow rate. With this assumption the mechanical work can be calculated by the steam specific enthalpy at the entrance and the exit and the flow rate w_s.

$$P = w_s \cdot \left(h_i - h_o\right) \qquad \text{Eq 3.8}$$

in which P represents the mechanical work of the turbine, h_i and h_o are the specific enthalpies of steam enters and exits the turbine. In the situations that the power plants generates at a relatively stable demand, the specific enthalpy in each stage of generation is relatively stable, as a result the $h_i - h_o$ in this equation can be considered as a constant k_P when there is not big impacts in the plant output (Eq 3.9).

$$P = k_P \cdot w_s \qquad \text{Eq 3.9}$$

3.1.3 FLOW RATE CALCULATIONS

The mass flow rates in the boiler tubes between each stage of the superheater can be expressed as the equation of the pressure between different stages, which is adopted in many research articles to calculate the fluid or gas flow rate (Gu *et al.*, 2009, Wei *et al.*, 2009, Guo *et al.*, 2014). The mathematical description of these flow rates can be summarized as Eq 3.10.

$$w_{boil} = k_{w\_b} \cdot \sqrt{p_i - p_o} \qquad \text{Eq 3.10}$$

where k_{w_b} stands for the parameter to be identified that related to the flow rate in the boiler, p_i and p_o are the pressure at the different end of the boiler. However this equation is not applicable when steam flows into a turbine system because there is an expansion stage involved. As a result Eq 3.11 is introduced to represent the flow rate for the turbine systems. This equation has shown a good agreement with the result obtained by a simulator (Salisbury, 1950, Shinohara and Koditshek, 1996).

$$w_{turb} = k_{w\_t} \cdot \frac{p}{\sqrt{T}} \cdot a_v \qquad \text{Eq 3.11}$$

in which a_v is the valve position of the steam turbine , k_{w_t} is an unknown parameter to be identified for the calculation of the turbine flow rate.

3.1.4 PARAMETERS IDENTIFICATION

From the equations of the first principle model, it can be seen that there are 32 unknown parameters to be identified, including 20 from the four stage heat exchangers in the boiler, 4 from the heat distribution between the heat exchangers, one time constant that refers to the time required by the combustion, 6 from the flow rate calculation and 2 from the calculation of turbine mechanical power output. These parameters are listed as the following table:

Table 3-1: Parameters of the first principle model

Parameter	Relevant variables of the unknown parameters
$k_{i1}, k_{i2}, k_{i3}, k_{i4}$	Outlet pressures in the Economizer, Waterwall, Superheater and Reheater
$k_{o1}, k_{o2}, k_{o3}, k_{o4}$	Outlet pressures in the Economizer, Waterwall, Superheater and Reheater
$k_{a1}, k_{a2}, k_{a3}, k_{a4}$	Outlet pressures in the Economizer, Waterwall, Superheater and Reheater
$k_{b1}, k_{b2}, k_{b3}, k_{b4}$	Outlet temperatures in the Economizer, Waterwall, Superheater and Reheater
$k_{c1}, k_{c2}, k_{c3}, k_{c4}$	Outlet temperatures in the Economizer, Waterwall, Superheater and Reheater
$k_{w\_b1}, k_{w\_b2}, k_{w\_b3}, k_{w\_b4}$	Flow rates of the Economizer, Waterwall, Superheater and Reheater
$k_{ECON}, k_{WW}, k_{SH}, k_{RH}$	Heat distribution between the Economizer, Waterwall, Superheater and Reheater
τ	Time required for the combustion
k_{w_t1}, k_{w_t2}	Flow rates of the HP and IP/LP turbines
k_{P1}, k_{P2}	Parameters of turbine mechanical work from the steam flows through the HP and IP/LP turbines

A Genetic Algorithm (GA), which is an evolutionary algorithms for both constrained and unconstrained system optimizations, is used to identify the parameters in the first principle model as it is capable to jump from the local optima towards the global optimum (Wei, 2007, Mohamed, 2012). Historical data at the rated capacity of the power plant is fed into the model as input and the Genetic Algorithm can generate a group of individuals with random parameter values in the range that the user defined as the first generation. Then the fitness values are evaluated by the fitness function, which is described as Eq 3.12:

$$fitness = \sum_{1}^{n} (R_m - R_s)^2 \qquad \text{Eq 3.12}$$

where R_m is the measured data and R_s is the simulated result. Following the natural rule 'survival of the fittest', these results are ranked and sent to the operators of selection, crossover and mutation if the optimization criterion is not satisfied. The offspring of this generation is generated for the optimization. The best individual in the end will be chosen as the parameters of the model when the optimization criterion is satisfied. The identified parameters enables the model to represent the supercritical power plant near the rated capacity.

3.1.5 LIMITATIONS OF THE MODEL

The thermal characteristics of steam, including pressure, temperature enthalpy etc., vary when the output of the real power plant changes. Many of the parameters in the boiler and turbine models have a high dependence on these thermal characteristics. Theoretically one group of parameters is only able to represent the supercritical power plant at one particular load level, but there is normally some tolerance to the parameters so that they can be used if the load variation is small enough (Mohamed, 2012).

One possible approach to address this weakness is to use the dynamic parameters. Data grouped by different load levels can be fed into the parameter identification process and different groups of parameters are assigned to the power plant model for different plant duty stages through a look-up table. But some of the parameters, including the percentage of chemical energy distributed to different

heaters in the furnace (k_{ECON} to k_{RH}), the parameters represent the change of specific enthalpy when the steam passes through the turbine k_{turb}, and the flow rate calculation by the pressure k_{w_b} and k_{w_t}, has little relevance to the generation process so constant value can be given to these parameters in all the power outputs for a faster identification.

3.2 FLUIDIC NETWORK BASED SIMULATOR

Another model approach used in the project is the simulator resulting from the cooperation with the Tsinghua University (THU) and the North China Electrical Power University (NCEPU), which the author is involved in. Both THU and NCEPU have an outstanding research record in supercritical process and power plant modelling and simulation (Fan and Lv, 1998, Fan *et al*., 2000, Liu *et al*., 2002, Liu, 2007).

The initial purpose for the simulator development is to provide a training platform for the site engineers to improve their skills in plant operation. With the development in the simulation technologies and improvement of model accuracy, the simulator is increasingly used for different purposes, for example, simulation evaluation of safe and economized generation, failure analysis and optimization of the power plant design and operation. First principle approach is used to describe every individual component in the system, and all physical components implemented in the simulator are interconnected through the fluid network. The

parameters of the simulator are based on a real 600MW supercritical power plant operating in China.

The power plant simulator is developed under the SimuEngine 2000, a commercial visual simulation support platform between simulation systems and computer operating systems. This platform is able to provide real-time database and complete simulation functions, including data visualization, on-line testing, collaborative development, multitask parallel running, multiple processes and distributed simulation. The power plant simulator is divided into two parts in the SimuEngine: plant process modelling and the control system. FORTRAN source code files as the basic element are added to the task that represent the corresponding function of the plant model. The codes are compiled with the library and then the whole task is made into an executable file (Figure 3.1). The software environment also provides the database for the each subsystem so that the saved variables can be visited and shared between different tasks as global when the simulator is running.

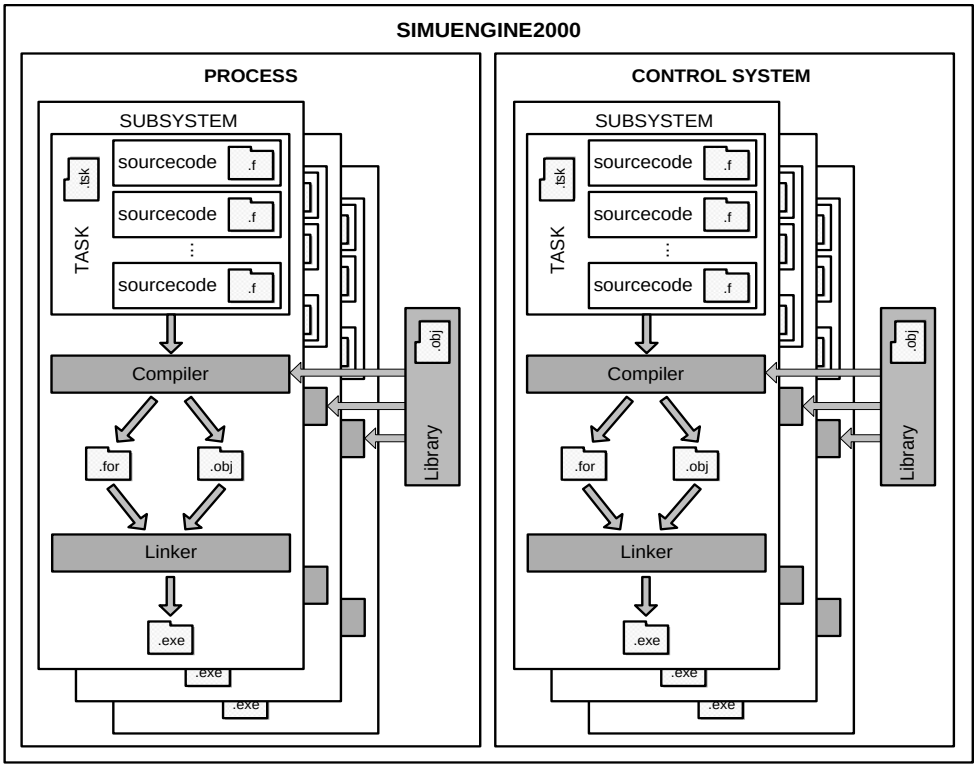

Figure 3-1: Structure of the Simulator

3.2.1 POWER PLANT PROCESS MODEL OF THE SIMULATOR

The mathematical model of the power plant simulator is far more complicated than the model derived via the first principle model presented in the earlier sections. Instead of proportional distributing the chemical energy to the heaters in the boiler, the simulator considers the complete path of the flue gas: from the air preheating in the air preheater, the combustion with coal, then the waterwall, the superheater, the reheater and the economizer, to the emission at the end from the chimney. Additionally the feedwater from the deaerator and condensed water after the LP turbine are also considered, therefore a complete water-steam cycle is established. Figure 3.2 shows a simplified figure of the water-steam cycle and the four sections including feedwater, boiler, turbine and condensed water are

marked in the figure. The red lines in this figure represent the steam flows; the blue lines represent the water flow; the green lines represent the cooling water for the condenser and the grey lines are the air flow to ensure the negative pressure in the condenser. The complete system design will be provided in the appendix of the thesis.

The supercritical power plant simulator can be divided into two parts from their functions in the simulator: the fluidic network calculation and the block model. The fluidic network calculation focuses on the pressure and the flow rate in the supercritical system, which play an important role in the block model, while the block model considers more on the thermodynamics and the characteristics of the network which may affect the flow rate calculation.

3.2.1.1 Water property databases

Thermodynamic properties, including heat capacity, saturation temperature, specific entropy, specific enthalpy, specific enthalpy of vaporization and specific volume (density), are the very fundamental data in the thermodynamic calculation. As water is the most common substance in the world, many research activities and measurements can be found to focus on these properties and a very detailed look-up table can be found to calculate these properties from any two others of them. All these look-up tables have been implemented in the simulator. With the implementation of these databases, the simulator is able to solve the parameter problem found in the first principle model as they cover all the conditions of water and steam in the power generation unit.

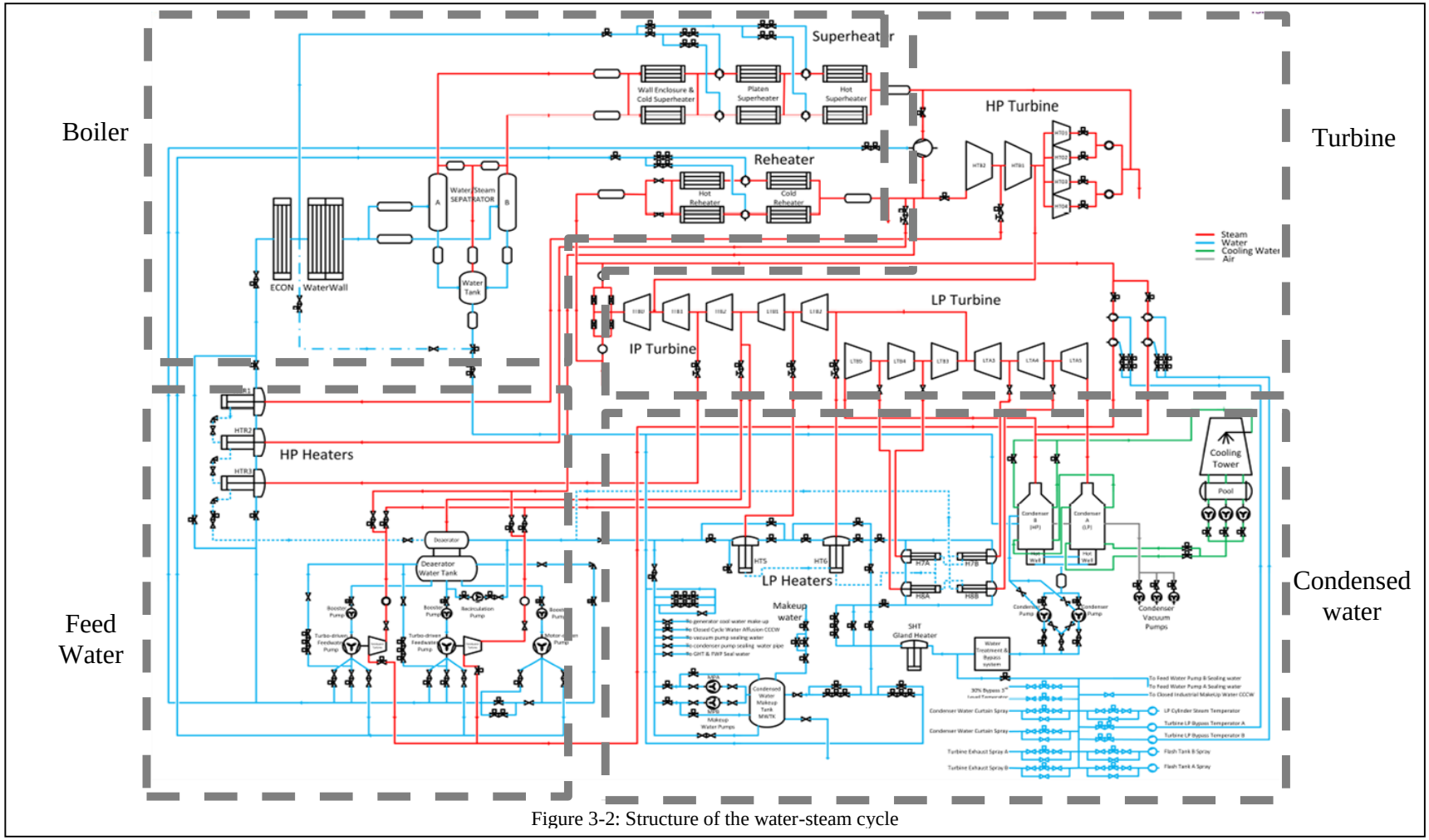

Figure 3-2: Structure of the water-steam cycle

3.2.1.2 Fluidic network calculation

It can be seen from Figure 3.2 that the water-steam cycle in the simulator is a network other than a simple flow as the first principle model considers, therefore a simple flow equation is not enough for the flow rate calculation in such a huge system. The fluidic network calculation, which is also the most significant difference between simulator and the first principle model, is implemented for the flow rate calculation.

Fluidic network is an analysis of the fluid which flows through a hydraulics network that containing several or many interconnected branches. To simplify the calculation, the first task of a fluidic network calculation is to separate the whole water-steam cycle into different subsystems. Usually the boundary blocks of a subsystem are pressure vessels as their pressure that is important in the fluidic network can be calculated from the inlet and outlet flow properties. In this simulator, the water steam cycle is divided into four major subsystems and four auxiliary subsystems. The major subsystems are the feedwater system, the main steam system (including superheating session, reheating session and turbine sessions), the condensing water system, the feedwater pump steam system and the auxiliary system includes the cooling water system, the heater drain system, the turbine gland system and the turbine vacuum system (Ren and Gao, 1999).

Once the subsystem is defined, all these boundaries and nodes, which are defined as the junctions which connect more than two branches or components in the

subsystem, are sorted with number for the calculation. Then simultaneous equations of the network analysis can be then established and the flow rate between the nodes can be described by the pressure of the nodes. The fluidic network has an important fact that the pressure change of different nodes in the fluidic network is independent of the path taken. Following this rule, as all the boundary pressures are available, the network problem can be solved by the Hardy Cross method, which is an iterative method that employs the Newton-Raphson method (Ren and Gao, 1999, Luo, 1988).

Based on the principle of the fluidic network calculation, there are two elements that can affect the calculation result: the pressure in the boundaries and the fluid conductance of the blocks in the network. These two variables can be obtained from the model of each block in the subsystem.

3.2.1.3 Modelling of the subsystem blocks

The block models can be classified as valve model, superheater/reheater model, turbine model and node model.

As introduced in the last section, the fluid conductance is an important element in the fluidic network calculation. Therefore this characteristic is considered as a very important variable in the simulator. A valve is the most common unit for flow rate control in power plants and the principle is to control the conductance by different valve position. Most of the fluid flow rates in the power generation are controlled by valves. In the simulator the branch characteristic (defined as R_B in the simulator) is employed to represent the fluid conductance of the valves

and other thermodynamic blocks. This branch characteristic is proportional to the fluid density as the calculation focuses on the mass flow rate instead of the volume flow rate. The mathematical description of this variable for valves and other blocks can be described as Eq 3.11 and 3.12.

$$R_B = k \cdot a_v^{\,2} \cdot \rho \qquad \text{Eq 3.11}$$

$$R_B = k \cdot \rho \qquad \text{Eq 3.12}$$

where a_v is the valve position, ρ is the fluid density k is the parameter related to the design of the valve.

Same as the first principle model, the model of the superheater, reheater, waterwall and the economizer are derived from the mass balance and the energy balance (Eq. 3.1 and Eq 3.2). As the database of water properties is available, instead of considering the pressure and temperature, this model focuses more on the specific enthalpy of the fluid (Li, 2009). The exit enthalpy at the exit of the system can be obtained by Eq 3.13:

$$\dot{h}_o = \frac{1}{\rho V} \cdot (\dot{Q}_{pws} + w_i(h_i - h) - w_o(h_o - h) + V\frac{dp_o}{dt}) \qquad \text{Eq 3.13}$$

where h_i, h_o are the specific enthalpy at the entrance and exit of the block while h is the average, p_o is the pressure at the exit. ρ is the average density of the fluid, which can be obtained in the look-up table from pressure and temperature, $\dot{Q}_{pws}$ is the heat transfer rate from the pipe and V represents the volume of the

water-steam in the block, which is a constant. As the pressure at the exit of the block can be found in the fluidic network calculation, the temperature, the outlet temperature, as well as the dryness of the steam if the outlet fluid is a mixture of water steam, can be obtained based on the look-up table from the specific enthalpy and the end pressure.

The variable $\dot{Q}_{pws}$ in the Eq 3.12 represents the heat transfer rate from the pipe to the water-steam following the Eq 3.13:

$$\dot{Q}_{pws} = A_i \cdot \Upsilon_i \cdot (T_p - T_{ws}) \qquad \text{Eq 3.13}$$

in which A_i and Υ_i are constant that represent the contact area and the heat transfer rate between the water-steam and the pipe, T_p and T_{ws} are the temperatures of the metal and the fluid. Similarly, the pipe temperature is calculated by Eq 3.14:

$$MC_j \frac{dT_p}{dt} = \dot{Q}_{fgp} - A_i \cdot \Upsilon_i \cdot (T_p - T_{ws}) \qquad \text{Eq 3.14}$$

$$\dot{Q}_{fgp} = A_o \cdot \Upsilon_o \cdot (T_{fg} - T_p) \qquad \text{Eq 3.15}$$

where the $\dot{Q}_{fgp}$ is the heat transfer rate from the flue gas to the pipe, A_o and Υ_o are constant that represents the contact area and the heat transfer rate between the flue gas and the pipe, T_p and T_{fg} are the temperatures of the metal and the flue gas (Li, 2009).

The steam turbine is the system component that extracts thermal energy from pressurized steam for conducting mechanical work via a rotating shaft. The model of the turbine system is based on the specific thermal balance. With the input specific enthalpy and pressure from the previous stage, the input specific entropy of the fluid, which is usually superheated steam, can be searched from the look up table. From the T-s diagram of an ideal supercritical power generation (Figure 2.5, Figure 3.3), it is obvious that the steam expanding process in the ideal turbine is an isentropic process (3-5 and 6-4). Therefore the specific entropy remains constant when flowing through the turbine. As the outlet pressure is available from the fluid network calculation, the outlet enthalpy can be then obtained by the look-up table.

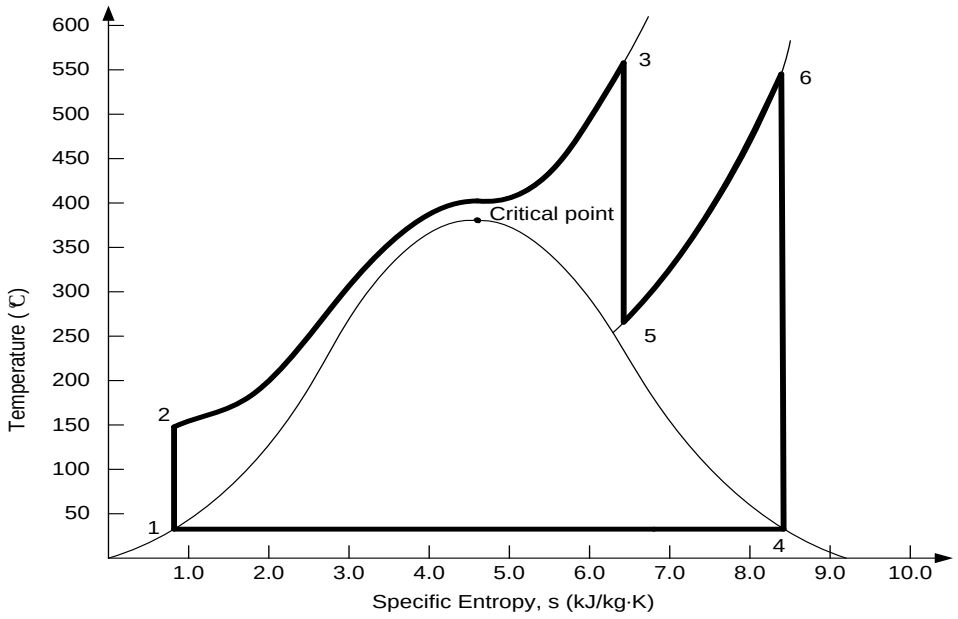

Figure 3-3: T-s diagram of an ideal supercritical power generation

The calculation of the mechanical work in the turbine system is introduced in the first principle model, described as:

$$P = w_s \cdot \left(h_i - h_o\right) \qquad \text{Eq 3.16}$$

where w_s is the flow rate, h_i and h_o are the inlet and outlet specific enthalpy of the steam. The temperature at the exit of turbine can be obtained by the specific enthalpy and the pressure from the look-up table.

The node introduced in the fluid network calculation is to mix or split the fluid that flows through, therefore the thermal property of the fluid is also important in the simulation implementation in additional to the flow rate. Figure 3.4 illustrates the structure of node model which has m inlet branches with different specific enthalpy and n outlet branches.

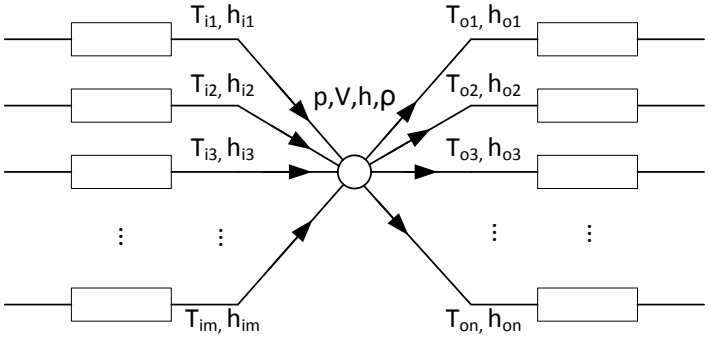

Figure 3-4: Node with m inlet branches and n outlet branches

Four types of node outputs are considered in the simulator including the flow rate of each branch, the node pressure, the node temperature, the node specific enthalpy, and the node density. The pressure and node density calculated in this node model are introduced to the fluid network, estimating the flow rate of each branch as introduced in Section 3.2.1.2, while the temperature, the specific enthalpy, the branch flow rate and the pressure are employed as the input of the following component in each branch.

As the node pressure and branch flow rate can be obtained in the fluid network, the node model focuses on the other three properties based on the mass and thermal balance. Considering the pressure in the node as a constant, the specific enthalpy of the node can be obtained by the enthalpy brought by the fluid into and out of the node volume V , described as the following equation:

$$\dot{h} = \frac{\sum_{1}^{m} w_i \cdot (h_i - h) - \sum_{1}^{n} w_o \cdot (h_o - h)}{\frac{\rho V}{dt} + (\sum_{1}^{m} w_i - \sum_{1}^{n} w_o)} \qquad \text{Eq 3.17}$$

where ρ and V are the density and the volume of the fluid in the node, w_i and w_o are the flow rate of different branch that flows into and out of the node. h_i and h_o are the specific enthalpy of fluid at the entrance and exit while h is that of the average in the node. Again, the density can be calculated from the look-up table as the end pressure and the specific enthalpy are available.

3.2.2 CONTROL SYSTEM IMPLEMENTED IN THE SIMULATOR

The control system is important to maintain the normal power generation process in a power plant. The control system implemented in the simulator can be divided into two parts: the control of individual subsystem blocks and the load control. An individual subsystem block is usually controlled by a PI or PID controller that provides the capability for the block to follow the demand output. The controls of this part are usually realised through valves or pumps whose reaction is relatively straightforward and fast. The target of the load control is to regulate the boiler and the turbine operation to ensure the power generation can follow the power demand requested from the grid and to maintain the stability of the whole system with a wide range of operational conditions. Among all the control variables, the power output and the main steam pressure are most important to the whole plant optimal operation.

The load control system of a power plant is mainly organised into two key subsystem controls: The boiler subsystem and turbine subsystem. The role of the boiler control is to deliver the internal demand of the hot steam. This control subsystem mainly focused on adjusting the flow rate of coal feed into the furnace.

The control of air flow rate follows the optimised fuel air ratio of the combustion. There is also an optimised proportion between the feedwater and the total fuel to maintain the main steam temperature. These three corresponding inputs are usually called the firing rate in industrial operation (Xiao, 2006).

The purpose of the turbine control is to match the output of the power plant with the load demand from the grid by changing the mechanical work delivered to the generator, which is shown proportional to the steam flow rate through the turbine from the Eq 3.16. As a result the valve positions before the turbines are usually controlled to regulate the power output. (Xiao, 2006)

The turbine response to the load demand is usually as fast as 6 to 15 seconds, which is much faster than the heat exchanging process in the boiler that may take several minutes, therefore balancing the turbine response and the operational condition is also very important in the system control.

Considering the requirements of the plant control, boiler follow and turbine follow are two well adopted modes to form the control strategies in the power generation load control. Boiler follow mode represents that the turbine response first, utilizing the stored energy in the boiler to provide immediate load response, the boiler response is carried out at once to bring pressure back to the set point. The problem of the boiler follow mode is that the main steam and reheated steam pressure is less stable. Turbine follow mode increase the firing rate to match the load and the valves before the turbines are controlled to maintain the main steam pressure. Comparing the boiler follow mode it provides a better stability of the

operational condition but the response is much slower. Both control strategies are implemented in the simulator (Xiao, 2006).

Coordinated control is another control strategy implemented in the simulator that the control of turbine response and the boiler response are carried out simultaneously. In the simulator, the main steam pressure demand, which is calculated by the load demand and the power generated, is sent to a PI controller with the power delivered to the grid therefore the firing rate demand can be obtained. As both the turbine and the boiler are controlled immediately, the coordinated control system is able to provide fast response with a relatively stable main steam characteristics (Xiao, 2006).

The same as a real power plant, the simulator also has a Distributed Control System (DCS) that links all the control actions and displays the information of temperature, the pressure and the flow rate at different position of the power plant, including the boiler and the turbine.

3.3 COMPARISON OF THE TWO MODELLING APPROACHES

Both the approach of the first principle model and using the power plant simulator were considered at the beginning of the project which focuses on different aspects of plant process with their own strengths. The selection of the modelling approach should consider both the purpose of the modelling and what characteristics that the project is interested in.

Comparing with the first principle model, the simulator is able to provide a more detailed representation of the power plant as the thermodynamics of almost every component in the power generation progress, from coal feed to the furnace to the mechanical work delivered to the generator, are considered. Although some of these components in the system play little role in the study of post combustion capture, for example the auxiliary subsystems and the condensed water subsystem, some other features are still of great importance. One example is that the intermediate pressure turbine (IP) and the low pressure turbine (LP) in the first principle model are considered as a whole turbine (IP/LP) to simplify the calculation while the simulator separated them as two. It makes almost no difference in the mechanical work calculation of the IP/LP in the whole process simulation, as the steam extraction in these two turbines is not considered in the model. However as the steam used to heat the reboiler in the post combustion capture usually comes from the end of IP before it comes to the LP, further calculation, for example the steam pressure and the temperature at the exit of IP, and the work from IP and LP respectively, is necessary and some of the parameters need to be re-identified.

Another difference of the two approaches is that the plant control system that is implemented in the simulator cannot be adapted to the first principle model. With the consideration of both the system block control and the load control, the simulator provides the capability to test different control modes of power plant in different situations, especially when the post combustion carbon capture is introduced to the power plant.

There are also limitations caused by the control system implemented in the simulator. As the control command of the feedwater is forced following the coal consumption flow rate with a gain for the optimised main steam property, individual control of the coal, air and feed water is not accessible. On the other hand, as no control is involved to maintain this feedwater coal ratio, the first principle model is able to avoid this problem that the flow rates are treated as irrelevant inputs. One disadvantage of the simulator is that the impact caused by the change of this ratio can only be studied in the first principle model unless some changes are carried out in the simulator.

Another disadvantage of the simulator is that the simulator is developed under FORTRAN which is a fixed step calculation. Integration calculation in FORTRAN is simplified and its accuracy is limited by the time step, which is 0.25s in this system due to the massive calculation. The integration in the first principle model is more accurate as a variable step solver ode45 is available in the Matlab/SIMULINK environment, which is based on the forth-fifth order Runge-Kutta algorithm. However the simulation result shows that the error caused by the integration calculation can be controlled within an acceptable range.

Following the comparison of the two models, the simulator can represent the power plant more than the first principle model can. Therefore this approach is chosen to study the dynamic response when the post combustion is implemented.

3.4 SUMMARY

This chapter introduces different modelling approaches for supercritical power plant simulation. The discussion focuses on the first principle model and the simulator based on the thermodynamics and the fluid network calculation. It compares the advantages and limitation of both models and the simulator, as it provides more functions and more complexity, will be used to study the impact of introducing post combustion carbon capture to the power plant.

Chapter 4.

MODELLING STUDY OF POWER PLANT COAL MILLING PROCESS

The fuel preparation is a very important process in power generation, which is usually achieved through coal mills that crush raw coal into small particles with greater contact surface with air to improve the combustion. The coal mills deliver the pulverised fuel to the furnace after the milling process. The flow rate of the feeding coal is an important input for the post combustion capture as it can affect the content and flow rate of the flue gas. However the mill model in the simulator can provide little information to the capture process simulation because it is simplified as a transfer function of the coal feed into the coal mill. Therefore the study of the coal mill is carried out in this project to enhance the mill model therefore more useful information to the post combustion carbon capture can be estimated.

This chapter contributes to introduce the mathematical model of the foster-wheeler tube-ball coal mill. It begins with the study of the fundamental working principles of different coal mills, and then the mathematical model based on these working principles of the coal mill is developed. Genetic algorithm is employed to identify the unknown parameters of the model and the validation work is carried out based on the data from the industrial partner.

This chapter also describes the approaches that can implement this mathematical model on-line in the power plant, by which additional information can be provided to the plant operators for the coal mill condition monitoring. Further analysis and applications based on the model on-line implementation are also discussed in this chapter to improve the mill performance.

4.1 CLASSIFICATION OF COAL MILLS

The coal mills can be classified by their rotation speed into high speed, medium speed, and low speed mills.

High speed coal mills, including beater wheel mill and hammer mill, usually have the most compact design therefore they are usually used in small scale applications like demonstration plants. A beater wheel mill is just like a fan, with an impeller of 8-10 blades at the rotate speed of 750 – 1500 rpm. The coal was fed into the mill with the drying hot air, crashed by the impeller and the blades and then splashed to the armour plates at high speed for a further crush. A classifier is installed in the beater wheel mill where the coal fine enough will

continue its journey to the furnace while the bigger ones are sent back to the mill and continue the milling process (Figure 4.1 (left)).

A hammer mill is another kind of high speed coal mill with the rated rotation speed of 750 rpm. When the coal was fed into the mill, it is hit by a rotating hammer at a speed of about 60 m/s and smashed into fine powder. The coal fine enough will be discharged at the bottom. (Figure 4.1 (Right))

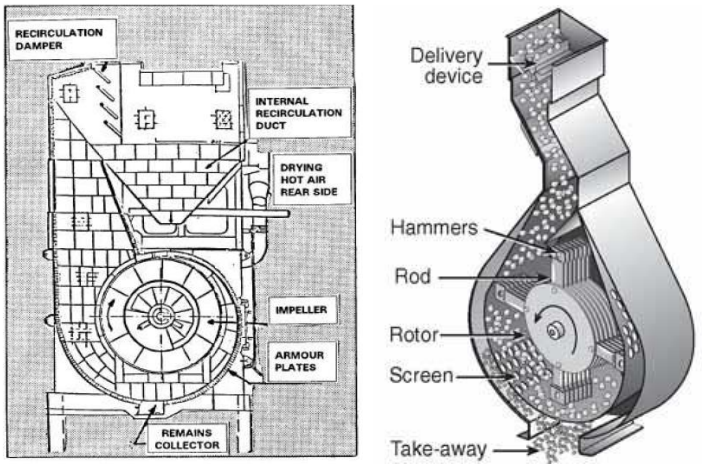

Figure 4-1: Beater wheel mill (left) and Hammer mill (right)

As these coal mills work at high rotating speed, they usually have a relative shorter life time and are not suitable for hard coals to prevent from damage. Heavy maintenance is also required by the high speed mill. As a result, this type of mill is no longer widely used for the coal pulverizing systems.

Medium speed mills, which are also known as vertical spindle mills, are the most widely used in power generation industry. The medium speed mills work on the principles of crushing and attrition. The grinding action takes place between two surfaces. The two surfaces rotate in the opposite direction at a speed between 50

– 300 rpm and the raw coal is crushed into fine coal between. There are two different types of the rolling elements in the medium speed coal mills: balls or ring-shaped rolls. Hot primary air is sent to the mill to dry the coal and to carry the pulverized coal to the classifier, where the ones fine enough is brought to the burner. The oversized coals particles are separated out and fall down, back to the mill grinding part.

Figure 1.2 shows the E-type vertical spindle mill equipped in the RWE Innogy Plc (DidcotA power station) (RWE Innogy Plc, 2000, Wei *et al*., 2007).

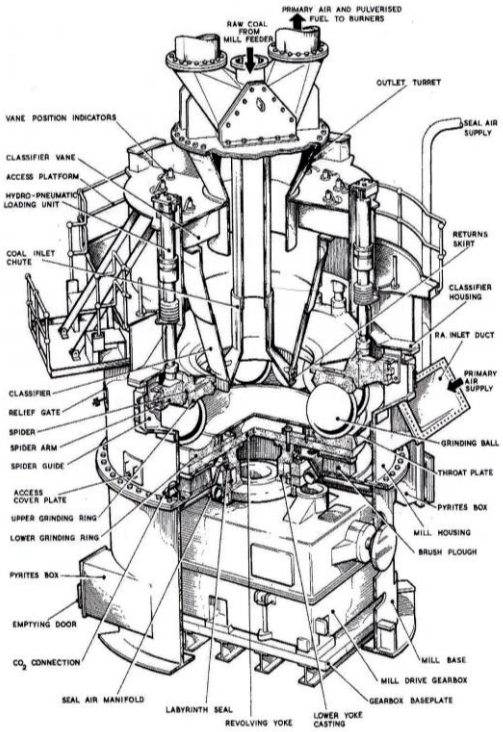

Figure 4-2: Medium speed mill (RWE Innogy Plc, 2000)

The vertical spindle mills are bigger than the high speed mills, but they are still relatively small, energy saving, and less noisy comparing with the low speed

mills. Similarly to the high speed mills, the vertical spindle mills are also not very good at dealing with hard coal.

Low speed coal mills stand for coal mills with rotation speed of 15 – 25 rpm, commonly known as tube-ball mills. A tube-ball mill has a horizontal rotating cylinder and a number of tumbling or cascading steel balls inside. Raw coals are fed into the mill body, crushed and smashed by the tumbling steel balls into powder and brought out to the classifier by the primary air for the fuel separation. There are two different mechanical designs of the tube-ball mill available in industry. Figure 4.3 shows the tube ball mill that is currently used in EDF Energy plc (Cottam Power Station) while Figure 4.4 is the coal mill from the Eggborough Power Ltd (Eggborough Power Station).

The tube-ball mills are relatively big, noisy, and consume more energy comparing to the medium speed coal mills, but it can be implemented reliably to grind coal with very high hardness.

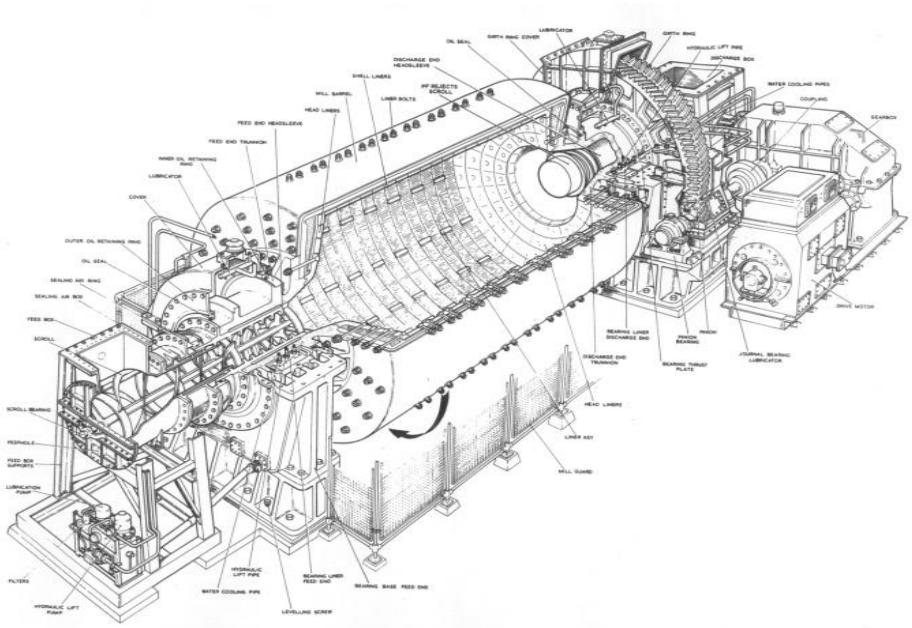

Figure 4-3: Low speed mill (EDF Energy) (Armitage, 1983)

The Foster wheeler low speed mill is studied as there is cooperation with the industrial partner Eggborough Power Ltd and data is available for the parameter identification.

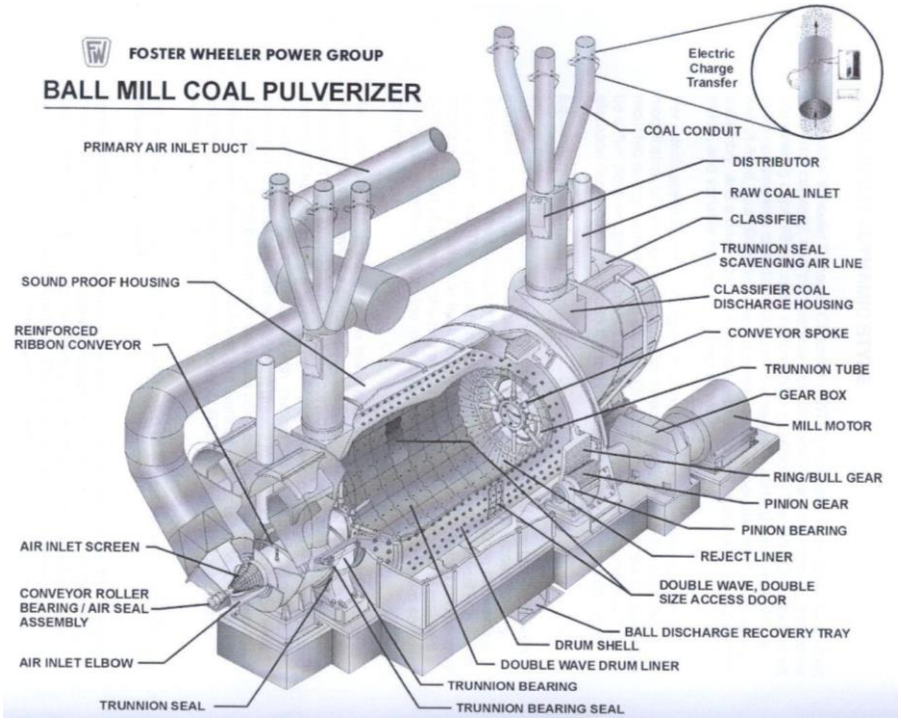

Figure 4-4: Low speed mill (Foster Wheeler) (Kukoski, 1992)

4.2 WORKING PROCESS OF LOW SPEED TUBE-BALL MILL

The main objective for pulverizing coal into fine particles is to create larger contact surface areas with the air so that it is easier to burn. This milling process is formed of four different functions: coal feeding, coal pulverization, coal separation, and coal delivery.

In the FOSTER WHEELER ball mill system (Figure 4.4), raw coal is firstly transported by a conveyor to the power plant. Once it arrives at the plant, it will be stored into the bunkers. Then the raw coal enters the mill from the raw coal inlet, mixes with the coal rejected by the classifiers and then drops to the feeders which feed the coal into the mill. It enters the mill and spins in a large drum where it is brought up with hundreds of steel balls and drops down back to the

bottom. The coal is ground into fine powder by the steel balls in this process. Preheated air from the power plant is sent to the mill from the Primary air inlet duct, as drying and transporting media of the fine coal powders. It carries the fine coal powder to the classifiers which located at both ends of the coal mill through the annular space between the fixed trunnion tube and the rotating hot air tube (Figure 4.5 & 4.6). (Kukoski, 1992)

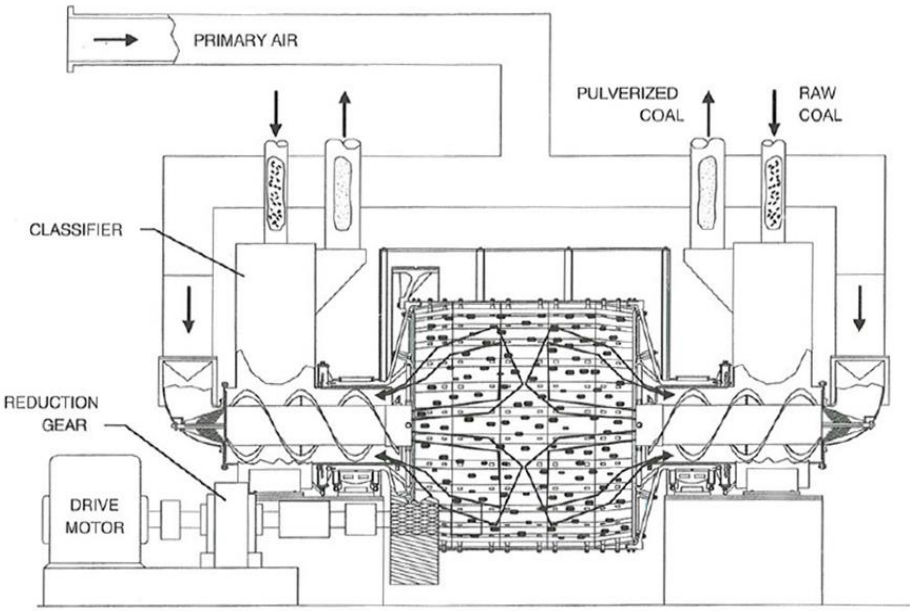

Figure 4-5: Primary air flow in the Ball Mill Coal Pulverizer (Kukoski, 1992)

The role of the classifiers is to filter the pulverised coal to ensure the coal leaving the mill is ground finely enough. Fine coal is blown to the coal conduit by the primary air easily, continues its journey to the furnace for combustion with the primary air. The bigger particles are rejected by the classifier, dropping down and being sent back to the drum for another grinding cycle (Figure 4.6) (Kukoski, 1992).

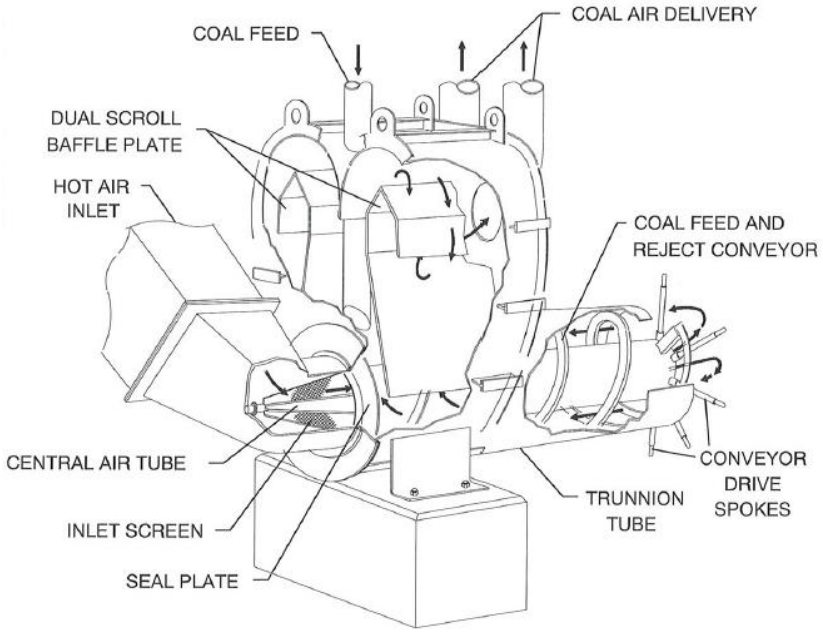

Figure 4-6: Classifier of the Ball Mill Coal Pulverizer (Kukoski, 1992)

4.3 MATHEMATICAL MODELLING OF THE COAL MILL

The procedure for coal mill modelling follows the following three steps:

1. To study the basic mill model dynamic equations based on the analysis of the milling process and physics principles;
2. To identify unknown parameters using intelligent algorithms based on the on-site data;
3. To analyse the results and return to and repeat steps 1 and 2 if modifications to the model are required or conduct further simulation to validate the model.

The design of the mathematical model of the Foster Wheeler tube-ball mill is based on the mass balance and thermal balance of the normal grinding process.

4.3.1 INPUT AND OUTPUT VARIABLES OF THE PROCESS

From the study of the mill design and the operation guidance, there are two feeders to provide raw coal into each mill: one is on the drive end (DE) while the other is on the non-drive end (NDE). The speeds of feeders are considered as the main inputs that are related to the flow rate of the raw coal into coal mill. The properties of the primary air that boost into the mill from both DE and NDE are also input variables that can affect the mill dynamics. Mill power (mill motor power or current) consumed is another model input that related to the thermodynamics of the milling process. The temperature and the differential pressure of the pulverized fuel and the hot primary air at the exit of the mill, which are measured directly and provided in the data from the Eggborough Power Station, are treated as the model outputs.

Some important variables of the coal mill are not measurable due to the lack of suitable sensors or difficulties to placing sensors. As a result these variables, for example mass flow rate of raw coal into the mill W_c (kg/s), mass of coal in mill M_c (kg), mass of pulverized coal in mill M_{pf} (kg), and mass flow rate of pulverized coal out of mill W_{pf} (kg/s), cannot be adopted as the output of the model because it is impossible to validate. Therefore they are treated as intermediate variables so that they can be estimated in the simulation. The full list of variables is given in Table 4.1.

Table 4-1: List of coal mill input and output variables

Coal mill variables		
Input variables	Intermediate variables	Output variables
Feeder 1 speed (%) Feeder 2 speed (%) Primary air temperature inlet the mill (°C) Mill Motor Current/Power (Amp/Watt) Primary air flow (%)	Mass flow rate of raw coal into the mill W_c (kg/s) Mass of coal in mill M_c (kg) Mass of pulverized coal in mill M_c (kg) Mass flow rate of pulverized coal out of mill W_{pf} (kg/s)	Mill outlet temperature T_{out} (°C) Mill outlet pressure ΔP_{out} (mBar)

To simplify the model, the coal in the mill is classified as pulverized and un-pulverized only, and the grinding process is considered separately with the transportation of pulverized coal.

4.3.2 MASS BALANCE

As introduced in Section 4.3.1, two feeders are equipped in the ball-mill mill manufactured by foster wheeler. Each feeder can be operated separately and therefore the flow rate of raw coal entering the mill can be controlled. With the help of the measurement of feeder speeds, the mass flow rate of the coal into the mill can be obtained by the following equation:

$$W_c = C_1 \cdot \left(k_{f1} \cdot v_{f1}\right) + C_2 \cdot \left(k_{f2} \cdot v_{f2}\right) \qquad \text{Eq 4.1}$$

where v_{f1} is the feeder 1 speed; v_{f2} is the feeder 2 speed. k_{f1} and k_{f2} are parameters that reflects the relationship between the feeder speeds and the raw coal flow rates. C_1 and C_2 are variables to avoid errors of feeder speeds which are caused by the inaccurate of measurements when the mill is idle. $C_1 = 1$ if the

feeder speed $v_{f1} > 5$, otherwise, $C_1 = 0$. $C_2 = 1$ if the feeder speed $v_{f2} > 5$, otherwise, $C_2 = 0$.

The raw coal is fed into the mill from the feeders at a mass flow rate of W_c, and then it is pulverized by tumbling with steel balls. Finally the fine coal is brought out of the mill by the primary air at a flow rate of W_{pf}. From mass balance point of view, the change of coal mass in the mill should be equal to the difference between the total mass of the pulverized coal that leaves the mill at the flow rate W_{pf} and the total mass of the raw coal mill that enters the mill at the flow rate W_c. The mass flow process in the mill is shown as the following figure:

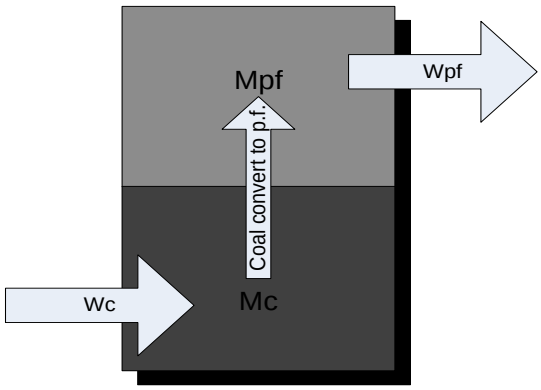

Figure 4-7: Illustration of mass flow process

Based on the mass flow balance, the following equations can be obtained (Guo *et al.*, 2014):

$$\dot{M}_c(t) = W_c(t) - k_1 \cdot M_c(t) \qquad \text{Eq 4.2}$$

$$\dot{M}_{pf}(t) = k_1 \cdot M_c(t) - W_{pf}(t) \qquad \text{Eq 4.3}$$

$$W_{pf}(t) = k_2 \cdot \Delta P_{out} \cdot M_{pf}(t) \qquad \text{Eq 4.4}$$

where k_1 and k_2 are unknown coefficients to be identified.

Eq 4.2 represents that the change of mass of coal in the mill. $\dot{M}_c(t)$ is decided by the raw coal flow rate into mill $W_c(t)$ and the fraction of coal pulverized from raw coal, which is proportional to the mass of coal in mill $M_c(t)$. Eq 4.3 describes the change of mass of pulverized fuel in mill $\dot{M}_{pf}(t)$ which is related to this fraction of coal turned into pulverized coal $k_1 \cdot M_c(t)$ and the flow rate pulverized coal that leaves the mill $W_{pf}(t)$. Eq 4.4 gives the mathematical description of the pulverized fuel flow rate out of the mill by the differential pressures at the end of classifier ΔP_{out} and the mass of pulverized coal in mill $M_{pf}(t)$.

4.3.3 THERMAL BALANCE

The coal mills in power plants are also involved with thermodynamics. Preheated primary air is blown into the mill and acts as the drying and transporting agent of the coal. Following the heat balance rule, the heat change in the mill Q_{mill} is equal to the difference between the heat sent into the mill Q_{in}, including the heat from raw coal Q_{coal}, the hot air Q_{air} and the power from the mill motor Q_p, and the heat out from the coal mill Q_{out}, which is a sum of the heat brought out by the pulverized coal with primary air Q_{pf} and the heat

emitted from the mill body to the environment Q_e. The thermal balance of the coal mill is given as Figure 4.8.

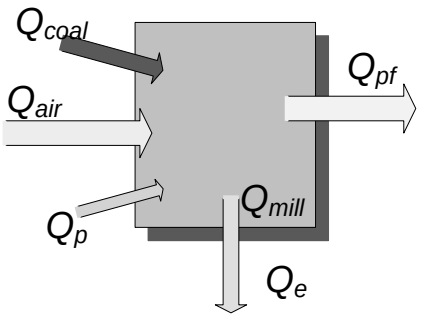

Figure 4-8: Thermal balance

Based on the heat balance and all the variables related to the thermodynamics, the following equation of the mill outlet T_{out} can be obtained:

$$\dot{T}_{out}(t) = k_3 \cdot T_{in\_DE}(t) + k_4 \cdot T_{in\_NDE}(t) + k_5 \cdot W_{air\_DE}(t) + k_6 \cdot W_{air\_NDE}(t) - k_7 \cdot W_c + k_8 \cdot P - k_9 \cdot T_{in} \cdot T_{out} + K_{10} \cdot T_{out}$$

Eq 4.5

where $k_3 \sim k_{10}$ are the unknown coefficients to be identified.

4.3.4 MILL PRODUCT PRESSURE

As there are not any exhaust fans equipped in this mill design, the primary air sent to the mill is the only element to bring the fine coal flow out to the burner. Therefore the outlet differential pressure $\Delta\dot{P}_{out}$ can be modelled by the following equation:

$$\Delta\dot{P}_{out}(t) = k_{11} \cdot M_{pf} + k_{12} \cdot M_c + k_{13} \cdot W_{air\_DE} + k_{14} \cdot W_{air\_NDE} + k_{15} \cdot \Delta P_{out}$$

Eq. 4.6

where $k_{11} \sim k_{15}$ are the unknown coefficients to be identified.

4.3.5 AVERAGE MILL LEVEL INDICATION

The coal in the mill drum is supposed to be maintained at an optimal level when the coal mill is working. Too much coal will reduce the impact from the steel balls to the coal that can lead to an inefficient milling while too little coal will potentially harm the mill because the steel balls may drop onto the mill drum directly. Therefore monitoring the coal level in the mill drum is another important factor that the industrial concerns. From Eq 4.1 to Eq 4.5, it is possible to obtain the quantity of the intermediate variables, two of which are very important to the mill level indication. These variables: mass of coal in mill M_c and mass of pulverized coal in mill M_{pf}, reflects the mass of coal inside mill. With the help of coal density and the specification of the balls inside the mill, it is possible to find out the volume of the coal and the mill balls, and then the mill level can be obtained by geometry calculations.

Figure 4.9 can briefly describe the geometry process in the mill. l in this figure represents the mill level while r represents the radius of the mill. α is an angle that related with the mill radius r and the mill level l, which can be described by the equation:

$$\alpha = \arccos(\frac{r-l}{r}) \qquad \text{Eq. 4.7}$$

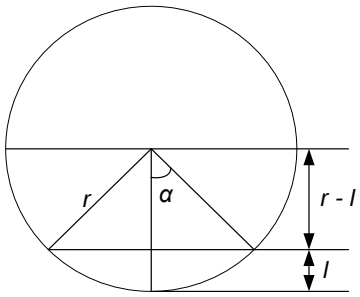

Figure 4-9: Geometry description of mill level calculation

The average mill level in proportional β can be obtained by:

$$\beta = \frac{l}{2 \bullet r} \qquad \text{Eq 4.8}$$

Substituting Eq 4.8 into Eq 4.7 we have:

$$\alpha = \arccos(1-2\beta) \qquad \text{Eq 4.9}$$

From the geometry analysis, the following equation can be obtained:

$$\frac{(V_{coal}+V_{ball})}{V_{mill}} = \frac{(\frac{2\alpha}{2\pi})\cdot\pi - \frac{\sin(2\alpha)}{2}}{\pi} \qquad \text{Eq 4.10}$$

where V_{coal} represents the volume of the raw coal and the pulverized in the mill, V_{ball} is the volume of the mill balls, and V_{mill} is the space of mill. Therefore:

$$\frac{((M_c+M_{pf})/\rho_{coal}+V_{ball})}{V_{mill}} = \frac{2\arccos(1-2\beta)-\sin(2\cdot\arccos(1-2\beta))}{2\pi}$$

Eq 4.11

The mill level β can be calculated by solving Eq 4.11.

4.3.6 IMPROVEMENT OF THE COAL MILL MODEL

From the industrial data of the coal mill from the Eggborough power station (Figure 4.10 & 4.11), the outlet differential pressure at each side of the coal mill has a significant difference. The possible reason for this difference is that as the design of this ball mill is not completely axisymmetric. On the other hand, it can be shown that the difference of outlet temperature at each side is much smaller than the differential pressure as the mill temperature is not as sensitive as its pressure, therefore the average temperature at the exit of the mill can be used as the mill outlet temperature.

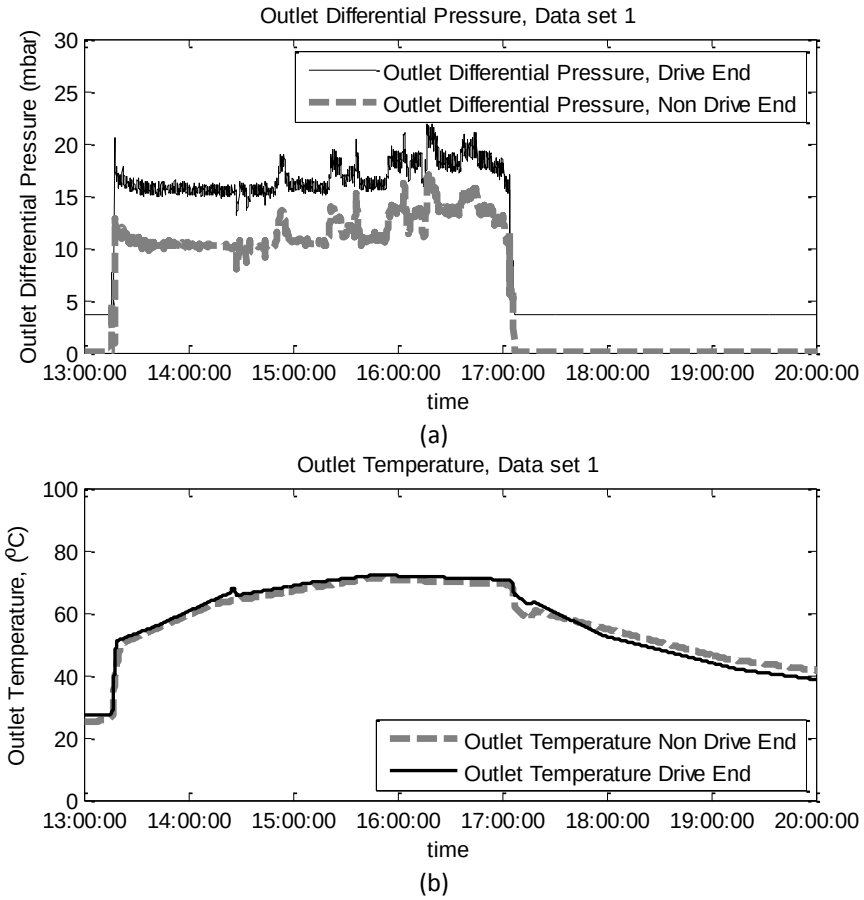

Figure 4-10: Outlet Differential Pressure (a) and Temperature (b) (measurement data, Group 1)

The difference between the outlet differential should be considered in the model. However the only result obtain from the Eq. 4.6 cannot represent the dynamics of both ends. Changes are implemented to the mathematical descriptions related to the outlet differential pressure (Eq 4.6) so that the inlet flow rate of both sides are considered as the inputs of the calculation on each end, as Eq 4.12 and 4.13.

$$\Delta\dot{P}_{out\_\mathrm{DE}}(t) = k_{11}\cdot M_{pf} + k_{12}\cdot M_c + k_{13\_\mathrm{DE}}\cdot W_{air\_\mathrm{DE}} + k_{14\_\mathrm{DE}}\cdot W_{air\_\mathrm{NDE}} + k_{15\_\mathrm{DE}}\cdot \Delta P_{out\_\mathrm{DE}} \quad \text{Eq 4.12}$$

$$\Delta\dot{P}_{out\_\mathrm{NDE}}(t) = k_{11}\cdot M_{pf} + k_{12}\cdot M_c + k_{13\_\mathrm{NDE}}\cdot W_{air\_\mathrm{DE}} + k_{14\_\mathrm{NDE}}\cdot W_{air\_\mathrm{NDE}} + k_{15\_\mathrm{NDE}}\cdot \Delta P_{out\_\mathrm{NDE}} \quad \text{Eq 4.13}$$

As there are two outlets for primary air to carry the pulverized coal to the furnace, $W_{pf}(t)$ can be calculated from the differential pressure of both the drive end and the non-drive end, therefore the Eq 4.4 can be replaced by:

$$W_{pf}(t) = k_2\cdot\Delta P_{out\_\mathrm{DE}}\cdot M_{pf}(t) + k_2\cdot\Delta P_{out\_\mathrm{NDE}}\cdot M_{pf}(t) \quad \text{Eq 4.14}$$

4.4 IDENTIFICATION OF UNKNOWN MODEL PARAMETERS

The basic mill model has 23 parameters in which the coefficient between the feeder speed and coal feed flow rate k_{f1} and k_{f2}, the coal density ρ, the volume of the mill drum V_{mill} and the steel balls in the drum V_{ball} can be obtained from the industrial documents provided by the Eggborough power station. The values of the other 18 model parameters need further investigation. In this project these parameters are identified from the industrial data collected in the power station based on the genetic algorithm, which is an optimization approach to find

the global optimal. Three groups of steady state data are available from the industrial partner for the identification and the model validation, which is introduced in the table 4.2. The data set 1 introduced previously in Figure 4.10 is used for the identification.

Table 4-2: List of steady state mill data

Data sets	Description	Usage
Data set 1	13 August 2010 13:30:00 ~ 17:00:00	Identification
Data set 2	09 August 2010 08:00:00 ~ 13:00:00	Validation
Data set 3	18 August 2012 17:00:00 ~ 22:00:00	Validation

A fitness function, which evaluates how close the simulation result is to the on-site data, is introduced to the genetic algorithm to change the parameter identification problem into an optimal searching problem. Three main outputs of the mill model: T_{out}, $\Delta P_{out\_\mathrm{DE}}$ and $\Delta P_{out\_\mathrm{NDE}}$ are compared with the on-site measurement in the parameter identification. A number of fitness function has been studied and the sum of the mean squared error with a gain as weight value gives the algorithm a good convergence and leads to more accurate solutions in the parameter identification problems (Mohamed, 2012). The fitness function can be described as Eq 4.15 ~ Eq 4.18.

$$e_1 = \sum_{n=1}^{N} \left(\frac{(T_{out\_\mathrm{S}}(t) - \frac{T_{out\_\mathrm{DE}}(\mathrm{t}) + T_{out\_\mathrm{NDE}}(\mathrm{t})}{2})}{T_{out\_\mathrm{TOP}}} \right)^2 \qquad \text{Eq 4.15}$$

$$e_2 = \sum_{n=1}^{N} \left(\frac{\Delta P_{out\_\mathrm{DE\_S}}(t) - \Delta P_{out\_\mathrm{DE}}(\mathrm{t})}{\Delta P_{out\_\mathrm{DE\_TOP}}} \right)^2 \qquad \text{Eq 4.16}$$

$$e_3 = \sum_{n=1}^{N} \left(\frac{\Delta P_{out\_\mathrm{NDE\_S}}(t) - \Delta P_{out\_\mathrm{NDE}}(\mathrm{t})}{\Delta P_{out\_\mathrm{NDE\_TOP}}} \right)^2 \qquad \text{Eq 4.17}$$

$$ff = W_1 \cdot e_1^2 + W_2 \cdot e_2^2 + W_3 \cdot e_3^2 \qquad \text{Eq 4.18}$$

where T_{out_S}, $\Delta P_{out\_\mathrm{DE\_S}}$ and $\Delta P_{out\_\mathrm{NDE\_S}}$ are the simulation estimated outlet temperature and differential pressure of the classifier in D.E. and N.D.E; T_{out_DE}, T_{out_NDE}, $\Delta P_{out\_\mathrm{DE}}$ and $\Delta P_{out\_\mathrm{NDE}}$ are the data values from the on-site measurements; T_{out_TOP}, $\Delta P_{out\_\mathrm{DE\_TOP}}$ and $\Delta P_{out\_\mathrm{NDE\_TOP}}$ are the top range of the variables; W_1, W_2 and W_3 are weight coefficients that refers to the importance of the output in the fitness function; N is the number of sample points of the recorded measured data.

Measured model input data from data set 1 were sent to the coal mill model and the fitness function evaluated the fitness value by the simulation estimated result and the measured data. Then the genetic algorithm operators (selection, crossover and mutation) are employed to search the proper set of parameters of the model until the fitness value meets the requirements. After a number of iterations of the parameters can be identified as Table 4.3.

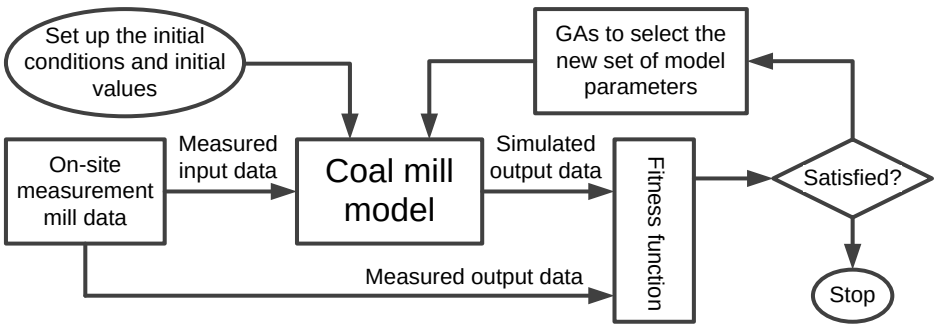

Figure 4-11: Schematic of the model's coefficients identification

Table 4-3: Identified mill parameters

Parameter	Value	Parameter	Value
k_1	0.00029	k_2	0.5615
k_3	0.0165	k_4	0.0172
k_5	27.684	k_6	31.646
k_7	0.0089	k_8	0.018
k_9	0.0009	k_{10}	-0.0692
k_{11}	3.21 e-006	k_{12}	4.9 e-006
k_{13_DE}	1.7510	k_{13_NDE}	1.8235
k_{14_DE}	0.5875	k_{14_NDE}	0.6987
k_{15_DE}	-0.0955	k_{15_NDE}	-0.1337

4.5 SIMULATION RESULTS AND MODEL VALIDATION

In this section the simulation results of the mill model are reported discussed. Data set 2 and Data set 3 in the table 4.2 are employed as the reference data for the model validation. The simulated result and the measured data are shown as Figures 4.12 and 4.13.

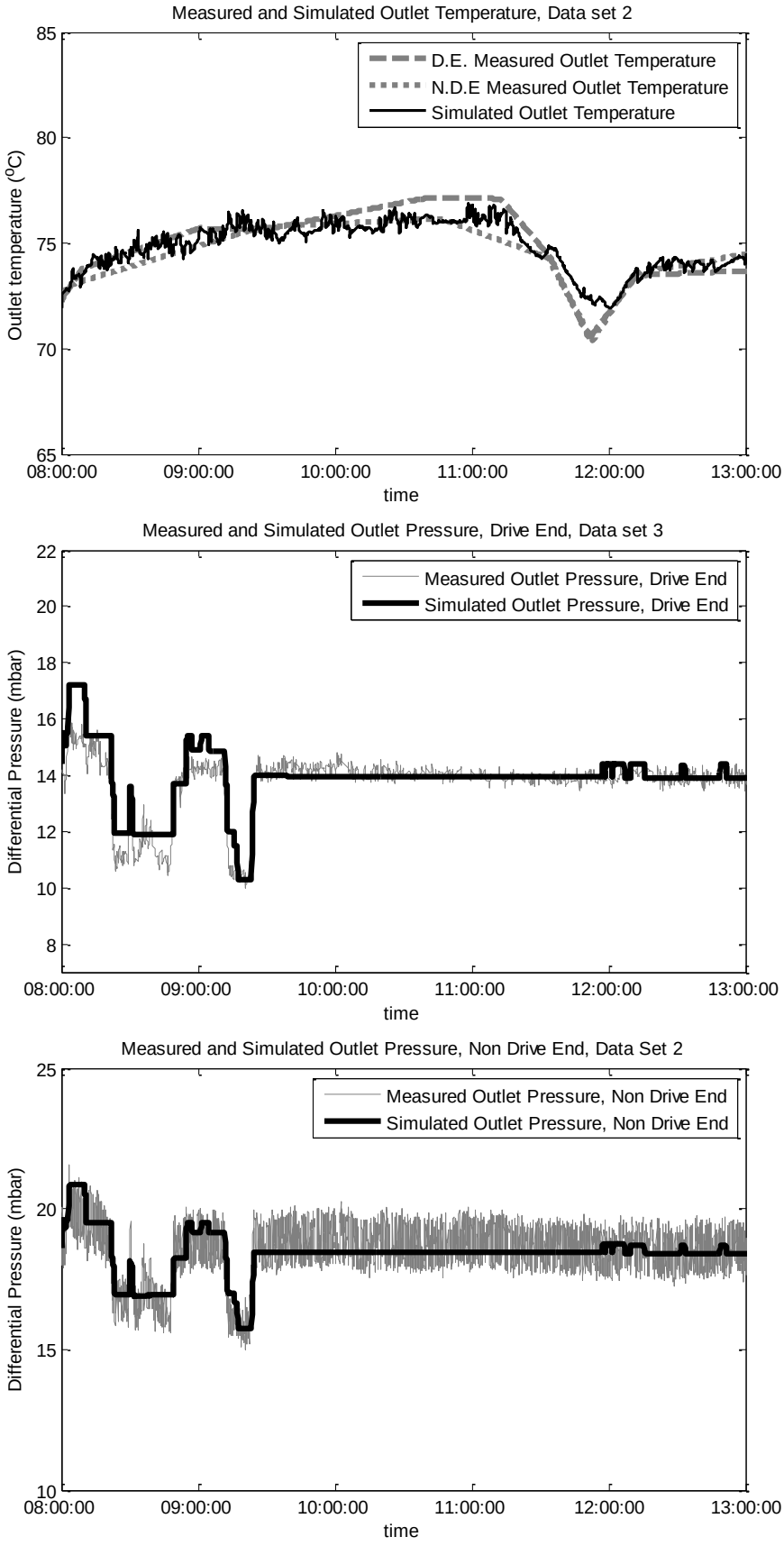

Figure 4-12: Model Validation on Data set 2

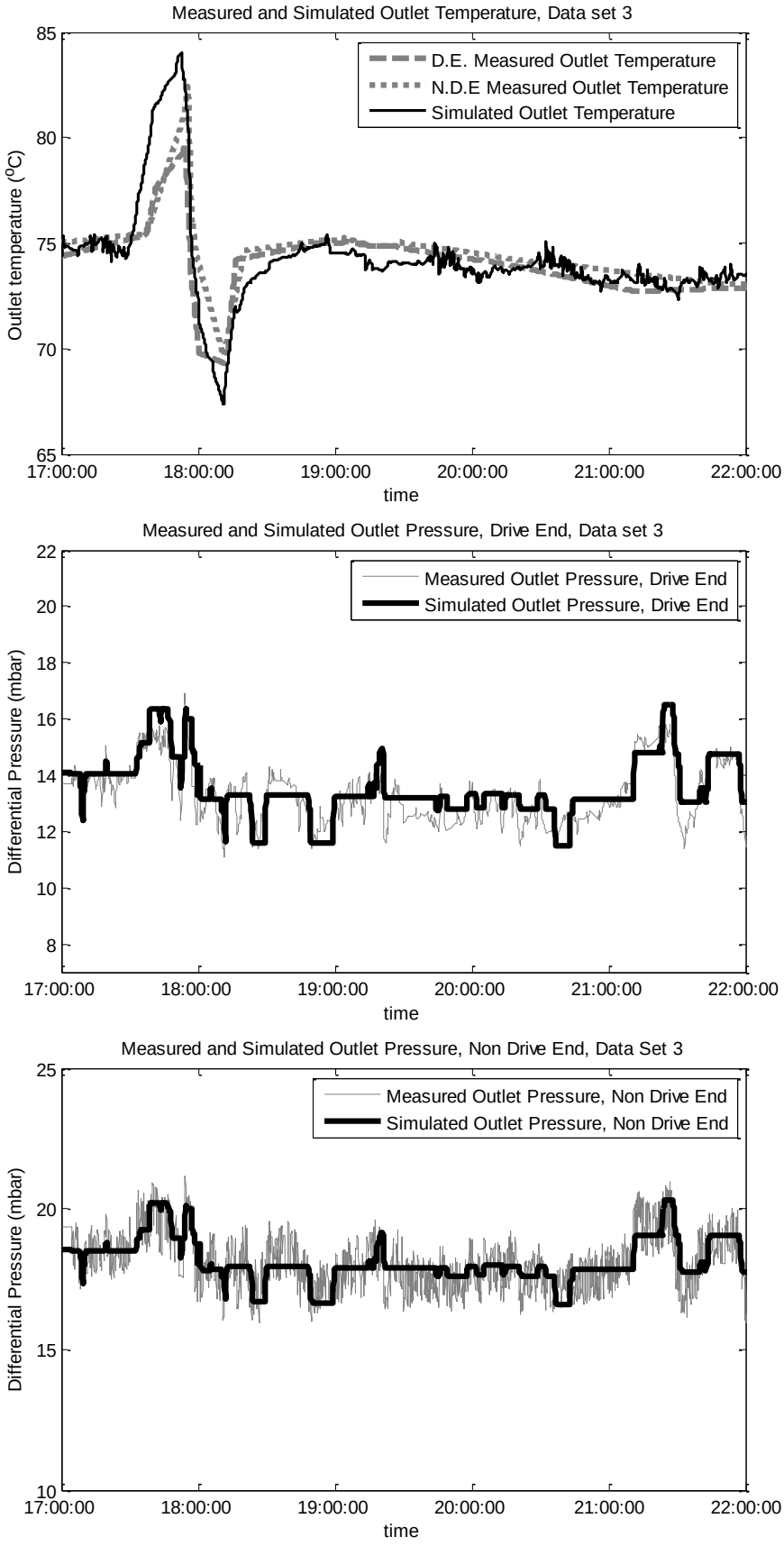

Figure 4-13: Model Validation on Data set 3

It is clear from the figures that the simulation results show a good agreement with the data measured in the power station. Numeric analysis is carried out based on the mean squared error and the mean squared relative errors of the outlet temperature and pressures are given as Table 4-4.

Table 4-4: Absolute errors of validation

Parameter	Data set 1	Data set 2
Outlet temperature e_1	0.96%	1.37%
Outlet pressure: Drive end e_2	0.75%	2.71%
Outlet pressure: Non-drive end e_3	1.27%	1.76%

It has been seen that the error is small enough compared with the measured data sets so the model is able to represent the main trend of the dynamic response of a tube ball mill with the parameters introduced in table 4-3.

4.6 ON-LINE IMPLEMENTATION OF THE COAL MILL MODEL

The application of the coal mill model refers to the calculation of the model intermediate variables that cannot be measured directly based on the data measured from the power plant. As a result, the on-line implementation which means the connection between the model and the measurements is the most important part of the model application. In order to represent the dynamics of the mill, the on-line implementation needs to be rapid enough and the access to the real-time data from the power plant is also a prerequisite. Three different approaches are studied to collect the data from the power plant.

4.6.1 On-line implementation based on direct measurements and microcontrollers

The direct measurements by the sensors located in different places of the mill is the simplest way of data collection. The mathematical model that can represent the mill is written into a microcontroller and the data from the direct measurements are sent to this chip after pre-processing as the model inputs. The structure of this method is shown as Figure 4.14.

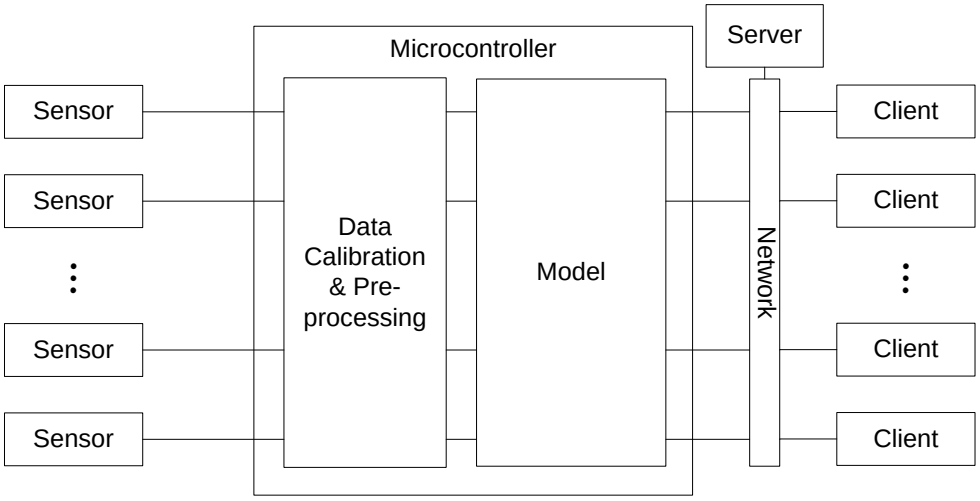

Figure 4-14: On-line implementation based on direct measurements and microcontrollers

Once the model results and intermediate variables are calculated, the estimated values of these variables results can be stored into the server and visited by the clients in the power plant through the network, like the other sensor measurements.

4.6.2 On-line implementation based on memory data sharing

The memory data sharing approach is introduced by Wei (2007) as a solution of the on-line implementation in his thesis. The idea is the data sharing between different computer programs via the computer memory. In most of the existing

power plants, the Plant Information (PI) System is used for the plant condition monitoring and the on-line data collection in real time. The data from the sensor is first broadcast to the network which enables PI system in the server and the clients can read these values for storage and monitoring. By adding a short data supplying program, a set of memory with a known base address is allocated to the PI system, which is therefore capable to map the on-site measurements into the corresponding memory buffer in real time at a fixed updating rate.

The mathematical model of the coal mill is implemented in another program. This program checks and reads the data from the shared memory buffer at the same frequency as the data supplying program. The data is directed to the model implemented in this program as inputs therefore the program can estimate the intermediate mill variables on-line. The structure of the shared memory approach can be summarized as Figure 4.15.

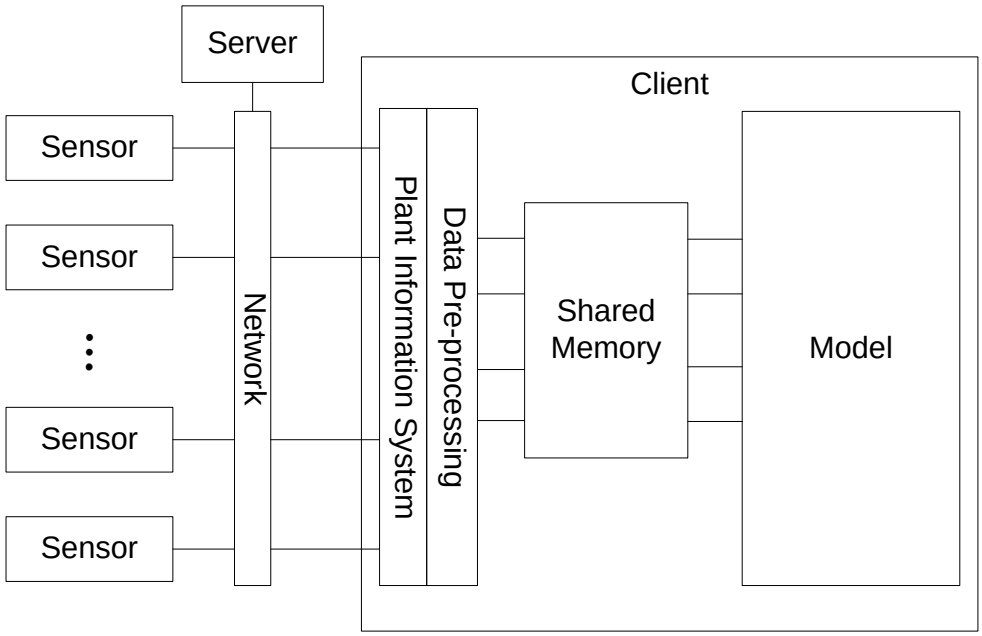

Figure 4-15: On-line implementation based on memory data sharing

4.6.3 ON-LINE IMPLEMENTATION BASED ON OPC NETWORK

Open Platform Communications (OPC) which was initially defined as the Object Linking and Embedding for Process Control is a standard that specifies the communication of real-time plant data between control devices from different manufacturers. This standard provides a connection between the Windows based software and process control hardware. As the OPC network is implemented in most of the power plants, it is possible for the model to bypass the plant information system and access the data directly from the server.

In the power plant, measured value from the sensor is regulated and reaches the OPC server where it is allocated to a unique tag, which is also called item ID, with some other defined information, including time stamp, quality, error state,

etc. The data can be accessed by clients in the network who knows the server name and the item ID.

In order to connect visit the data from the OPC server, the configuration work is supposed to be carried out. The first step is to define the data access client object that represents the address of the target server and establish the connection with the server. The group objects are defined and the required data are added to the group by providing their unique item ID. The data on the server has been accessed then and ready to read and write. The received data of the group is a structure array with all the information defined in the server side, in which the data value can be used as model inputs. The structure of the OPC based on-line implementation is given as Figure 4.16.

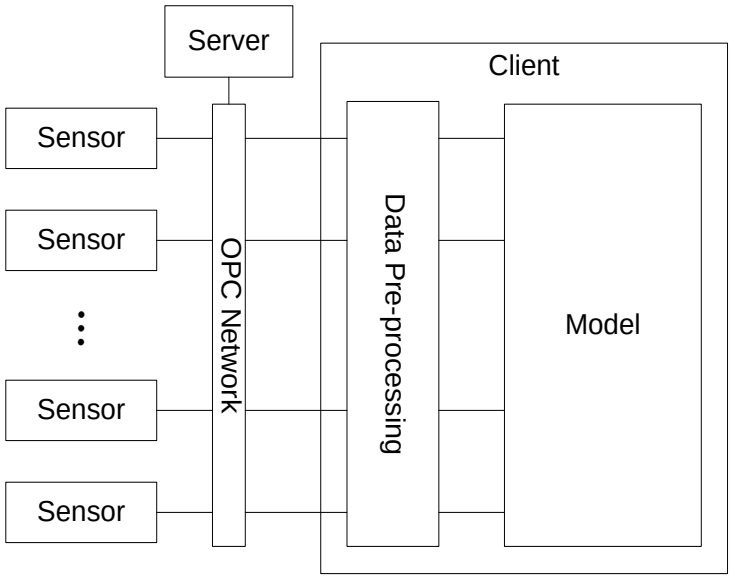

Figure 4-16: On-line implementation based on OPC network

4.6.4 COMPARISON OF DIFFERENT ON-LINE IMPLEMENTATION APPROACHES

As the microcontroller visits the sensors directly and the data comes from the direct measurements, one advantage of this approach is that the model is able to work without the network support therefore the required inputs can be always available unless the sensors are off. With the estimations send to the server, engineers can also access the intermediate variables on the clients from the plant information system. One problem of the direct measurement is that the sensor outputs are analogue data specific to the sensors other than the actual values therefore it normally cannot be used by the model directly without pre-processing. Another trouble is that the sensors are located all over the mill and it may need extra work to connect the right sensor from the bus to the microcontroller.

The characteristic of the memory sharing strategy is that the model visits the required data from the memory, which is shared from the plant information system directly. The PI system helps this approach to avoid the data problem in the direct measurements approach, but it causes a new problem. Figure 4.17 includes two parts of the data spreadsheets from the PI system, it can be easily find out that some of the data are strings instead of values, which is not readable for the model. There are two reasons of the invalid data: one is caused by the sensor or the data network failure, which is shown as 'Shutdown' and '#NULL!' in the figure; the other one is caused by the regulate algorithms in the PI system who replaces the over range and under range data by the strings 'Under Range' or 'Over Range' instead of the actual readings. Pre-processing algorithms can be

implemented to address the invalid data problem but this may result in some minor errors as the model inputs are not the value that the sensors measured.

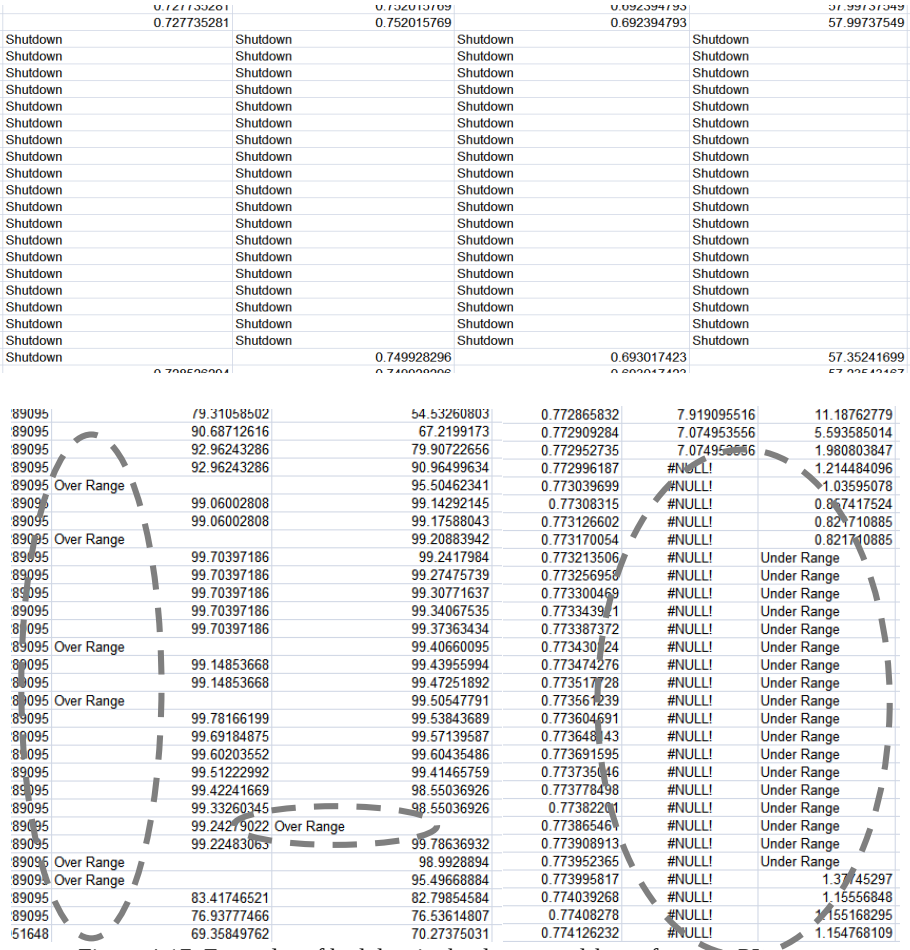

0.727735281	0.752015769	0.692394793	57.99737549
Shutdown	Shutdown	Shutdown	Shutdown
Shutdown	Shutdown	Shutdown	Shutdown
Shutdown	Shutdown	Shutdown	Shutdown
Shutdown	Shutdown	Shutdown	Shutdown
Shutdown	Shutdown	Shutdown	Shutdown
Shutdown	Shutdown	Shutdown	Shutdown
Shutdown	Shutdown	Shutdown	Shutdown
Shutdown	Shutdown	Shutdown	Shutdown
Shutdown	Shutdown	Shutdown	Shutdown
Shutdown	Shutdown	Shutdown	Shutdown
Shutdown	Shutdown	Shutdown	Shutdown
Shutdown	Shutdown	Shutdown	Shutdown
Shutdown	Shutdown	Shutdown	Shutdown
Shutdown	Shutdown	Shutdown	Shutdown
Shutdown	Shutdown	Shutdown	Shutdown
Shutdown	Shutdown	Shutdown	Shutdown
Shutdown	Shutdown	Shutdown	Shutdown
Shutdown	Shutdown	Shutdown	Shutdown
Shutdown	Shutdown	Shutdown	Shutdown
Shutdown	0.749928296	0.693017423	57.35241699

89095	79.31058502	54.53260803	0.772865832	7.919095516	11.18762779
89095	90.68712616	67.2199173	0.772909284	7.074953556	5.593585014
89095	92.96243286	79.90722656	0.772952735	7.074953556	1.980803847
89095	92.96243286	90.96499634	0.772996187	#NULL!	1.214484096
89095	Over Range	95.50462341	0.773039699	#NULL!	1.03595078
89095	99.06002808	99.14292145	0.77308315	#NULL!	0.857417524
89095	99.06002808	99.17588043	0.773126602	#NULL!	0.821710885
89095	Over Range	99.20883942	0.773170054	#NULL!	0.821710885
89095	99.70397186	99.2417984	0.773213506	#NULL!	Under Range
89095	99.70397186	99.27475739	0.773256958	#NULL!	Under Range
89095	99.70397186	99.30771637	0.773300469	#NULL!	Under Range
89095	99.70397186	99.34067535	0.773343921	#NULL!	Under Range
89095	99.70397186	99.37363434	0.773387372	#NULL!	Under Range
89095	Over Range	99.40660095	0.773430824	#NULL!	Under Range
89095	99.14853668	99.43955994	0.773474276	#NULL!	Under Range
89095	99.14853668	99.47251892	0.773517728	#NULL!	Under Range
89095	Over Range	99.50547791	0.773561239	#NULL!	Under Range
89095	99.78166199	99.53843689	0.773604691	#NULL!	Under Range
89095	99.69184875	99.57139587	0.773648143	#NULL!	Under Range
89095	99.60203552	99.60435486	0.773691595	#NULL!	Under Range
89095	99.51222992	99.41465759	0.773735046	#NULL!	Under Range
89095	99.42241669	98.55036926	0.773778498	#NULL!	Under Range
89095	99.33260345	98.55036926	0.77382201	#NULL!	Under Range
89095	99.24279022	Over Range	0.77386546	#NULL!	Under Range
89095	99.22483063	99.78636932	0.773908913	#NULL!	Under Range
89095	Over Range	98.9928894	0.773952365	#NULL!	Under Range
89095	Over Range	95.49668884	0.773995817	#NULL!	1.37745297
89095	83.41746521	82.79854584	0.774039268	#NULL!	1.15556848
89095	76.93777466	76.53614807	0.77408278	#NULL!	1.155168295
51648	69.35849762	70.27375031	0.774126232	#NULL!	1.154768109

Figure 4-17: Examples of bad data in the data spreadsheets from the PI system

The same as the memory data sharing, the on-line implementation based on OPC network also solved the data problem in the first approach. This method also have the same problem caused by the sensor or network failure, but as it bypasses the PI system the data received by the model can represent the sensor readings even it is not in the range that the PI system ruled. This feature could potentially increase the accuracy of the model. Additionally another benefit from this

implementation approach is that the OPC network allows the client to broadcast data back to the server when necessary if the corresponding item ID can be assigned in the server, therefore with this function the site engineers is possible to monitor the model estimated intermediate variables on any client in the network.

Previous analysis of different approach shows that the OPC network can be achieved by an individual software in one of the clients, without any further hardware knowledge. Therefore the on-line implementation of coal mill in this project will adopt this method.

The on-line implementation program that includes the mathematical model is developed under the Matlab simulation environment and the built-in OPC toolbox that provides the library of the OPC server data access in the Matlab can make the development much easier.

4.7 MODEL UPDATE STRATEGY AND APPLICATIONS

In additional to controlling the mill operation in a better way by providing the coal reserve and feed rate information to the power generation process control, the model accuracy can also benefit from the access of on-line real-time data. One particular situation is that the mill performance may be changed by various reasons, for example the refill of steel balls to the mill drum in a normal maintenance, the change of coal type or the biomass injection to the mill. Despite these changes of the operational condition, some other problems that are unpredictable may also affect the mill dynamics. These unexpected reasons are

supposed to be avoided and actions are supposed to take when necessary as these unexpected changes can cause potential incidents, in which the most typical case is the coal choking that blocks the coal to the furnace.

The change of the mill performance, no matter caused by normal maintenance or other unknown reasons, means that the model cannot represent the mill and the simulation result will drift away from the measured data. So the model should be updated when the simulation result shows a significant difference with the real-time measurement in the power plant. As the basic principle of the milling process remains, it is not necessary to change the mathematical equations in the model therefore the idea of the model update is actually to update its key parameters based on the measurements.

Monitoring the intermediate variables of the coal mill is supposed to be a continuous process and the unexpected problem takes place randomly. Therefore the update of model parameters must be capable to start automatically whenever necessary. For this purpose the on-line implementation program is composed of two main functions: the modelling and the parameter update. With the real-time input data collected from OPC network the modelling function estimates the mill outputs and the intermediate variables which are then broadcasted back to the OPC server. These variables can be displayed either on the program or in the Process Information system of the power plant control room. With another function in the program that accumulates the absolute error of the calculation in a defined period, which can be from minutes to hours, the periodic error in the past period can be obtained. When the result is smaller than the pre-set threshold,

which means that current model is accurate enough to represent the mill, the mill model will continue running without further actions. On the other side when the result exceeds the threshold, which means the mill performance has changed, all the input and output data from the past period will be saved and the re-identification will be carried out in parallel with the modelling based on these data. A set of new parameters can be generated after the direct search by the genetic algorithms, which is then shard to the model so the new model can represent the mill performance in time. The block diagram of the whole mill update system is shown as Figure 4.18.

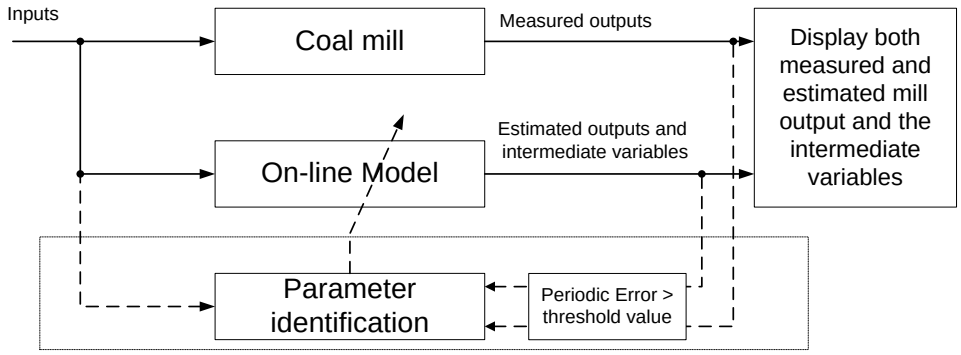

Figure 4-18: Block diagram of the mill model update system

Based on the on-line mill mathematical model, further applications and algorithms are developed to monitor the mill condition and to enhance the mill operation. As introduced in this chapter that the intermediate variables of the mill, including the mass flow rate of raw coal into the mill W_c, the mass of coal in mill M_c, the mass of pulverized coal in mill M_c, the mass flow rate of pulverized coal out of mill W_{pf} and the mill level can be estimated by the mathematical model. By broadcasting these intermediate variables to the OPC

server the software can be very helpful to the mill condition analysis and can improve the mill control and performance to control the mill level at an optimised range.

The on-line implementation with the automatically update of the signature parameters can also greatly strengthen the condition monitoring. From the further analysis of the mathematical model and the change of the re-identified model parameters, it has been observed that some particular parameters are much more sensitive to irregular performances. For example the model parameter k_1 can potentially reflect the change of fuel type fed into the mill; k_{10} refers to the heat accumulation in the mill; and k_{15_DE} and k_{15_NDE} is related to the mill choking problems. As the heat accumulation and the mill choking are abnormal events in the normal milling process that can potentially cause mill incidents, additional actions should be carried out as soon as a significant change of k_{10}, k_{15_DE} or k_{15_NDE} can be observed for safety reason. However further studies on these key parameters and the mill failure are not studied in this project as there is not enough data for the investigation.

4.8 SUMMARY

The coal mill plays an important role in the fuel preparation process which is highly relevant to the post combustion carbon capture due to the contents of flue gases. So it is essential to understand the coal milling process. The coal mill modelling is reported in the chapter. A mathematical model based on the

working principles of the coal mill has been developed which is used to provide extra information to enhance the dynamic control. The unknown parameters of the model are identified by adopting the evolutionary computation technique with the data obtained from a real power plant in the UK.

Model validation shows that the model is able to represent the coal mill in normal grinding operation conditions. Extra information of the mill can be obtained via the model prediction, for example the coal flow rate and the mill level, which can be provided to the mill operators to enhance the mill operation. This chapter also introduced different approaches for on-line implementation of the mill model at a power plant. Self-adaptive parameters has been introduced in this on-line implementation to update the model when there is a maintenance work, or when an unexpected problem takes place. Monitoring some of the key parameters can be helpful to predict potential incidents but further investigation is needed before any conclusions can be drawn.

Chapter 5.

MODEL DEVELOPMENT OF POST COMBUSTION CARBON CAPTURE

Different post combustion carbon capture technologies have been reviewed in Chapter 2. The process of the amine based chemical absorption has been studied in detail as it is currently the most established capture approach and is selected for study in this PhD project. In this chapter, further analysis of MEA based post combustion carbon capture is reported. The mathematical description of the capture system will be derived and the plant model including the carbon capture process is extended.

5.1 THE MATHEMATICAL MODELLING OF THE CHEMICAL ABSORPTION BASED ON AQUEOUS MEA SOLUTION

Carbon capture based on chemical absorption can be accomplished by a series of absorption/regeneration process to remove the carbon dioxide from the flue gas. In this project it refers to the amine based post combustion carbon capture, in which the flue gas is absorbed into the bulk phase of aqueous monoethanolamine solution. This technology has been commercialized and used in the natural gas industry for over 60 years and is regarded as the most mature technology (Yang *et al*., 2008, Bhown and Freeman, 2011).

The basic principle of absorption capture is that the carbon dioxide can react with the absorbent at the flue gas temperature (40 – 60 ˚C) while the rest of the flue gas (majorly nitrogen) cannot. The "tower" that the flue gas contacts the absorbent is called "Absorber". Most of the carbon dioxide is removed from the flue gas via the process therefore the CO_2 emission can be greatly reduced. The rich CO_2 solvent is then directed to a "regeneration unit", which is also called stripper, where the solvent is heated to reverse the reaction and to release CO_2 (Yang *et al*., 2008, Bhown and Freeman, 2011, Wang, 2011). The CO_2 released is captured, compressed and then ready for transportation. Usually the hot lean CO_2 solvent can be used to preheat the rich CO_2 solvent from absorber in a cross heat exchanger and then it is sent back to the storage tank of the lean MEA solution (Figure 5.1). In real power plants, the steam from the boiler-turbine steam-water system usually takes the role of heating source for the regeneration.

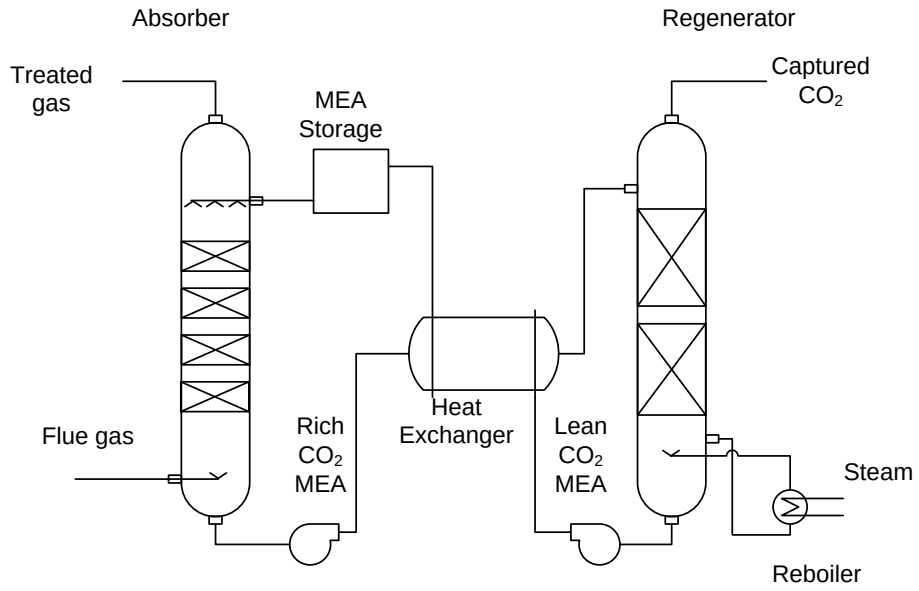

Figure 5-1: Post combustion carbon capture with aqueous amines

Based on the working principle, a typical amine based post combustion carbon capture system can be divided into four important sections: the absorber, the regenerator, the reboiler and the main heat exchanger. Each part is modelled separately and they are then connected together to represent the whole capture process. In most situations of this project, outlet temperature is assumed to be equal to the module temperature, which is considered as a constant in the same side of the same work media. To simplify the whole process, this modelling focuses more on the thermal dynamics of those four modules than the flow dynamics, which means that the simple control strategy is implemented to balance the mass flow.

Up to the time of completion of this thesis, there was not enough data of thermal measurements of the monoethanolamine available, especially the specific

enthalpy versus different temperatures and pressures. The only thermal property available is the heat capacity at normal temperature C_{MEA} , which is a given constant of $2.78\ \mathrm{J/(kg\cdot °C)}$ (Haynes, 2013) . Therefore this project will not take the effect of temperature and pressure to the heat capacity and the pressure effect to the specific enthalpy into consideration. The enthalpy calculation is therefore simplified as a product of the solution heat capacity and the temperature, which is described as $h = C_p \cdot T$.

The heat capacity of a mixture usually represents the average heat capacity of different substances in the mixture. In the situation of an amine solution loaded with loaded CO_2, it depends on different factors including the concentration of the amine solution and the CO_2 load which means a complicated calculation. However a group of experiments has been carried out to estimate the heat capacity of different types of amine under different concentration and different CO_2 loads. The experiments focus on the measurement of the temperature rise with a known mass of sample in response to a known electrical energy input via an immersed ohmic resistance (Weiland *et al*., 1997, Chen and Li, 2001, Chen *et al*., 2001). As the monoethanolamine is the only amine considered in this project, a look up table is built in this project based on the measurements of monoethanolamine only for the purpose of the heat capacity estimation.

Table 5-1: Heat Capacity ($J \cdot g^{-1} \cdot K^{-1}$) of CO_2-Loaded MEA Solutions at 25 °C (Weiland *et al.*, 1997)

Loading (mol/mol)	10 mass % MEA	20 mass % MEA	30 mass % MEA	40 mass % MEA
0.00	4.061	3.911	3.734	3.634
0.05	4.015			
0.10		3.823	3.656	3.508
0.20	3.917	3.766	3.570	3.343
0.30	3.915	3.670	3.457	3.238
0.40	3.891	3.648	3.418	3.163
0.50	3.857	3.597	3.359	3.109

The specific enthalpy calculation based on the measured heat capacity has a limitation that it cannot be used when there is a phase change in one or more substances in a mixture. Despite the difference of heat capacity for water and steam, the latent heat of vaporization should also be considered. Therefore the approach presented in this section is only employed in the analysis of absorber and the heat exchanger systems in which the temperature at steady state is lower than the saturation temperature of water.

For the regenerator and reboiler as they are working around the water saturation temperature at different pressures, the average specific enthalpy is calculated from the values for water, steam and monoethanolamine. The concentration of the solution and the vapour quality of water in the mixture should also be considered.

5.2 MATHEMATICAL DESCRIPTION OF THE ABSORBER

The absorber tower is the only module that has a direct contact with the flue gas. The role of the absorber is to remove CO_2 from the flue gas to the MEA solution.

Flue gas from the main duct is cooled down to approximately 35 ˚C after the disulphate process in the Flue-gas desulfurization (FGD) system of power station and then it is fed to the bottom of the absorber. At the same time, the lean MEA solution at about 40 ˚C is pumped up from the storage tank and fed into the absorber from the top part of the absorber. The MEA solution contact with the flue gas and the reaction of CO_2 with MEA takes place in the middle part of the absorber, which is specially designed to maximise the contact of the solution and the gases for a higher CO_2 removal rate. The CO_2 rich amine stream exits from the bottom of the absorber and is pumped to the next stage, while the other gases from the flue gas leaves from the top of the tower and is sent to the plant chimney. Solvent vapour and mist generated in the absorber is captured by a downstream water wash, and the water wash also has an influence on the liquid concentration in the absorber. The MEA flowing into the absorber is achieved by two inlet streams instead of one in this project by taking the consideration of further improvement.

Based on the design, the absorber tower can be treated as a liquid tank with gas/liquid reactions involved, which contains four inlet streams and two outlet streams. There are different important properties for each streams, including pressure, temperature, enthalpy, and the flow rate. For the gas streams, the CO_2 concentration is another important characteristic while the MEA concentration and CO_2 load are also important to the absorber. The full list of input/output of the absorber are given in Table 5.2 by following the definition rules in the simulators.

Table 5-2: Inputs and outputs of the absorber model

	Inlet streams				Outlet streams	
	Flue gas	MEA1	MEA2	Water wash	Flue gas	MEA
Pressure (MPa)	p_{GE}	p_{ME1}	p_{ME2}	p_{WE}	p_{GL}	p_{ML}
Temperature (°C)	T_{GE}	T_{ME1}	T_{ME2}	T_{WE}	T_{GL}	T_{ML}
Specific Enthalpy(kJ/kg)	h_{GE}	h_{ME1}	h_{ME2}	h_{WE}	h_{GL}	h_{ML}
Flow rate (kg/s)	w_{GE}	w_{ME1}	w_{ME2}	w_{WE}	w_{GL}	w_{ML}
Concentration (%)	ω_{GE}	ω_{ME1}	ω_{ME2}	-	ω_{GL}	ω_{ML}
CO_2 load(mol/mol)	-	L_{ME1}	L_{ME2}	-	-	L_{ML}
Heat capacity(kJ/(kg·°C))	c_G	c_{ME1}	c_{ME2}	-	c_G	c_{ML}

Due to lack of industrial data, it is assumed that the initial mass of MEA and water in the tower, which are represented by the variable ' m_M ' and ' m_W ' in the model. These values can be controlled by the input and output flow rate. The flow in rate of MEA and water can be calculated from the following equations.

$$w_{ME\_total} = \omega_{ME1} \cdot w_{ME1} + \omega_{ME2} \cdot w_{ME2} \qquad \text{Eq 5.1}$$

$$w_{WE\_total} = w_{ME1} \cdot (1 - \omega_{ME1}) + w_{ME2} \cdot (1 - \omega_{ME2}) + w_{WE} \qquad \text{Eq 5.2}$$

where w_{ME} is the mass flow rate of the solute (pure MEA) entering the absorber and w_{WE_total} is that of the solvent water. The average CO_2 load of the MEA flows in can be described as:

$$L_{ME} = \frac{L_{ME1} \cdot \omega_{ME1} \cdot w_{ME1} + L_{ME2} \cdot \omega_{ME2} \cdot w_{ME2}}{w_{ME}} \qquad \text{Eq 5.3}$$

The flow out rate of MEA w_{ML} and water w_{WL} can be calculated from the outlet flow out rate and the concentration:

$$w_{ML} = \omega_{ML} \cdot w_{MWL} \quad \text{Eq 5.4}$$

$$w_{WL} = w_{MWL} \cdot (1 - \omega_{ML}) \quad \text{Eq 5.5}$$

therefore the ' m_M ' and ' m_W ' can be calculated by:

$$\dot{m}_M = w_{ME} - w_{ML} \quad \text{Eq 5.6}$$

$$\dot{m}_W = w_{WE} - w_{WL} \quad \text{Eq 5.7}$$

The outlet concentration is supposed to equal to the concentration of the MEA in the absorber, therefore:

$$\omega_{ML} = m_M / (m_M + m_W) \quad \text{Eq 5.8}$$

From the amine chemistry study in Chapter 2, the maximum load capacity for the MEA is 0.5 mol CO_2 /mol amine. Therefore the maximum capture rate of the carbon dioxide w_{CA_max} by the amine flows in can be obtained by:

$$w_{CA\_max} = M_{CO_2} \cdot \left(\frac{(0.5 - L_{ME}) \cdot w_{ME}}{M_{MEA}} \right) \quad \text{Eq 5.9}$$

where M_{CO_2} is the molar mass of CO_2 which is 44.01 g/mol (Haynes, 2013) and M_{MEA} represents that of monoethanolamine, which is 61.08 g/mol respectively (Haynes, 2013). When the carbon dioxide flows in the absorber ($w_{CA} = w_{GE} \cdot \omega_{GE}$) is greater than this value, only this part of CO_2 can be captured in the absorber:

$$w_{CA} = \begin{cases} w_{CA\_MAX} & \left(w_{CE} > w_{CA\_MAX}\right) \\ w_{CE} & \left(w_{CE} \le w_{CA\_MAX}\right) \end{cases} \qquad \text{Eq 5.10}$$

In order to balance the internal pressure, it is assumed that the flue gas leaves the absorber from both the bottom (majorly CO_2 in the rich MEA solution) and the top (other contents in the flue gas including the rest of CO_2 not absorbed) is equal to the flue gas flow in rate. Therefore the flue gas flow rate can be calculated from the outlet and the percentage of CO_2 in this outlet flue gas: $w_{CL} = w_{CE} - w_{CA}$,

$w_{GL} = w_{GE} - w_{CA}$, $\omega_{GL} = \dfrac{w_{CL}}{w_{GL}}$.

Similarly, control activities are carried out to maintain the water level in the absorber. In order to simplify the calculation the flow rate of MEA solution is divided into two parts: MEA solution (MEA + water) and CO_2:

$$w_{MWL} = w_{WE} + w_{ME1} + w_{ME2} \qquad \text{Eq 5.11}$$

and the flow rate of the carbon dioxide can be obtained directly by the flow rate, concentration and mol load of CO_2 by

$$w_{CAL} = M_{CO_2} \cdot L_{ML} \cdot \left(\frac{\omega_{ML} \cdot w_{ML}}{M_{MEA}} \right) \qquad \text{Eq 5.12}$$

The thermal properties of the absorber outlet is based on the thermal balance that considers the model inputs and the thermal inertia. As introduced at the beginning of this chapter, the average specific enthalpies of the inlet streams can be described by their temperatures, the concentrations and the CO_2 loads.

The enthalpy calculation is focused, which can be summarized as the following equation:

$$\begin{aligned}&\frac{dh_{\mathrm{ML}}}{dt}\cdot\left(m_{\mathrm{M}}+m_{\mathrm{W}}\right)+h_{\mathrm{ML}}\cdot\left(w_{\mathrm{ME1}}+w_{\mathrm{ME2}}+w_{\mathrm{WE}}\right)\\&\quad=h_{\mathrm{GE}}\cdot w_{\mathrm{GE}}+h_{\mathrm{ME1}}\cdot w_{\mathrm{ME1}}+h_{\mathrm{ME2}}\cdot w_{\mathrm{ME2}}+h_{\mathrm{WE}}\cdot w_{\mathrm{WE}}+Q_{\mathrm{abs}}\cdot w_{\mathrm{CA}}\\&\quad-k_{\mathrm{a}}\cdot\left(T_{\mathrm{sat}}-T_{\mathrm{a}}\right)-c_{\mathrm{G}}\cdot w_{\mathrm{GE}}\cdot\left(T_{\mathrm{GL}}-T_{\mathrm{GE}}\right)\end{aligned}$$

Eq 5.13

T_{sat} in the equation is the temperature in the absorber, T_{a} is the atmosphere temperature, while the k_{a} represents the heat loss coefficient from the absorber to the atmosphere caused by this temperature difference, whose value is obtained from other thermal modules in the simulator condensed water system. The Q_{abs} stands for the reaction heat generated from the absorption process, but there is not an authoritative measurement of the reaction heat yet. In this thesis the value of 1720.75kJ/kg which is derived from 18.1 kcal·mol^{-1} ($18.1\mathrm{kcal}\cdot\mathrm{mol}^{-1}\times4.184\mathrm{kJ}\cdot\mathrm{kcal}^{-1}\times0.04401\mathrm{kg}\cdot\mathrm{mol}^{-1}$) following the measurements by Hikita *et al*. (1977). $c_{\mathrm{G}}\cdot w_{\mathrm{GE}}\cdot\left(T_{\mathrm{GL}}-T_{\mathrm{GE}}\right)$ represents the energy wasted to heat the flue gas in the absorber where c_{G} represents the average heat capacity of the flue gas, which is approximately equal to 1.04 based on literature (Nordlander, 2003, Persson *et al*., 2006).

With one step further calculation, the outlet temperature can be obtained by the division of the enthalpy and the heat capacity related to the specific solution

concentration and CO_2 load, which can be found out through the look-up table introduced at the beginning of this section.

5.3 MATHEMATICAL DESCRIPTION OF THE HEAT EXCHANGER

The main role of the heat exchanger in the post combustion Carbon Capture is to preheat the rich CO_2 amine solution before sending to the regenerator. There are several heat exchangers as heaters in the condensing water and feed water system in the power generation process, introducing the steam from the turbine system to heat the condensed water and the feed water. Latent heat of vaporization plays a very important role in the heating job as the steam condensed into water, releasing a big amount of heat. However instead of using steam from the turbine the heat exchanger here employs the lean CO_2 amine solution to preheat the rich CO_2 amine. There is not any phase change in the shell side therefore none of these heat exchanger models can be used directly in the post combustion carbon capture. Additionally, instead of steam and water, the working media in the heat exchanger in the system is amine solution, whose heat characteristics are also different.

The heat exchanger is a two-inlet-two-outlet system that can be divided into shell side (hot side) and tube side (cold side). For the post combustion capture, the hot shell side is lean CO_2 amine solution while the tube side is the rich CO_2 amine solution. The physical properties that refer to the heat exchanger thermal dynamics are the pressure, the temperature, the specific enthalpy, the flow rate,

the MEA concentration, the CO_2 load, and the heat capacity. The full list of inputs and outputs for the heat exchanger model are as shown in Table 5.3:

Table 5-3: Inputs and outputs of the absorber model

	Inlet streams		Outlet streams	
	Rich	Lean	Rich	Lean
Pressure (MPa)	p_{RE}	p_{LE}	p_{RL}	p_{LL}
Temperature (°C)	T_{RE}	T_{LE}	T_{RL}	T_{LL}
Specific Enthalpy(kJ/kg)	h_{RE}	h_{LE}	h_{RL}	h_{LL}
Flow rate (kg/s)	w_R	w_L	w_R	w_L
Concentration (%)	ω_R	ω_L	ω_R	ω_L
CO_2 load(mol/mol)	L_R	L_L	L_R	L_L
Heat capacity(kJ/(kg·°C))	c_R	c_L	c_R	c_L

From the industrial data, the rich CO_2 amine solution from the absorber is pumped into a pressure of approximately 6 - 7 bar (0.606 – 0.707 MPa) and lifted to the heat exchanger, where it is preheated for the CO_2 regeneration. As the regenerator is around 30 meters high and the rich amine is sent to the upper level, the author assumes that the pressure drop caused by the gravity is around 0.3 - 0.4 MPa. Therefore the Rich flow inlet pressure (p_{RE}) is given as 0.65 MPa and the outlet (p_{LE}) is 0.3 MPa. The lean flow in pressure is the outlet pressure from the reboiler, but there is not any data available from industry for the outlet pressure of lean flow. It is pre-assumed that the lean amine was sent to the storage tank directly and control actions are employed to ensure the target flow rate can be achieved when necessary.

There is not any mixing or chemical reactions in either the shell side or the tube side of the heat exchanger. Therefore the properties of the rich and lean amine,

including pressure, flow rate, amine concentration, the CO_2 load and the heat capacity, are constant at the entrance and exit of the heat exchanger. Based on this assumption the only variables are the temperature and enthalpy the heat exchanger model can be built based on the thermal balance.

From the structure of the heat exchanger, the pipe between the shell side and the tube side is the key media to achieve the heat transfer: hot lean amine heats the pipe by radiation and the heat is then transferred to the rich amine in the same way. The heat transfer rate, however, is directly related to the temperature difference of the radiation media on both side. Therefore another assumption of the heat exchanger model is made that the temperature of the shell side is evenly distributed, while that of the tube side is proportionally increased through the whole tube, as shown in Figure 5.2:

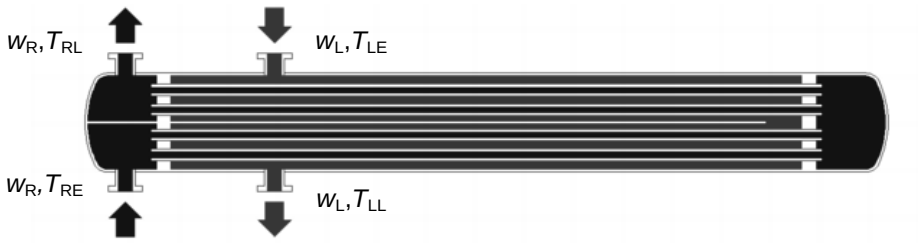

Figure 5-2: Post combustion capture with aqueous amines

Following the heat flux calculation and the definition of the Heat transfer coefficient, the heat transferred between the solid and liquid through the surface can be described as

$$\dot{Q} = S \cdot \Upsilon \cdot \Delta T \qquad \text{Eq 5.14}$$

where S is the contact surface, Υ is the heat transfer coefficient of the contacting media, and ΔT is the temperature difference between the two. In the situation of the model, the pipe temperature and the tube side temperature, is different at different position of the pipe, therefore this equation can be improved as $\dot{Q} = 2\pi r \cdot \Upsilon \cdot \int_0^l \Delta T \cdot dl$ where r is the radius of the pipe and l is the length of the pipe in the heat exchanger. As the temperature change of the rich amine not linear, the pipe temperature also has a non-linear change, therefore shell side heat transfer from the lean amine to the pipe $\dot{Q}_{\text{L-P}}$ is simplified as in this project as:

$$\dot{Q}_{\text{L-P}} = 2\pi r \cdot \Upsilon_{\text{L-P}} \cdot \int_0^l \Delta T_{\text{L-P}} \cdot dl = \kappa \cdot S_{\text{L-P}} \cdot \Upsilon_{\text{L-P}} \cdot \left(T_{\text{LE}} - T_{\text{p}}\right) \quad \text{Eq 5.15}$$

in which T_{p} represents the pipe temperature, κ stands for the effectiveness that describes the ratio of actual heat transfer divided by the maximum possible heat transfer.

In the heat exchanger, the lean amine flow into the shell side heats the lean amine already in the heat exchanger and also the pipe at the same time. Study of the lean amine shows the following equation that can represent the thermal dynamics based on the heat balance:

$$\frac{dh_{\text{LL}}}{dt} \cdot m_{\text{L}} + h_{\text{LL}} \cdot w_{\text{L}} = h_{\text{LE}} \cdot w_{\text{L}} - \dot{Q}_{\text{L-P}} - k_{\text{a}} \cdot \left(T_{\text{LL}} - T_{\text{a}}\right) \quad \text{Eq 5.16}$$

in which m_{L} is the mass of lean amine in the heat exchanger, which is constant as it was assumed that the outlet flow rate is controlled and equal to the inlet flow rate; and $k_{\mathrm{a}} \cdot \left(T_{\mathrm{LL}} - T_{\mathrm{a}}\right)$ represents the heat loss caused by the temperature difference with the atmosphere in which T_{a} is the atmosphere temperature and k_{a} is a coefficient of the heat transfer.

Similar to the thermal calculation in the shell side, the heat transfer in the tube side $\dot{Q}_{\mathrm{P\text{-}R}}$ and the outlet enthalpy of the tube side h_{RL} is described as:

$$\dot{Q}_{\mathrm{P\text{-}R}} = 2\pi r \cdot \Upsilon_{\mathrm{P\text{-}R}} \cdot \int_0^l \Delta T_{\mathrm{P\text{-}R}} \cdot dl = \kappa \cdot S_{\mathrm{P\text{-}R}} \cdot \Upsilon_{\mathrm{P\text{-}R}} \cdot \left(T_{\mathrm{P}} - T_{\mathrm{RE}}\right) \quad \text{Eq 5.17}$$

$$\frac{dh_{\mathrm{RL}}}{dt} \cdot m_{\mathrm{R}} + h_{\mathrm{R}} \cdot w_{\mathrm{R}} = h_{\mathrm{RE}} \cdot w_{\mathrm{R}} - \dot{Q}_{\mathrm{P\text{-}R}} \quad \text{Eq 5.18}$$

The enthalpy of the pipe can be described calculated from the heat transferred from the lean and to the rich amine, the mass of pipe m_{pipe} and the heat capacity of the metal c_{pipe}:

$$\dot{T}_{\mathrm{S}} = \frac{\dot{Q}_{\mathrm{P\text{-}R}} - \dot{Q}_{\mathrm{P\text{-}R}}}{m_{\mathrm{pipe}} \cdot c_{\mathrm{pipe}}} \quad \text{Eq 5.19}$$

From the specific enthalpy of the tube side and the shell side, the outlet temperature of the rich and lean amine flows can be calculated by the division of the specific enthalpy and the heat capacity:

$$T_{\mathrm{RL}} = \frac{h_{\mathrm{RL}}}{c_{\mathrm{R}}} \quad \text{Eq 5.20}$$

$$T_{\mathrm{LL}} = \frac{h_{\mathrm{LL}}}{c_{\mathrm{L}}} \qquad \text{Eq 5.21}$$

5.4 MATHEMATICAL DESCRIPTION OF THE REGENERATOR

The rich amine from the preheated in the heat exchanger is then introduced to the upper level of the next module, the regenerator. Opposite to the absorber, the regenerator is used to release the carbon dioxide that was absorbed in the amine under a relatively high temperature to achieve the separation of CO_2. The hot steam, which is one of the output from the reboiler, is fed into the regenerator from the bottom part to heat the whole regenerator. The regenerator has a similar design as the absorber so that the steam can have more sufficient contact with the rich amine. The steam temperature was first de-superheated by heating the amine to the saturation temperature and some of the steam then was condensed to water for further heating until the system was balanced. The condensed water is mixed with the amine solution therefore the concentration of solution changes in the regenerator. The amine solution also releases the CO_2 absorbed when temperature increases therefore the CO_2 load is reduced from rich to lean and the solution flows to the reboiler from the lower part of the tower. The rest of the steam that is not condensed into water is mixed with the regenerated CO_2 and the air left in the regenerator. These constituents of the gases left the regenerator together when the regenerator pressure was high. These outlet gases are introduced to another condensing unit to remove the steam from the CO_2 to ensure the purity of CO_2. The condensed water from the condensing unit refluxes

back to the regenerator and joins the make-up water as another inlet of the regenerator.

The regenerator is also treated as a tank with the inlet and outlet as described before. Table 5.4 shows the variables that are involved in the regenerator model in both inlet and outlet streams. It can be found that, similar to the absorber model, the important characteristics related to the amine solution are the pressure, the temperature, the flow rate, the concentration, the CO_2 load, the heat capacity and the specific enthalpy. For the steam, make-up water and the regenerated CO_2, the related properties are the pressure, the temperature, the flow rate and the specific enthalpy. The concentration of CO_2 in the outlet gases can also be calculated.

Table 5-4: Inputs and outputs of the regenerator model

	Inlet streams				Outlet streams	
	MEA1	MEA2	Steam	Water wash	Gases	MEA
Pressure (MPa)	p_{ME1}	p_{ME2}	p_{SE}	p_{WE}	p_{GL}	p_{ML}
Temperature (°C)	T_{ME1}	T_{ME2}	T_{SE}	T_{WE}	T_{GL}	T_{ML}
Specific Enthalpy(kJ/kg)	h_{ME1}	h_{ME2}	h_{SE}	h_{WE}	h_{GL}	h_{ML}
Flow rate (kg/s)	w_{ME1}	w_{ME2}	w_{SE}	w_{WE}	w_{GL}	w_{ML}
Concentration (%)	ω_{ME1}	ω_{ME2}	-	-	ω_{GL}	ω_{ML}
CO_2 load(mol/mol)	L_{ME1}	L_{ME2}	-	-	-	L_{ML}
Heat capacity(kJ/(kg·°C))	c_{ME1}	c_{ME2}	-	-	-	c_{ML}

The regenerator has four inputs from which the liquids and gases can flow in. The equivalent flow in rate of the amine w_{ME_total} and water w_{WE_total} can be calculated by the following equations:

$$w_{\mathrm{ME\_total}} = \omega_{\mathrm{ME1}} \cdot w_{\mathrm{ME1}} + \omega_{\mathrm{ME2}} \cdot w_{\mathrm{ME2}} \qquad \text{Eq 5.22}$$

$$w_{\mathrm{WE\_total}} = w_{\mathrm{SE}} + w_{\mathrm{WE}} + \left(1-\omega_{\mathrm{ME1}}\right) \cdot w_{\mathrm{ME1}} + \left(1-\omega_{\mathrm{ME2}}\right) \cdot w_{\mathrm{ME2}} \qquad \text{Eq 5.23}$$

where $w_{\mathrm{ML\_total}}$ and $w_{\mathrm{WL\_total}}$ are the equivalent amine and water flow rate into the regenerator. As the outlet of lean amine at the bottom of this regenerator is the only way of the liquid water and MEA to flow out, the outlet water flow rate and outlet amine flow rate can be calculated by:

$$w_{\mathrm{ML\_total}} = \omega_{\mathrm{ML}} \cdot w_{\mathrm{ML}} \qquad \text{Eq 5.24}$$

$$w_{\mathrm{WL\_total}} = \left(1-\omega_{\mathrm{ML}}\right) \cdot w_{\mathrm{ML}} \qquad \text{Eq 5.25}$$

where $w_{\mathrm{ML\_total}}$ and $w_{\mathrm{WL\_total}}$ are the equivalent amine and water flow rate out of the regenerator. The mass balance of the steam and water can be then described as:

$$\dot{m}_{\mathrm{WS}} = w_{\mathrm{WE\_total}} - w_{\mathrm{WL\_total}} - w_{\mathrm{SL}} \qquad \text{Eq 5.26}$$

$$\dot{m}_{\mathrm{M}} = w_{\mathrm{ME\_total}} - w_{\mathrm{ML\_total}} \qquad \text{Eq 5.27}$$

in which M_{WS} represents the mass of water and steam; M_{M} is the mass of MEA in the regenerator and w_{SL} is the steam that flows out from the top of this tower. The mass fraction of the MEA versus the steam-water mixture is defined as:

$$\omega_{\mathrm{M}} = \frac{m_{\mathrm{M}}}{m_{\mathrm{M}} + m_{\mathrm{WS}}} \qquad \text{Eq 5.28}$$

This mass fraction of amine versus both steam and water ω_{M} is introduced to the system in the regenerator model to help the analysis of the thermodynamics. This concentration plays a very important role in the calculation between the specific enthalpy in the regenerator with the other thermal properties. The H_2O has two possible phases in the regenerator, which can be changed from one to the other based on temperature and heat balance, and the mass of water and steam is defined as m_{S} and m_{W}. The vapour quality of the steam/water is also an important parameter in the model to estimate the contents in the regenerator, described as X_{WS} in the model. Therefore:

$$m_{\mathrm{S}} = X_{\mathrm{WS}} \cdot m_{\mathrm{WS}} \qquad \text{Eq 5.29}$$

$$m_{\mathrm{W}} = \left(1 - X_{\mathrm{WS}}\right) \cdot m_{\mathrm{WS}} \qquad \text{Eq 5.30}$$

The average specific enthalpy of the amine/water/steam in the regenerator can be obtained by:

$$\begin{aligned} &\frac{dh_{\mathrm{MWS}}}{dt} \cdot m_{\mathrm{MWS}} + h_{\mathrm{MWS}} \cdot \left(w_{\mathrm{ME1}} + w_{\mathrm{ME2}} + w_{\mathrm{SE}} + w_{\mathrm{WE}}\right) \\ &\quad = h_{\mathrm{ME1}} \cdot w_{\mathrm{ME1}} + h_{\mathrm{ME2}} \cdot w_{\mathrm{ME2}} + h_{\mathrm{WE}} \cdot w_{\mathrm{WE}} + h_{\mathrm{SE}} \cdot w_{\mathrm{SE}} \\ &\qquad - k_{\mathrm{a}} \cdot \left(T_{\mathrm{MWS}} - T_{\mathrm{a}}\right) - Q_{\mathrm{reg}} \cdot w_{\mathrm{CR}} \end{aligned}$$

Eq 5.31

in which $k_a \cdot (T_{MWS} - T_a)$ is the heat transfer with the atmosphere by the temperature difference of the regenerator T_{MWS} and the atmosphere T_a where k_a is the coefficient of the heat transfer. $Q_{reg} \cdot w_{CR}$ represents the reaction heat necessary for the CO_2 regeneration with the reaction speed of w_{CR}, which is related to the outlet amine CO_2 load, but there is not any useful information of how the load capacity of the lean amine can be determined by the regenerator properties, therefore a constant output is employed which value is chosen by the load from the storage tank to the absorber. The mathematical description of the CO_2 regeneration rate is similarly as that of the CO_2 absorption rate in the absorber:

$$w_{CR} = M_{CO_2} \cdot \left(\frac{(L_{ML} - L_{ME}) \cdot w_{ML\_total}}{M_{MEA}} \right) \qquad \text{Eq 5.32}$$

The same as the absorption equation, the M_{CO_2} is equal to 44.01 g/mol to represent the molar mass of CO_2 and that of the monoethanolamine M_{MEA} is 61.08 g/mol. The variables L_{ML} and L_{ME} are the CO_2 load of the MEA flows into and out of the regenerator.

The regenerator works at around 120°C, therefore this temperature of the regenerator is supposed to be maintained at this temperature. But liquid water can never reach this temperature in the standard pressure as it is vaporized into steam at the saturated temperature. In the post combustion capture the pressure in the regenerator is controlled to increase the water temperature, and in this

project the set pressure of 0.2MPa is proposed, at which the saturated temperature of water is 120.212°C. As works at the saturated temperature, both water and steam exist in the steady state. Water and steam are the same substance in different state caused by the temperature or pressure, but they have different heat capacity and enthalpy change rate vs the temperature at the same pressure. Monoethanolamine, on the other side, has a much higher saturation temperature which means there is only liquid phase amine. Additionally the energy required by the phase change is also an important issue to the modelling work.

As the steady state of the regenerator covers both gaseous steam and liquid water, the calculation of specific enthalpy based on the heat capacity is no longer available in the modelling development. A new approach is designed based on the steam water enthalpy look-up tables. In this approach the first job is to calculate the phase of the water in the regenerator: liquid water, steam or the mixture of the two. As amine has a higher saturated temperature, there is only liquid phase amine in the regenerator, therefore the specific enthalpy calculation of amine can also follow the rule with the heat capacity and the temperature as $h = C_p \cdot T$. Based on this assumption, the average specific enthalpy for the mixture of MEA with saturated water h_{MWsat} or saturated steam h_{MSsat}, which is treated at the boundaries of the water-steam mixture system, can be calculated by:

$$h_{\mathrm{MWsat}} = \left(h_{\mathrm{Wsat}} \cdot \left(1-\omega_{\mathrm{ML}}\right) + C_{\mathrm{MEA}} \cdot T_{\mathrm{MWS}} \cdot \omega_{\mathrm{M}}\right) \qquad \text{Eq 5.33}$$

$$h_{\mathrm{MSsat}} = \left(h_{\mathrm{Ssat}} \cdot (1 - \omega_{\mathrm{ML}}) + C_{\mathrm{MEA}} \cdot T_{\mathrm{MWS}} \cdot \omega_{\mathrm{M}} \right) \qquad \text{Eq 5.34}$$

in which T_{MWS} is the regenerator temperature; h_{Wsat} and h_{Ssat} are the specific enthalpy of water and steam, and C_{MEA} represents the heat capacity of pure monoethanolamine, which is $2.78\ \mathrm{J/(kg \cdot °C)}$ based on chemical database (Haynes, 2013). Comparing the h_{MWS} with this two boundary specific enthalpy the phase of water in the regenerator can be obtained: if the h_{MWS} calculated is greater than the h_{Ssat}, all the H_2O in the regenerator is evaporated into superheated steam; if the h_{MWS} is lower than h_{Wsat} there is not steam in the regenerator; a h_{MWS} value between means both steam and water exists in the regenerator, which is the easiest way to control the regenerator temperature as the regenerator works at the saturation temperature of water.

When the H_2O in the regenerator is in its liquid phase, there is not any steam in the regenerator, the vapour quality of the fluid X_{ML} is 0. Replacing the specific enthalpy of the amine by $c_{\mathrm{MEA}} \cdot T_{\mathrm{MWS}}$, the definition of the average specific enthalpy can be transformed into:

$$h_{\mathrm{MWS}} \cdot \left(m_{\mathrm{M}} + m_{\mathrm{W}} \right) = c_{\mathrm{MEA}} \cdot T_{\mathrm{MWS}} \cdot m_{\mathrm{M}} + h_{\mathrm{W}} \cdot m_{\mathrm{W}} \qquad \text{Eq 5.35}$$

An assumption value σ_{W0} is introduced to simplify the relationship between the water specific enthalpy and the temperature, defined as $h_{\mathrm{W}} = \sigma_{\mathrm{W0}} \cdot T_{\mathrm{MWS}}$. Therefore the regenerator temperature can be calculated by

$$T_{\mathrm{MWS}} = \frac{h_{\mathrm{MWS}} \cdot \left(m_{\mathrm{M}} + m_{\mathrm{W}}\right)}{c_{\mathrm{MEA}} \cdot m_{\mathrm{M}} + \sigma_{\mathrm{W}} \cdot m_{\mathrm{W}}} = \frac{h_{\mathrm{MWS}}}{c_{\mathrm{MEA}} \cdot \omega_{\mathrm{ML}} + \sigma_{\mathrm{W}} \cdot \left(1 - \omega_{\mathrm{ML}}\right)}$$

Eq 5.36

For most of the steady state condition the regenerator works at the saturation temperature and the value of h_{MWS} is between the h_{MWsat} and the h_{SWsat}, which means both steam and water are existing in the regenerator. The regenerator temperature can be obtained from the saturation temperature $T_{\mathrm{MWS}} = T_{\mathrm{sat}}$ without any further calculations. The main fluid is mainly composed of three parts: liquid Monoethanolamine, saturated water and saturated steam and as a result the specific enthalpy balance can be established:

$$\begin{aligned} & h_{\mathrm{MWS}} \cdot \left(m_{\mathrm{M}} + m_{\mathrm{W}} + m_{\mathrm{S}}\right) \\ & \quad = c_{\mathrm{MEA}} \cdot T_{\mathrm{sat}} \cdot m_{\mathrm{M}} + h_{\mathrm{Wsat}} \cdot m_{\mathrm{W}} + h_{\mathrm{Ssat}} \cdot m_{\mathrm{S}} \\ & \quad = c_{\mathrm{MEA}} \cdot T_{\mathrm{sat}} \cdot m_{\mathrm{M}} + h_{\mathrm{Wsat}} \cdot X_{\mathrm{ML}} \cdot m_{\mathrm{WS}} + h_{\mathrm{Ssat}} \cdot \left(1 - X_{\mathrm{ML}}\right) \cdot m_{\mathrm{WS}} \end{aligned}$$

Eq 5.37

X_{ML} in this equation represents the vapour quality of the $\mathrm{H_2O}$; h_{Wsat} and h_{Ssat} are the specific enthalpy of the saturated water and saturated steam. Therefore the vapour quality X_{ML} can be deducted by these variables and the ω_{ML} defined in Eq 5.28:

$$X_{\mathrm{ML}} = \frac{\left(h_{\mathrm{MWS}} - c_{\mathrm{MEA}} \cdot T_{\mathrm{sat}}\right) \cdot \omega_{\mathrm{M}} / (1 - \omega_{\mathrm{M}}) + \left(h_{\mathrm{MWS}} - h_{\mathrm{Wsat}}\right)}{h_{\mathrm{Ssat}} - h_{\mathrm{Wsat}}}$$

Eq 5.38

Therefore the mass of steam and water in the regenerator can be calculated by the following equations:

$$m_{\mathrm{S}} = X_{\mathrm{ML}} \cdot m_{\mathrm{WS}} \qquad \text{Eq 5.39}$$

$$m_{\mathrm{M}} = \left(1 - X_{\mathrm{ML}}\right) \cdot m_{\mathrm{WS}} \qquad \text{Eq 5.40}$$

As the steam leaves the regenerator from the top, the actual concentration and specific enthalpy of the amine solution out of the tower to the reboiler are:

$$\omega_{\mathrm{ML}} = \frac{m_{\mathrm{M}}}{m_{\mathrm{M}} + m_{\mathrm{W}}} \qquad \text{Eq 5.41}$$

$$h_{\mathrm{MWS}} = \frac{h_{\mathrm{MWS}} \cdot \left(m_{\mathrm{M}} + m_{\mathrm{WS}}\right) - h_{\mathrm{Ssat}} \cdot m_{\mathrm{S}}}{m_{\mathrm{M}} + m_{\mathrm{W}}} \qquad \text{Eq 5.42}$$

The last situation when there is no liquid water in the regenerator therefore the specific enthalpy equation in the regenerator is:

$$h_{\mathrm{MWS}} \cdot \left(M_{\mathrm{M}} + M_{\mathrm{S}}\right) = c_{\mathrm{MEA}} \cdot T_{\mathrm{MWS}} \cdot M_{\mathrm{M}} + h_{\mathrm{S}} \cdot M_{\mathrm{S}} \qquad \text{Eq 5.43}$$

As the specific enthalpy of steam versus temperature is also nearly linear but with a different slope with that of water at the same pressure, the project uses another equation to describe the specific enthalpy of the steam h_{S} as:

$$h_{\mathrm{S}} = h_{\mathrm{Ssat}} + \sigma_{\mathrm{S}} \cdot \left(T_{\mathrm{MWS}} - T_{\mathrm{Ssat}}\right) \qquad \text{Eq 5.44}$$

where h_{Ssat} is the saturated specific enthalpy, T_{Ssat} is the saturated temperature of the steam under the regenerator pressure; σ_{S} represents the change of the

specific enthalpy defined as $\sigma_S = \frac{h_S - h_{Ssat}}{T_{MWS} - T_{Ssat}}$ from the previous step. Eq 5.44 can be transformed into:

$$h_{MWS} \cdot (m_M + m_S) = c_{MEA} \cdot T_{MWS} \cdot m_M + (h_{Ssat} + \sigma_W \cdot (T_{MWS} - T_{Ssat})) \cdot m_S$$

Eq 5.45

Therefore the T_{MWS} can be obtained by:

$$T_{MWS} = \frac{h_{MWS} \cdot (m_M + m_S) - h_{Ssat} \cdot m_S + \sigma_S \cdot T_{Ssat} \cdot m_S}{c_{MEA} \cdot m_M + \sigma_S \cdot m_S} = \frac{h_{MWS} - (h_{Ssat} - \sigma_S \cdot T_{Ssat}) \cdot (1 - \omega_M)}{c_{MEA} \cdot \omega_M + \sigma_S \cdot (1 - \omega_M)}$$

Eq 5.46

This calculation only theoretically exists because vaporizing all the water solvent should be avoided during the post combustion carbon capture. When there is no liquid solvent is fed into the reboiler, the high concentration monoethanolamine can be harmful to the regenerator and reboiler as a corrosive chemical. Additionally the outlet temperature of lean amine to the heat exchanger could be extremely high in this situation because there is not any phase change in the heat transfer process. Emergency operations like reducing the reboiler duty or introducing cooling water should be carried out when the vapour quality of regenerator raises to a critical percentage to avoid such situation.

The pressure of the regenerator is another very important factor which can influence the saturation temperature. The calculation of regenerator pressure is

based on the amount of all different gases inside, including steam, carbon dioxide, and some air. With the assumption that the flow rate of different gases is proportionally to their mass fractions, proportionally, the flow rate of each gases out of the regenerator can be obtained by:

$$w_{\mathrm{CL}} = w_{\mathrm{GL}} \cdot \frac{m_{\mathrm{C}}}{m_{\mathrm{C}} + m_{\mathrm{A}} + m_{\mathrm{S}}} \qquad \text{Eq 5.47}$$

$$w_{\mathrm{AL}} = w_{\mathrm{GL}} \cdot \frac{m_{\mathrm{A}}}{m_{\mathrm{C}} + m_{\mathrm{A}} + m_{\mathrm{S}}} \qquad \text{Eq 5.48}$$

$$w_{\mathrm{SL}} = w_{\mathrm{GL}} \cdot \frac{m_{\mathrm{S}}}{m_{\mathrm{C}} + m_{\mathrm{A}} + m_{\mathrm{S}}} \qquad \text{Eq 5.49}$$

Based on the ideal gas law $pV = nRT_{\mathrm{SI}}$, therefore $p = nT_{\mathrm{SI}} \cdot \frac{R}{V}$ in which $\frac{R}{V}$ is constant in the regenerator. Therefore $p / p_0 = nT_{\mathrm{SI}} \cdot \frac{R}{V} / \left(n_0 T_{\mathrm{SI0}} \cdot \frac{R}{V} \right)$ and the pressure can be calculated by:

$$p = \frac{n_{\mathrm{all}} \cdot \left(T_{\mathrm{MWS}} + 273.15 \right)}{n_0 \cdot \left(T_0 + 273.15 \right)} \cdot p_0 \qquad \text{Eq 5.50}$$

in which p_0 , T_0 and n_0 are constants representing the pressure, the temperature and the amount of gases in mol for the volume of regenerator in the standard state; n_{all} is the amount of gases in the tower in mol, which can be obtained by the masses of these gases:

$$n_{\mathrm{C}} = 1000 \cdot \frac{m_{\mathrm{C}}}{M_{\mathrm{C}}} \qquad \text{Eq 5.51}$$

$$n_{\mathrm{A}} = 1000 \cdot \frac{m_{\mathrm{A}}}{M_{\mathrm{A}}} \qquad \text{Eq 5.52}$$

$$n_{\mathrm{S}} = 1000 \cdot \frac{m_{\mathrm{S}}}{M_{\mathrm{S}}} \qquad \text{Eq 5.53}$$

and

$$n_{\mathrm{all}} = n_{\mathrm{C}} + n_{\mathrm{A}} + n_{\mathrm{S}} \qquad \text{Eq 5.54}$$

where M_{C}, M_{A} and M_{S} are the molar mass of the CO_2, air and steam. Defining $k_{\mathrm{pTn}} = \frac{p_0}{n_0 \cdot (T_0 + 273.15)}$ as a constant the pressure in the regenerator can be calculated by

$$p = n_{\mathrm{all}} \cdot k_{\mathrm{pTn}} \cdot (T_{\mathrm{MWS}} + 273.15) \qquad \text{Eq 5.55}$$

5.5 MATHEMATICAL DESCRIPTION OF THE REBOILER

The role of the reboiler in a post combustion capture is to provide the steam required for heating the regenerator therefore the target temperature of CO_2 regeneration can be obtained. The reboiler, which functions like a heat exchanger that lets the steam from the turbine pass through the next stage, is the only module directly connected to the steam water system, therefore it is the key part of the post combustion capture that can directly affect the dynamics of the power plant.

The carbon dioxide is released from the amine while the rich amine becomes lean and then flows into the tube side of the reboiler while high temperature steam from the intermediate pressure turbine is fed into the shell side. The steam condenses to water and releases a huge amount of heat. The heat is transferred to the amine solution so that part the solvent water is vaporized to steam. The steam and water are separated, in which steam ascends to the regenerator and water flows down and is pumped to the heat exchanger with the amine respectively. As a result the inlet of the shell side is the steam from the power plant and that of the tube side is the amine solution from the regenerator. The tube side outlet is separated into two parts including amine solution to the heat exchanger and the steam to the regenerator while the water from the shell side flows back to the power plant.

The same as other modules there are seven important amine properties (pressure, temperature, specific enthalpy, flow rate, concentration, CO_2 load and heat capacity) and four for the steam and water (pressure, temperature, specific enthalpy, flow rate). Table 5.5 gives the full list of the inputs and outputs for the reboiler model.

Table 5-5: Inputs and outputs of the reboiler model

	Inlet streams		Outlet streams		
	MEA	Steam	MEA	Steam	Water
Pressure (MPa)	p_{ME}	p_{SE}	p_{ML}	p_{SL}	p_{WL}
Temperature (°C)	T_{ME}	T_{SE}	T_{ML}	T_{SL}	T_{WL}
Specific Enthalpy(kJ/kg)	h_{ME}	h_{SE}	h_{ML}	h_{SL}	h_{WL}
Flow rate (kg/s)	w_{ME}	w_{SE}	w_{ML}	w_{SL}	w_{WL}
Concentration (%)	ω_{ME}	-	ω_{ML}	-	-
CO_2 load(mol/mol)	L_{ME}	-	L_{ML}	-	-
Heat capacity(kJ/(kg·°C))	c_{ME}	-	c_{ML}	-	-

Although the reboiler is a heat exchanger system, the modelling work of the reboiler is very different from the heat exchanger introduced earlier in the report for the following two reasons: the shell side is water and steam in the reboiler while it is amine solution in the heat exchanger; both the tube and shell side of the reboiler may contain liquid and gas at the same time while there is only liquid phase in the main heat exchanger. Therefore the reboiler is modelled as an individual module in the post combustion modelling.

The shell side of the reboiler is divided into three sections based on the liquid gas phase of water, including desuperheating section, condensing section and drain cooling section, with different heat transfer coefficient with the tube side. From the mass balance of the shell side:

$$\dot{m}_{WS} = w_{SE} - w_{WL} \qquad \text{Eq 5.56}$$

The average density of the shell side, which is full of saturated water and saturated steam in steady state, can be obtained by $\rho_{WS} = M_{WS} / V_S$ in which V_S

is the volume of the shell side. As the saturated steam and saturated water have different densities (ρ_{Ssat} and ρ_{Wsat}) corresponding to the pressure, it is possible to estimate the volume of water and steam in the shell side by:

$$V_{\mathrm{SW}} = V_{\mathrm{S}} \cdot \frac{\rho_{\mathrm{WS}} - \rho_{\mathrm{Ssat}}}{\rho_{\mathrm{Wsat}} - \rho_{\mathrm{Ssat}}} \qquad \text{Eq 5.57}$$

$$V_{\mathrm{SS}} = V_{\mathrm{S}} \cdot \frac{\rho_{\mathrm{Wsat}} - \rho_{\mathrm{WS}}}{\rho_{\mathrm{Wsat}} - \rho_{\mathrm{Ssat}}} \qquad \text{Eq 5.58}$$

The thermodynamics calculation of the shell side is divided into two parts: the first part is combination of a desuperheating section and a condensing section to calculate the shell side temperature while the second is the drain cooling section, with the water property calculation of the drain water at the end of the shell side. As both steam and water exists in the shell side, the shell side temperature T_{SW} can be treated as the temperature of the saturated water, corresponding to the specific enthalpy of water h_{S} at the surface of the water, which is obtained by:

$$\begin{aligned} &\frac{d}{dt}\left(h_{\mathrm{W}} \cdot V_{\mathrm{SW}} \cdot \rho_{\mathrm{Wsat}} + h_{\mathrm{S}} \cdot V_{\mathrm{SS}} \cdot \rho_{\mathrm{Ssat}}\right) \\ &\quad = w_{\mathrm{SE}} \cdot \left(h_{\mathrm{SE}} - h_{\mathrm{W}}\right) - U_{\mathrm{DS}} \cdot \left(T_{\mathrm{SE}} - T_{\mathrm{ML}}\right) \\ &\quad\quad - U_{\mathrm{CND}}\left(T_{\mathrm{sat}} - 0.5 \cdot \left(T_{\mathrm{ME}} + T_{\mathrm{ML}}\right)\right) - k_{\mathrm{a}} \cdot \left(T_{\mathrm{sat}} - T_{\mathrm{a}}\right) \end{aligned} \qquad \text{Eq 5.59}$$

where h_{W} and h_{S} are the water and steam specific enthalpy, U_{DS} and U_{CND} are the heat transfer coefficients for the desuperheating section and condensing section, k_{a} is the heat transfer coefficient related to the heat loss to the

atmosphere. The shell side temperature T_{SW} and pressure p_S can be obtained from the look up table by the specific enthalpy.

The specific enthalpy of the drain water is calculated as:

$$\frac{dh_{WL}}{dt} \cdot V_W \cdot \rho_{Wsat} = w_{WL}\left(h_W - h_{WL}\right) - U_{DRN} \cdot \left(T_{WL} - T_{ME}\right) - k_{da} \cdot \left(T_{WL} - T_a\right)$$

Eq 5.60

in which U_{DRN} is the heat transfer coefficient corresponding to the drain cooling section, k_{da} represents the coefficient of the heat loss of the drain cooling water with the atmosphere. The pressure at the end of the reboiler is related to the shell side pressure p_S and the water level, with the mathematical description of:

$$p_{WL} = p_S + \rho_{Wsat} \cdot g \cdot H \qquad \text{Eq 5.61}$$

where H represents the water level in the shell side obtained by the volume of water in the shell side V_{SW} and g is the gravitational acceleration. The temperature can be then searched from the look up table with the help of pressure and specific enthalpy.

From the thermal balance of the tube side:

$$\frac{dh_{ML}}{dt} \cdot \left(m_M + m_{WS}\right) = w_{ME} \cdot \left(h_{ME} - h_{ML}\right) + U_{DS} \cdot \left(T_{SE} - T_{ML}\right) + U_{CND}\left(T_{sat} - 0.5 \cdot \left(T_{ME} + T_{ML}\right)\right) + U_{DRN} \cdot \left(T_{WL} - T_{ME}\right)$$

Eq 5.62

where m_M is the mass of amine in the reboiler, m_{WS} is the mass of steam and water in this side, U_{DS}, U_{CND} and U_{DRN} are the heat transfer coefficients for the desuperheating section, condensing section and drain cooling section. As one of the tube side outputs is steam at steady state, the reboiler has same problem as the regenerator. The same algorithm can be used and the temperature, the vapour quality and the specific enthalpy of the amine solution can be calculated from Eqs 5.33 – 5.46.

5.6 SIMULATION STUDIES AND MODEL VALIDATION

Several pilot plants have used absorption/stripping with aqueous monoethanolamine for CO_2 capture. A complete data set from a baseline MEA campaign for the Separations Research Program pilot plant has been published in the thesis of Dugas (2006) to support other research programs. These data have been used for validation in different articles in the simulation of the post combustion capture area (Lawal *et al*., 2009, Harun *et al*., 2012). As it is only a pilot level plant, the limitation of the data is that the capture capacity is very low therefore it cannot represent the full scale Carbon Capture plant and can only show the trend of the capture or indicate its characteristics.

Lawal *et al*. (2009) have 'scaled-up' the pilot scale data in his publication based on the Rate-based dynamic model developed in gPROMS (Process System Enterprise Ltd.). With the assumption of the same working pressure, the paper managed to estimate the corresponding column diameters of the capture plant

for a 500MW supercritical power plant and the simulation result is also provided in this paper.

Based on the data and simulation results available, the validation and verification work of the post combustion model is organised into two parts: validation by the pilot scale capture plant and comparison with full scale simulation result. Some of the parameters and configurations for each validation are changed to represent the corresponding system.

5.6.1 VALIDATION BY THE DATA OF A PILOT SCALE CAPTURE PLANT

Data from the pilot scale capture plant was fed into the model for validation. Unlike the capture plant modelled in this project, which is targeting to capture CO_2 from flue gas in industry, this plant is used for test the idea of the capture technology. As a result there are several design differences compared with a capture plant integrated in a power plant.

The most significant difference is that the capture capacity of the pilot scale plant is very small. The flow rates of flue gas in the data are usually given as 0.1kg/s-0.2kg/s, which is less than 0.1% of the flue gas in a 600MW power plant. Resizing of the capture plant has to be carried out in the validation, which includes the dimensions, mass of different substance and this also affects the pressure calculation in different components.

Another important design difference that can affect the validation is that the pilot plant is not connected with a power plant therefore the reboiler duty cannot be satisfied by steam. Instead of a reboiler, an electricity heater is employed in this

plant therefore an exact reboiler duty can be measured by the power of the heater. As the reboiler model estimates the steam demand, there is not a direct variable to represent the heat duty, an alternative method is given for the validation. The steam specific enthalpy at the entrance and the water specific enthalpy at the exit of the reboiler are recorded, and the heat duty can be obtained by the product of their difference and the steam flow rate. In the pilot plant, the heat exchanger that is used to preheat the rich amine is also replaced by a heater. Similar calculation is used to validate the heat duty of the preheater.

Two sets of tests are chosen for the pilot scale validation. Based on the data, the values of the inputs are given as the Table 5.6:

Table 5-6: Input data for validation

Test set		7	19
Flue Gas Temperature	˚C	44.68	30.73
Flue Gas Pressure	MPa	0.101	0.101
Flue Gas CO2 Flow Rate	kg/s	0.0294	0.0174
CO2 Removal	%	95	95
Lean Amine Concentration	%	30	30
Lean Amine Temp	˚C	38.8	38.4
Lean Amine Loading	mol/mol	0.27	0.27

The validation of the model focuses on the thermal dynamics limited by the data available and the results are compared with the publication as Table 5.7:

Table 5-7: Validation of the pilot scale simulation

Test set		7		19	
		Measured value	Model Estimated	Measured value	Model Estimated
Required Lean Amine Flow	kg/s	0.66	0.56 (-15.2%)	0.46	0.41 (-10.9%)
Absorber Rich Amine Temp out	˚C	39.57	41.01 (3.6%)	44.08	46.1 (-4.6%)
Preheater (HX) duty	kW	130.2	100.6 (-22.8%)	100.67	85.7 (-14.9%)
HX Rich amine Temp out	˚C	73.53	75.8 (3.0%)	89.2	88.45 (-09%)
Regenerator Temp out	˚C	116.5	113.7 (-2.5%)	114.9	113.7 (-1.1%)
Reboiler Duty	kW	329	175.3 (46.7%)	137.7	119.5 (13.2%)

As the load of the rich and the lean amine in different positions of the pilot plant is not given in the published data, it is impossible to validate the relationship between the actual necessary flow rate, the CO_2 that is not captured, and the load of CO_2 in the rich and the lean amine. Additionally this project focuses on the process of the whole capture system other than the packing process, the maximum load capacity for the MEA in an ideal absorption process, which is 0.5 mol CO_2 /mol amine, is used in the absorber model as introduced in Section 5.2. This value is used in the controller to estimate the required feed MEA flow rated for the absorption. Therefore a smaller flow rate command of the lean amine is sent to the simulator, which can be found in the Table 5-7.

When lesser amine is introduced to the system, less heat is required to heat both the preheater and the reboiler to the same target temperature. The heat transfer efficiency, as the model uses specific enthalpy and flow rate to evaluate the heat duty, is also an important variable to affect the heat duty in the heat exchanger.

It can be found in the table that both preheater and reboiler have smaller duties when comparing with the plant data.

Another configuration that may affect the validation of reheater duty is the vapour fraction of water solvent that in the regenerator and reboiler. Data from the pilot plant does not provide the information of the flow rate of water and steam, but the steam extraction in this project is designed to maintain a 20% vapour fraction. The missing information would cause an uncertainty in the validation of reboiler duty. By changing the set point of the reboiler vapour fraction control, the reboiler duty can be regulated to a different level but this may cause either unnecessary energy for regeneration or a much longer time to reach the system balance.

5.6.2 VERIFICATION OF THE FULL SCALE SIMULATION

The idea of carbon capture is only at the stage of research and early stage of demonstration, therefore the validation of the model dynamics for the industrial scale capture plant from the operation data becomes not realistic at this stage of the project.

However Lawal *et al*. (2009) provides a set of simulation results from an equilibrium model of the capture system that focuses on the film around the interface between the liquid and gas. An alternative verification of the model to compare the simulation result with the result from this paper is carried out. However as this project focuses on the thermodynamics of the whole system, one difficulty in the verification is that the change of absorption rate is not

considered in the model. Therefore the flow rate of amine entering the absorber is controlled by balancing the target load of the rich amine introduced in the paper in the steady state simulation. The configuration of the full scale model are described in Table 5.8:

Table 5-8: Plant configuration for verification

Absorber Operating Pressure	MPa	0.101
CO_2 Mass Fraction in Flue Gas	%	21
CO_2 capture level	%	90
Regenerator Operating Pressure	MPa	0.162
Lean Amine Loading	mol CO_2/mol MEA	0.29

The work in this paper focuses more on the flow rate of the capture plant to represent the heat duty, limited information are provided to represent the thermal properties, for example the temperature, the pressure and the vapour qualities in different components of the plant. Additionally load of the amine in different locations of the capture plant is also unavailable. Therefore the verification work in the project focuses on the comparison of important flow rates in the flue gas and solvent circulation, which can be summarized in Table 5.9:

Table 5-9: Comparison of the full scale simulation

Test set		30 wt. % MEA		40 wt. % MEA	
		Simulation result (Laural *et al*)	Model Estimated	Simulation result (Laural *et al*)	Model Estimated
Fuel burn rate	kg/s	56.8	67.3	56.8	67.3
Flue Gas Flow Rate	kg/s	589.6	722.42	589.6	722.42
CO_2 Flow Rate	kg/s	123.8	120.0 (-3.0%)	123.8	120.0 (-3.0%)
Solution circulation rate	kg/s	3122	3135.7 (0.4%)	2964	2755 (-7.1%)
Steam draw-off flow rate	kg/s	139.8	147.9 (+5.8%)	113.2	127.0 (12.4%)

One important challenging in the verification is to use same input to both capture plant models. As the mass fraction of carbon in the coal depends on the coal type, same fuel burn rate introduced to different systems may result in both a different flow rate of flue gas and a different fluid content. As the CO_2 flow to the absorber is the most important input of the capture plant, different fuel burn rate is chosen in both systems so similar values can be feed into the capture plant models.

Due to the lack of thermal and load information in the journal paper, it is impossible to compare the condition of amine that enters and leaves the system. It is obvious that the solvent circulation demand and the steam draw-off demand have a high dependence to these conditions so the verification work is more based on these settings of the system in the project. Increasing the flow rate of amine will cause a smaller CO_2 load which is not shown in the data, and also a higher steam draw-off demand and vice versa.

Another variable that the reference model did not provide is the vapour fraction at the reboiler, which may affect the outlet flow rates. Vaporizing the water

solvent as the main role of the reboiler is the main objective, therefore a higher heat duty will be resulted from a higher set point of the vapour fraction, which causes further difference in the model verification.

5.7 SUMMARY

In order to represent the amine based post combustion capture process, a mathematical model of the capture plant is developed in this chapter based on the thermal and mass balance. The model can be divided into four modules that represent different roles in the capture process: the absorber, the heat exchanger, the regenerator and the reboiler. Due to the data limitation, the validation work has been carried out in two different plant scales: the pilot scale validation is based on the data from a pilot plant published in a thesis in The University of Texas at Austin, which has been employed by the validation work in many different organizations; the validation of full scale simulation compares the result obtained in this project with the simulation in a paper published by the University of Cranfield, who scaled up the plant data to a 500MW simulation environment.

The following chapter will be focused on the retrofit of the power plant simulator. Steam will be extracted with from the entrance of the LP turbines of the steam-water system, with a valve to regulate extraction flow rate. The impact of introducing the post combustion carbon capture to the power plant will be studied and the equivalent power that is reduced due to the steam extraction will be fed back to the command of the coal feeding to overcome the power penalty.

Chapter 6.

STUDY OF IMPACT ON POWER PLANT DYNAMICS WITH INTEGRATION OF POST COMBUSTION CARBON CAPTURES

The CO_2 regeneration in the post combustion carbon capture is an endothermic process therefore the regenerator must be maintained at high temperature. As introduced in Chapter 5, part of the steam, which is supposed to pass through the low pressure turbine to generate mechanical work to the generator, needs to be extracted to the reboiler and acts as the heat source for the CO_2 regeneration. As less steam flows through the low pressure turbine, the mechanical energy from this turbine drops which results in an overall power penalty.

This chapter introduces the study of plant dynamics with the carbon capture process integration. The regenerator and reboiler system at the steady state is normally kept at a relatively stable temperature that enables the regeneration reacts in a most efficient way. But the starting up process of the capture plant is much more complicated because heating the system to the required temperature efficiently remains as a challenging topic. This chapter focuses on the study of the dynamics of power plant with a starting process of the capture plant. The steady state of the capture plant with different capture loads is also investigated in this chapter. The shutting down of a capture plant, however, usually refers to a cool down system that is isolated from the power plant because all the feeding of flue gas, lean amine and steam are stopped. So the capture plant has almost no interactions with the power plant in this process.

In this chapter, a simple procedure of the starting up process is designed and the dynamics and steam demand from the power plant is modelled. The simulator environment is modified to form the "channels" to provide steam and flue gas to the capture plant. With the experiments on the simulator the impact of the post combustion capture to the power plant is then studied.

6.1 STARTING UP THE CAPTURE PROCESS

From the previous chapters, it is clear that the steam extracted from the turbine system does not have a direct contact with the amine solution. Instead, it is used to heat and vaporize the solvent water into steam in the reboiler to heat the regenerator. Therefore the starting-up segment of the capture plant must

establish the steady state of its working temperature for the reboiler in the regenerator before the flue gas and amine are introduced to the capture plant.

There are no an industrial documents available at the present to give a clarification for the steps to follow for starting up a post combustion capture plant, therefore a simplified starting up procedure is designed from the theoretical analysis, which is to establish the initial condition before the flue gas is introduced into the capture plant. Associated control strategies are introduced for estimation of the steam required by the normal operation.

Focusing on the regenerator and reboiler systems, the start up procedure is divided into four steps: to heat the reboiler up, to generate required steam for the regenerator, to increase the amine circulation and to establish the steady state.

The target of the first step is to heat up the solution in the reboiler and vaporize part of the solvent into steam. As soon as the request of CO_2 capture is received, the control valve of the steam is opened so the steam can be introduced to the reboiler. The steam is controlled to a relatively low level to maximise the heat exchange rate and to limit the temperature change rate of the reboiler.

When the reboiler reaches the evaporation temperature, which is usually 100 ℃, the plant enters the phase of the starting up process. In this step, the steam flow from the turbine is maintained at the same level and some of the solvent water in the reboiler evaporates into steam that ascents to the regenerator to heat the regenerator to the steady state temperature. The circulation of amine flow starts at a relatively low rate to prevent the solvent loss in the reboiler.

As soon as the steam fraction of the reboiler outlet solvent reaches a certain level, which is 20% in this thesis, the whole system starts up and the capture command is gradually increased to the target level. The minimum lean amine demand is estimated based on the CO_2 load of the rich amine that leaves the absorber and this estimated demand is satisfied by control valves of the amine flow to minimize the power penalty. The flow rate demand of the lean amine can be greatly affected by its concentration and initial load as well as the flue gas properties. As a more rich amine solution enters the regenerator, the reboiler duty increases so the steam extraction valve is controlled to evaporate more steam for the regenerator heating up. The control system aims to keep the tube side steam fraction to an optimised level, to reduce the power penalty by minimizing the vapour escape in the regenerator and give an enough heat reserve for the sudden increase of the capture target level. A series of different set points has been implemented in the control system, from 5% to 25%. It has been found that keeping the vapour fraction at 16% is enough to satisfy the heat reserve therefore this value is employed to regulate the steam demand to the power plant. The steady state of the capture plant will be gradually established in this process after a while.

Figure 6-1 records the dynamics of the important variables, including the flow rate of flue gas, amine and steam; the outlet temperature of each part of the capture plant and the vapour fraction of amine solvent water in the reboiler, of a starting up capture plant from idle to a 5% capture rate following the procedure.

The set concentration of lean amine is 30% with the initial CO_2 load of 0.29 mol/mol.

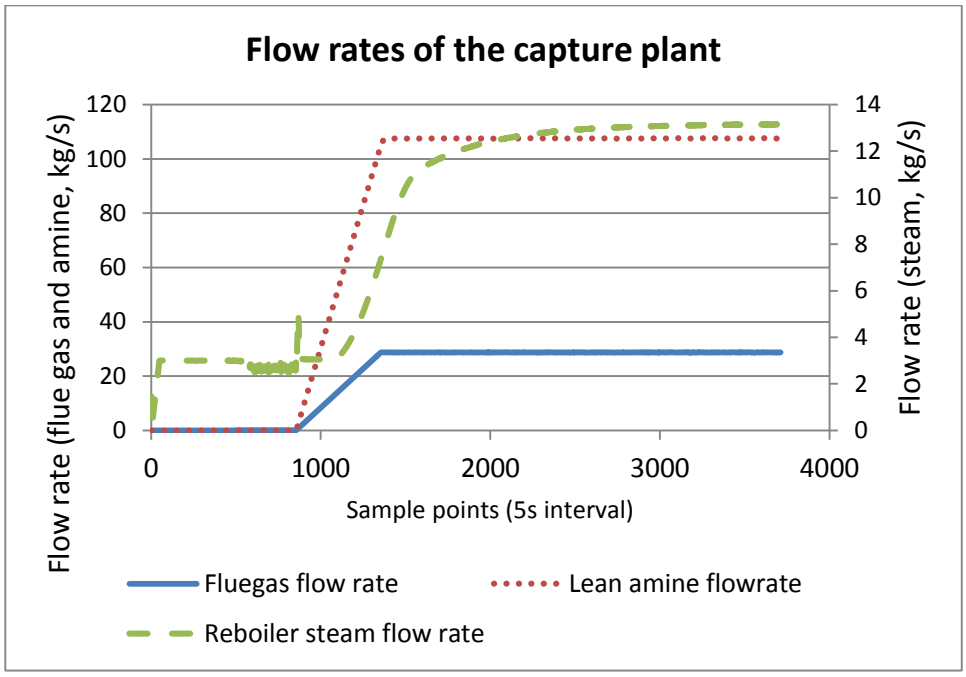

(a)

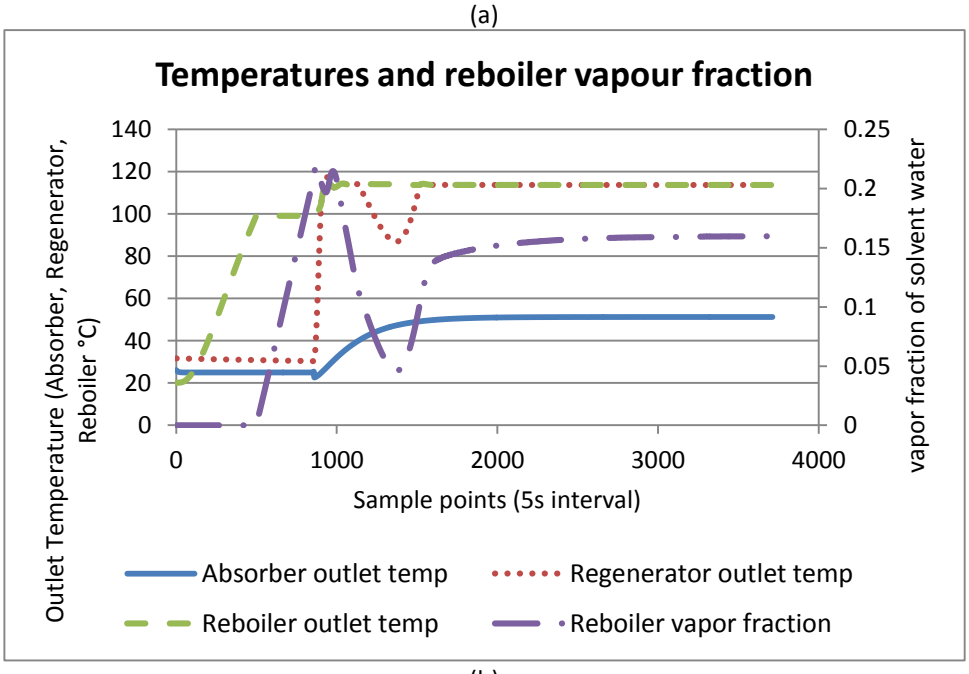

(b)

Figure 6-1: (a) flow rates of the capture plant for 5% capture rate on a supercritical power plant with 500MW power output; (b) temperature and vapour fraction of the capture plant

The steam flow rate in this figure represents the steam extraction from the power plant which is the most important feature that can significantly affect the dynamics of the power plant. This project is based on the assumption that the steam extraction can always satisfy the steam demand. It can be observed in Figure 6-1 that after the steam is introduced to the capture plant, the outlet temperature of the reboiler increases to 100 ℃, which is the saturation temperature of solvent water under 1 atm and the solvent water evaporates into vapour gradually. The flow rates of the flue gas is increased slowly to the given capture target when the vapour fraction of the reboiler reaches 20% and lean amine is introduced to a proper amount for a better capture efficiency. The outlet temperature of the regenerator rises rapidly because the flow rate of amine is very slow at the very beginning. However as the flow rate of amine increases, the heat provided by the steam is not high enough to maintain this temperature so the regenerator temperature drops down. This temperature is lifted back to the saturation temperature as more steam is introduced to the reboiler from the power plant. The system is stabilized at the steady state gradually and the vapour fraction of the lean amine solvent from the reboiler is maintained at 16% after the regenerator temperature is brought back.

6.2 IMPLEMENTATION OF THE INTEGRATION OF THE POST COMBUSTION CAPTURE TO THE POWER PLANT IN THE SIMULATOR

In the mathematical model introduced in the last chapter, only two fluids are directly connected to the power plant: the flue gas introduced to the absorber and

the steam connected with the reboiler. Therefore the modification work on these two connections must be considered to realise the integration of the post combustion carbon capture to the power plant. On one hand, the flue gas is introduced to the absorber at the chimney stage, which is located at the very end of the power generation process. The effect of the capture plant in the flue gas side is so small that it can be ignored. On the other hand the role of the steam piped to the reboiler is to satisfy the heat duty of the capture plant. As less steam passes through the low pressure turbine, the mechanical work delivered to the generator from the turbine system suffers from a significant penalty, which has a much greater and complicated impact to the power plant dynamics. The retrofit work in this project is focused on the steam extraction only, and, as the flow rate of the flue gas does not affect the plant dynamic responses, this process can be simply modelled as the flow rate of the flue gas passing the chimney multiplies the capture target percentage given by the operator.

6.2.1 MODELLING OF STEAM EXTRACTION PROCESS

Despite the capture process itself, two most important topics that researchers and the industry concern are the power penalty caused by the post combustion capture and the dynamic stability of the power plant. It has been recommended by most of the work published in this area (Ramezan and Skone, 2007, Lawal *et al*., 2009, Lucquiaud and Gibbins, 2009) that the steam at the IP/LP crossover is the best choice for steam extraction to satisfy the demand of the reboiler. Figure 6-2 shows the changes on the intermediate pressure turbine based on the fluidic network design diagram of the simulator based on the suggestion of these papers,

in which red lines represent the steam flow, blue lines are for the water. The dashed line in the figure that starts from the node 19 and ends with reboiler is the branch pipe added to the steam flow from which the steam can be extracted to the capture plant. A control valve is fitted in this branch to govern the flow rate so the extract flow rate of the steam needed can be regulated.

From the simulation a drop of the steam pressure can be observed at the position that steam is drawn. As this pressure change can significantly affect the upstream in the fluid network, especially the output of the intermediate pressure turbine, the dynamic response analysis of the power plant will focused on the pressure drop caused by the steam extraction.

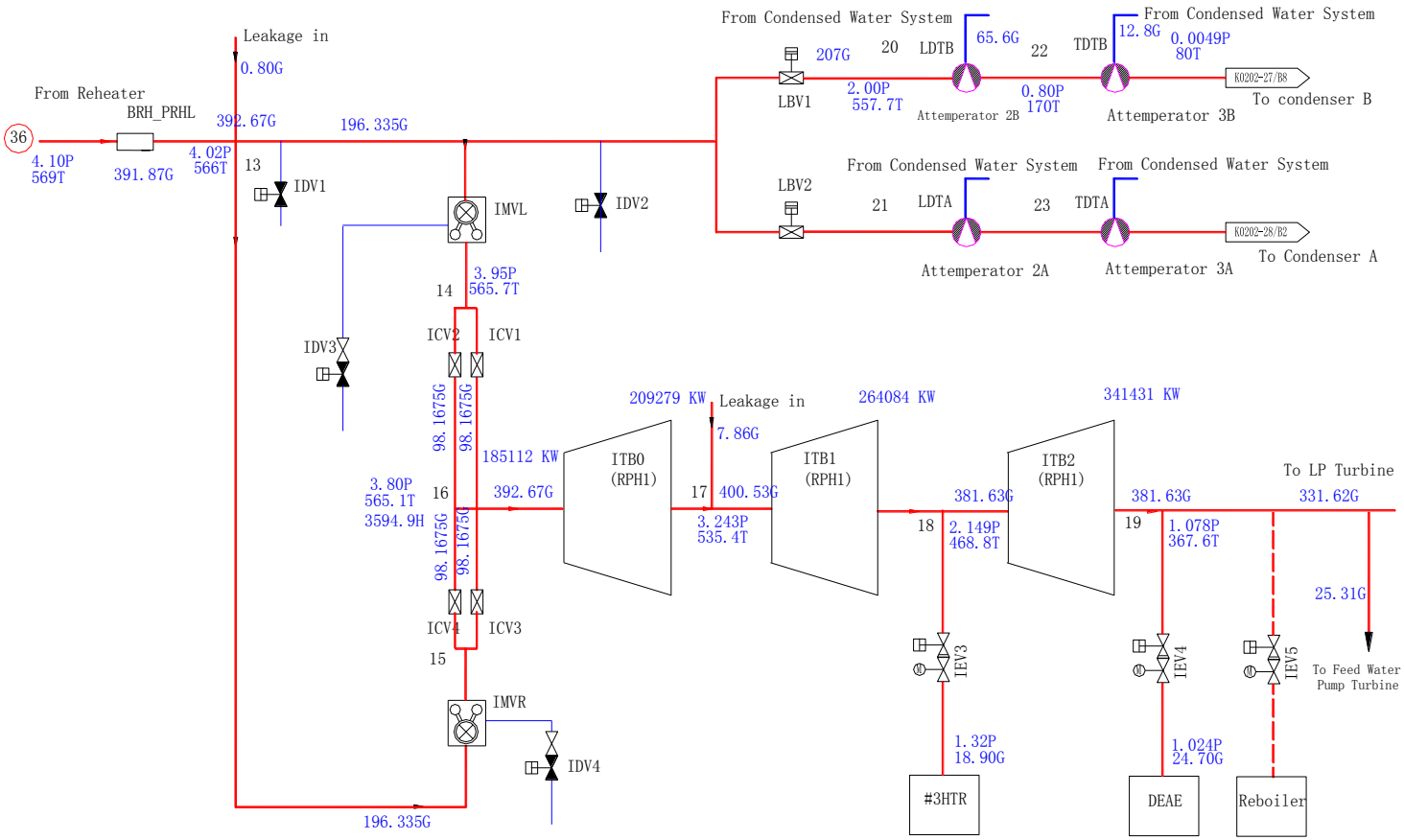

F0621S-K0202-02 Flow-net of Intermediate Pressure Turbine System

Figure 6-2: Flow-net diagram of the Intermediate Pressure Turbine System

In order to re-calculate the pressure at the exit of the intermediate pressure turbine, which is described as node 19 in Figure 6-2, the fluidic network calculation of the main steam system introduces a new branch connected with a new boundary block as the reboiler. The fluid conductance and the flow rate of this branch, which is limited by the valve position and the pressure of the upstream and the downstream, are calculated from the valve model. This information is shared with the fluidic network calculation in which the reboiler pressure is taken as the pressure for calculation therefore the pressure of the connection between IP and LP can be obtained. Once the new pressure and flow rate balance is established, the power output from each turbine stages can be obtained by Eq 3.16 introduced in Chapter 3:

$$P = w_s \cdot \left(h_i - h_o \right)$$

where w_s is the flow rate, h_i and h_o are the inlet and outlet specific enthalpy of the steam.

6.2.2 STUDY OF THE IMPACT OF POST COMBUSTION CAPTURE TO THE POWER PLANT DYNAMICS

In order to study the output dynamics of the power plant when a post combustion capture is engaged, simulation tests of the steam extraction have been carried out in the simulator environment. The control strategy adopted in the simulator is manual to maintain a constant feed coal and feed water flow rate. The steam extraction demand calculated to satisfy the heat duty of the reboiler is introduced and the steam extraction is governed by the control valve (IEV5 in Figure 6-2).

The shell side pressure of the reboiler is another important factor in the flow rate calculation of the steam extraction and it is used as a boundary condition for the plant fluidic network calculation in the system.

The experiment introduced previously, which is the starting up process of the capture plant from idle to a target capture rate of 5% in a 500MW plant, is employed for the dynamic study and the calculated steam demand is given to the controller of the control valve. From the simulation of the capture plant, it has been observed that the capturing 5% of CO_2 under 500MW power output by the 30% lean amine with 0.29 mol/mol CO_2 load in the capture plant needs approximately 7% of the steam from the power plant taken from the end of intermediate pressure turbine. Figure 6-3 (a and b) compares the relationship between the steam demand required to satisfy the heat duty of the starting capture plant and the dynamic response of the power plant mechanical power changes caused by this steam extraction in the steady state power plant. It is clear that an overall power penalty of more than 20MW is resulted from this process.

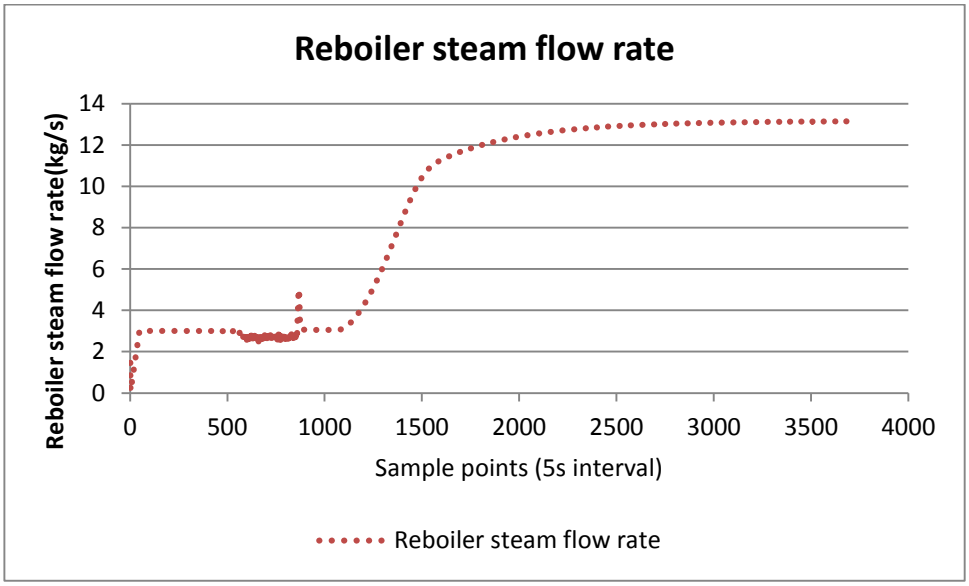

(a)

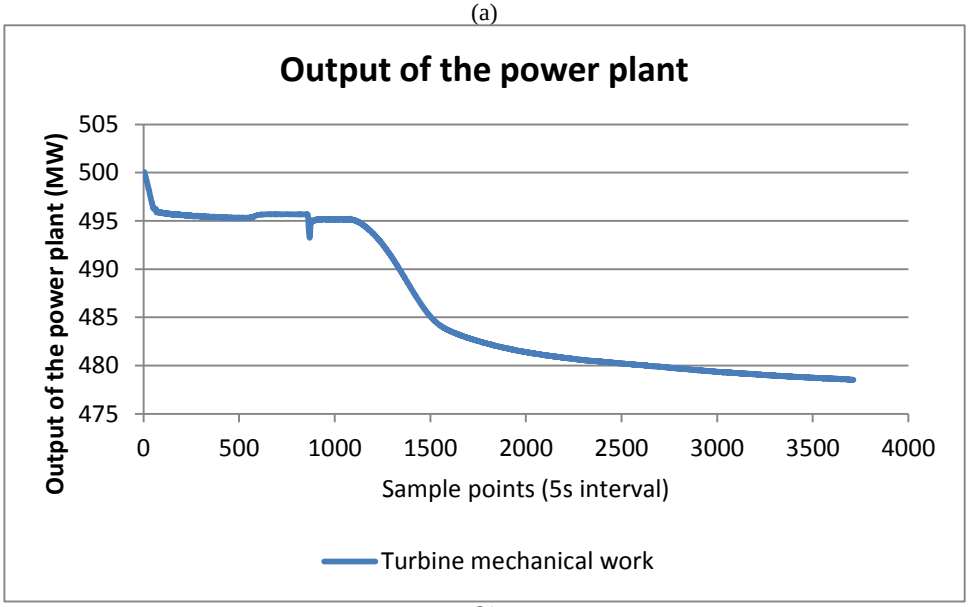

(b)

Figure 6-3: (a) Reboiler steam flow rate command; (b) Dynamic response of power plant when post-combustion capture integration is implemented

There is no supercritical power plant with post combustion capture available, therefore most of the research activities are now based on the approximation from the steady state simulation. It is almost impossible to validate the results of plant dynamics generated from the simulator using the data from an industrial

scale demonstration plant so this becomes the main obstacle of this study. However the estimated power penalty can be reasonably explained. From the study the power penalty in Figure 6-3 shows a very linear dependence on the steam introduced to the reboiler when all the other inputs are kept constant.

6.3 POWER PENALTY RECOVERY

Electricity is the product that a power station produces which is transmitted via the power grid to the end users. To ensure the power grid stability, the quality of the electrical power is very important, especially, keeping the frequency at a constant value. The frequency of the electricity will vary with the load and generation changes therefore the Automatic Generation Control (AGC) is used at power plants. AGC detects the frequency changes from the grid and adjusts the demand command to the power plant control system therefore to deliver matched mechanical power to the generator to bring the frequency back to the targeted value. When there is a power penalty caused by the integration of post combustion capture in the power generation process, the output of the plant power can no longer satisfy the power demand. Therefore it is essential to bring the power output back to meet the demand from the grid. The control system needs to be modified to be able to ensure the power output at various capture rate. In this project, a recovery strategy is proposed which is divided into two parts, namely rapid power recovery and precise power control.

6.3.1 RAPID POWER RECOVERY

The control target of the rapid power recovery is achieved by estimating the power penalty and giving a fast feedback to the control command of the coal preparation and feeding process. This approach provides a fast response in command to address the power short-fall caused by a fast increase of the steam extraction.

The most important task of the rapid power recovery is to estimate the power penalty from the post combustion capture. The low pressure turbine can be divided into five different stages (eight expansion chambers) as shown in the design diagram of the simulator of the low pressure turbine (Figure 6-4). Steam extraction at each stage is controlled to a flow rate for the heaters in the condensed water system. Although this flow rate is much lower compared with the main flow, the calculation of the mechanical power output is not accurate enough when it is calculated based on the ratio of steam extraction.

In order to estimate the energy penalty, a separate model of the low pressure turbine is established and is running in parallel with the original mode based on the same system implemented in the simulator. Without steam extraction to the capture plant the only steam flow leak out of the system is the steam to the deaerator at the normal operation condition therefore the steam extraction is added to each stage of the low pressure turbine in the parallel model.

The mechanical power calculated in this parallel model is compared with the actual output of the LP turbine and the difference between the results obtained

from the two models is added back to the load demand so that the coal, water and air command can be updated to bring the power back to compensate the power reduction caused by the capture process.

6.3.2 PRECISE POWER CONTROL

One limitation of the parallel model is that it ignores the changes in pressure distribution across the fluidic network for different situations when the steam is introduced to the capture plant. The fast power recovery is only possible to estimate an approximated power penalty but it cannot exactly match the demand from the grid. This difference of approximation is not big, but this brings big impact to the power output quality which may cause unstable output while is working in the manual mode. Therefore an additional compensation is necessary to be added to the command control to balance the demand variations and the turbine output.

In the control strategy of frequency response, a command bias calculated from the comparison of generation frequency with the rated grid frequency is introduced to the load set point which makes an alteration to the command obtained via the rapid power recovery and update the feed coal. A PI controller that can adjust the load command in a small range is added to the simulator before the frequency regulator to precisely control the load output balance when the post combustion capture is engaged in and disturbs the generation process.

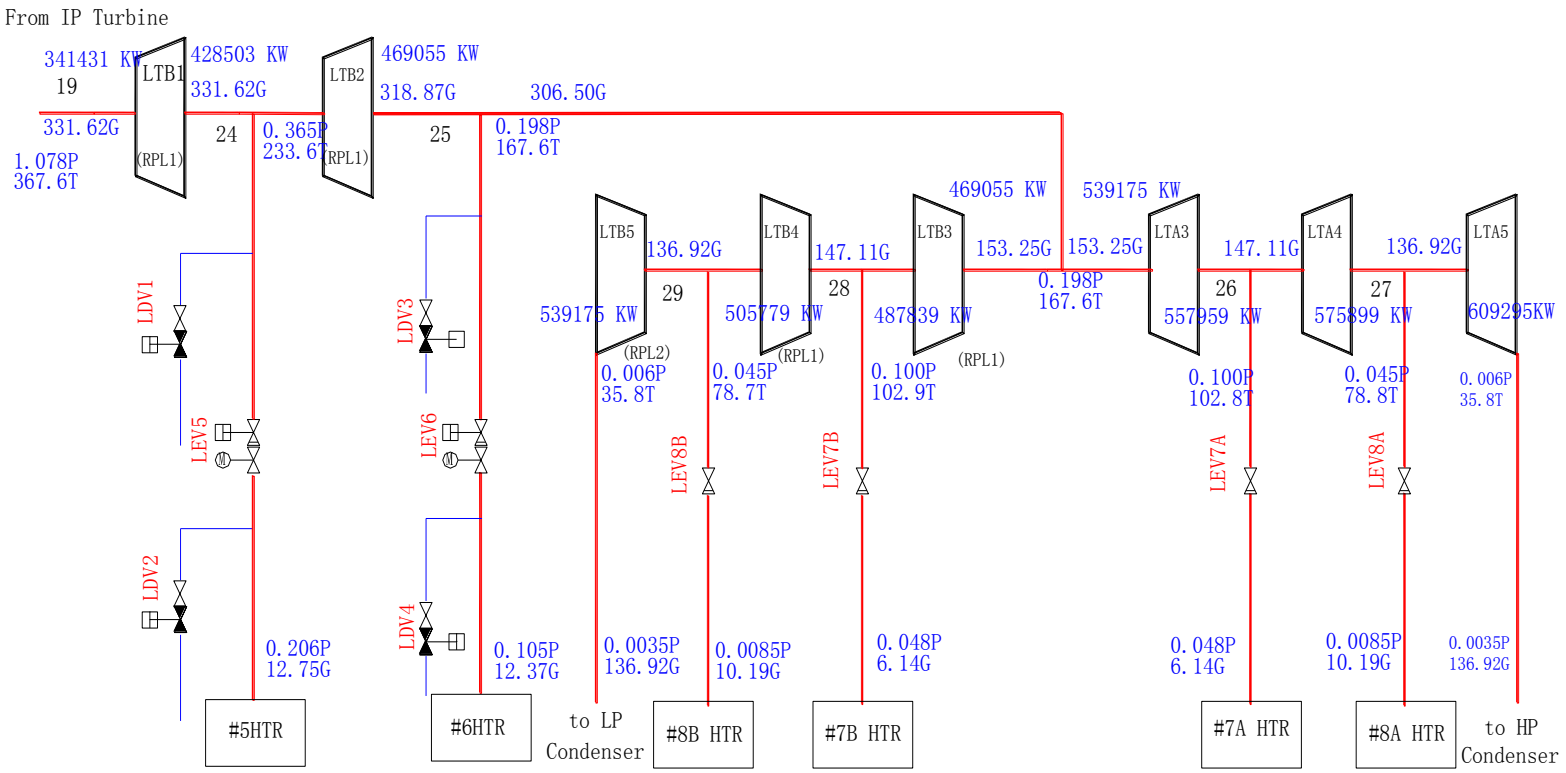

Flow-net of Low Pressure Turbine System

Figure 6-4: Flow-net diagram of the Intermediate Pressure Turbine System

6.3.3 IMPACT OF POST COMBUSTION CAPTURE TO THE POWER PLANT DYNAMICS WITH PENALTY RECOVERY

A group of start-up experiments of the capture plant with steam extraction from the power plant have been conducted in the simulator to test the algorithms of the penalty recovery strategy. Using the same conditions as the previous simulator, the power plant is initially operating at 500 MW steady state at the beginning of the experiment and a 3% capture rate of the flue gas is given to the system. The control system of the capture plant estimates the lean amine and steam demand in the way as shown in Figure 6-5 (a). With the power recovery strategy implemented to compensate for the power penalty caused by the steam introduced to the capture plant, the turbine system is able to deliver enough mechanical energy to the generator for power generation. Figure 6-5 (b) compares the dynamics of the set power demand from the grid, the actual power demand regulated by the penalty recovery, and the mechanical energy delivered from the turbine system.

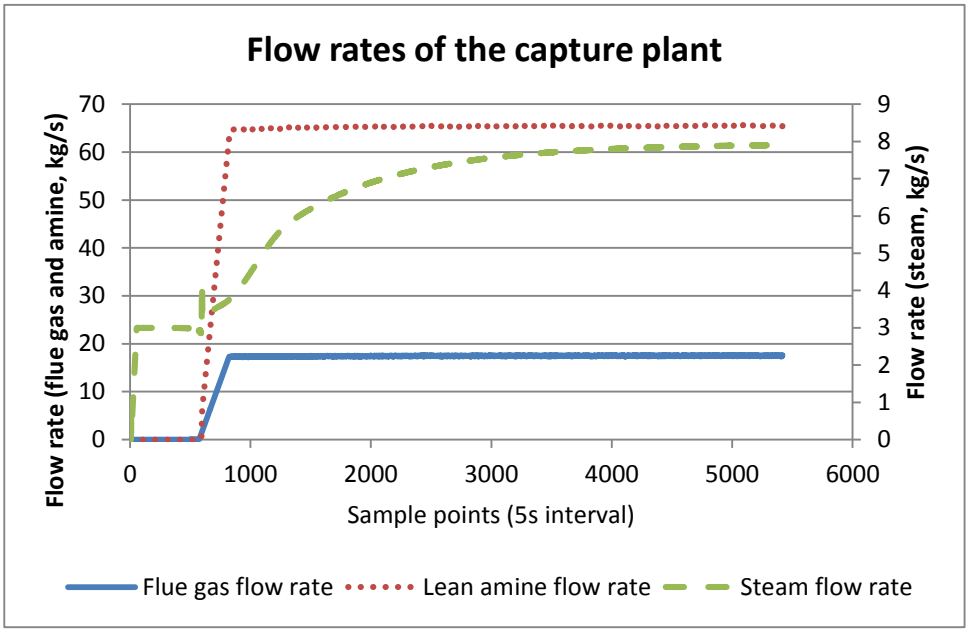

(a)

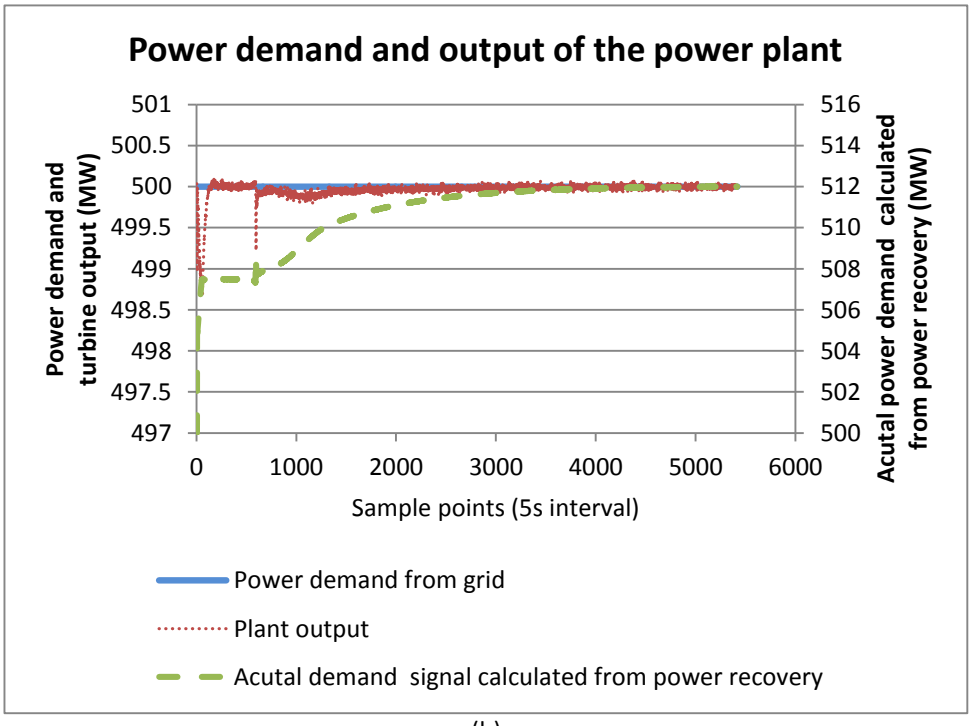

(b)

Figure 6-5: (a) flow rates of the capture plant for 3% capture rate on a supercritical power plant with 500MW power output (30%, 0.29mol CO_2/mol MEA); (b) Power demand and plant output

Following the starting up procedure of the capture plant, it can be observed that the steam duty calculated by the control system of the capture plant rises to 3kg/s rapidly at the beginning of this process to heat the reboiler up to generate steam for heating regenerator. This quick increase of steam extraction results in a sudden drop of the actual power output although the corresponding demand signal given to the feed coal flow rate is increased immediately to 507MW. The plant output was brought back to 500MW in a short time period within 10 minutes after the response of penalty recovery takes place.

The flue gas and lean amine are introduced to the capture plant when the reboiler is successfully heated up, providing steam for the regenerator. As the temperature of the rich amine is lower than the working temperature of the regenerator, a heat duty will be necessary after the system is warmed up, which follows the the flow rate of the rich amine. Steam from the power plant, which is around 350℃, acts as the heat source in the regenerator reboiler system to satisfy the heat duty. The simulation result shows that the steam demand is gradually increased to 8kg/s to satisfy the reboiler heat duty. Meanwhile, the penalty recovery algorithm raises the actual demand signal to approximately 512MW to make sure the power plant is able to deliver enough output as more steam bypasses the low pressure steam turbine. Figure 6-5 (b) shows that the second power loss of the plant output is much smaller than the first one when the reboiler regenerator is warming up to the rated temperature. A possible reason is that the modified recovery strategy is fast enough compared with the increase of steam extraction in this situation.

Another set of simulation test was conducted at the rate of 10% CO_2 capture from the flue gas with 40% 0.16 mol CO_2/mol MEA solution and the results are shown in Figure 6-6. The results of this test shows a much lower heat duty comparing with the capture with 30% 0.29 mol CO_2/mol MEA solution because less absorbent and less water solvent are required. The dynamics of the plant shows a similar result as the experiment presented in Figure 6-6.

6.4 IMPACT OF STEAM PRESSURE IN HIGH CAPTURE RATE AND FURTHER IMPROVEMENT OF POWER PLANT

Simulation studies shows that when increasing the capture load to 10% of the flue gas with 30% 0.29 mol CO_2/mol MEA solution, the simulator becomes very unstable and calculation error occurs. After several experiments in different capture loads and different lean amine configurations, it has been identified that the problem is related with the flow rate of the steam extraction.

Analysis of the fluidic network calculation shows that the pressure between the intermediate and low pressure turbine drops as steam is taken out from the turbine system from the branch connected with the reboiler. Figure 6-7 shows the dynamics of this steam pressure of the experiments introduced in Section 6.3.3 and it is clear that with the same downstream pressure, more steam losses will result in a greater pressure drop at that node. Figure 6-8 summarizes the steam pressure at the exit of the intermediate pressure turbine at different steam load when the simulator is working at 500MW.

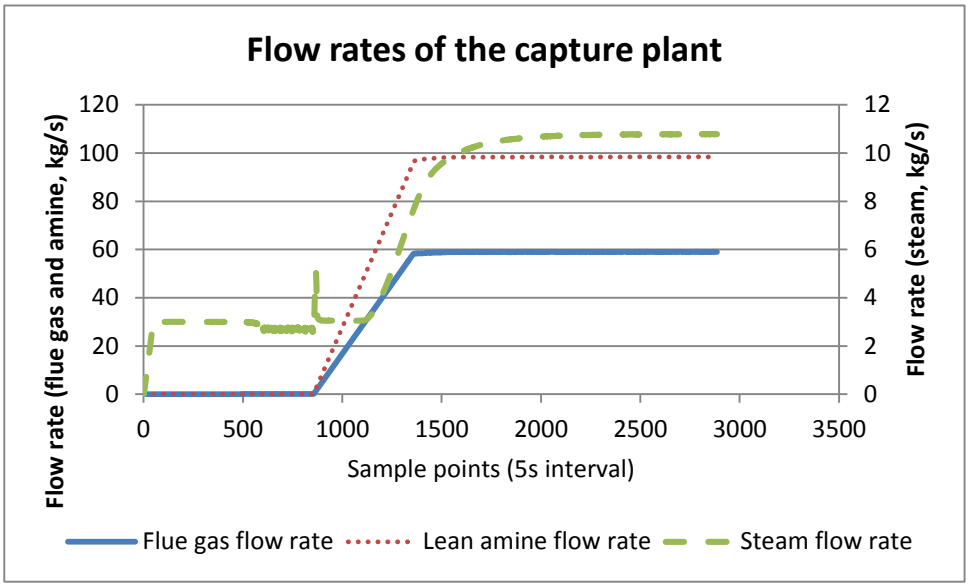

(a)

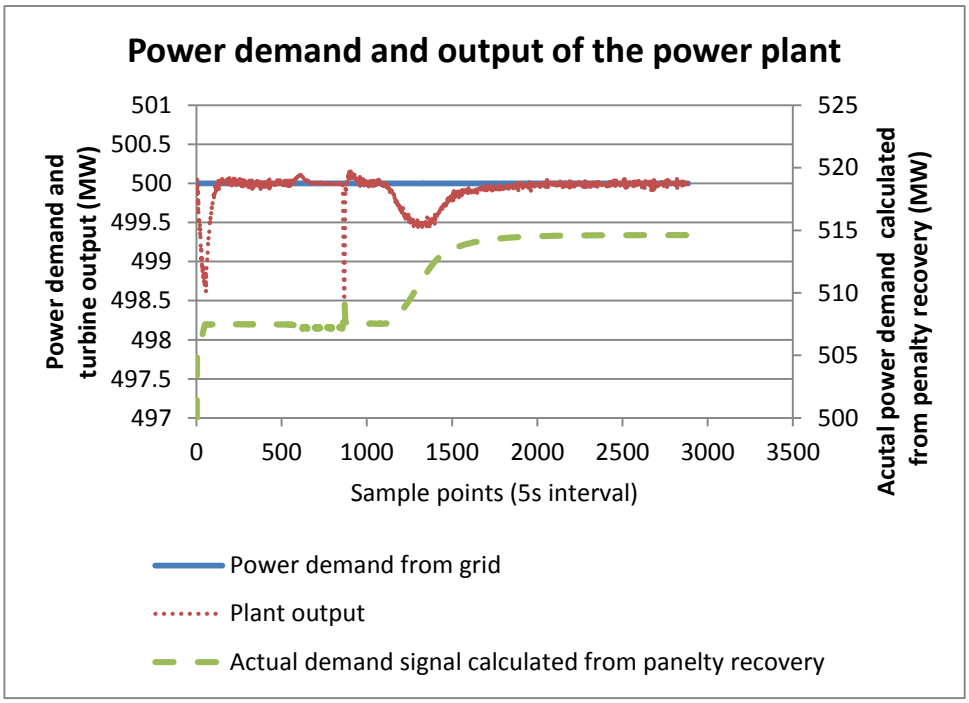

(b)

Figure 6-6: (a) flow rates of the capture plant for 10% capture rate on a supercritical power plant with 500MW power output (40%, 0.16mol CO_2/mol MEA) (b) Power demand and plant output

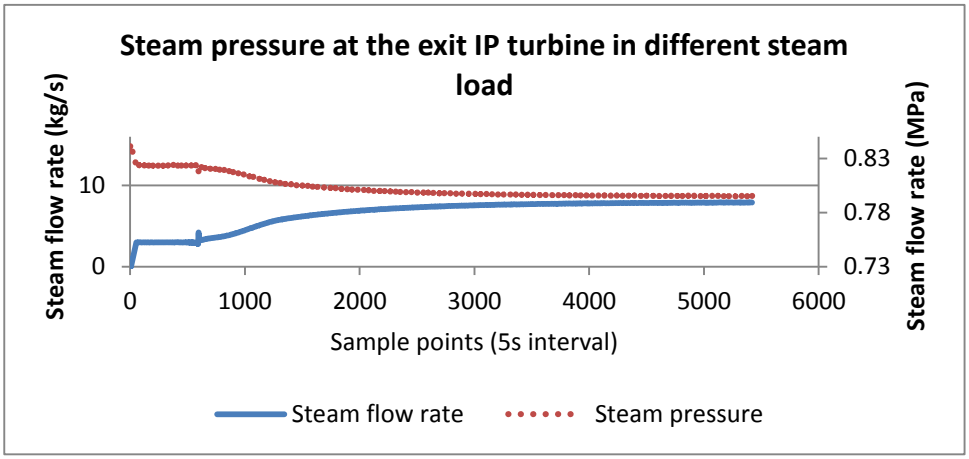

(a)

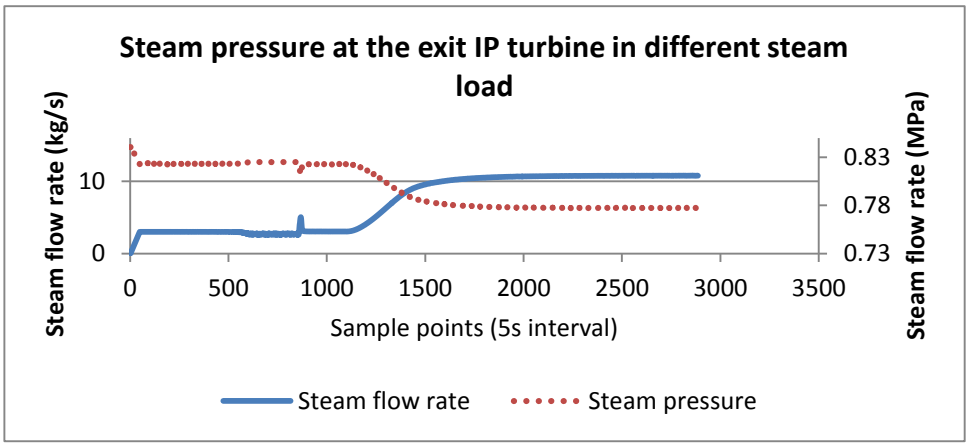

(b)

Figure 6-7: (a) Steam pressure at the exit of the intermediate pressure turbine in the starting up of capture plant (with 30% 0.29 mol CO_2/mol MEA solution); (b) Steam pressure at the exit of the intermediate pressure turbine in the starting up of capture plant (with 40% 0.16 mol CO_2 /mol MEA solution)

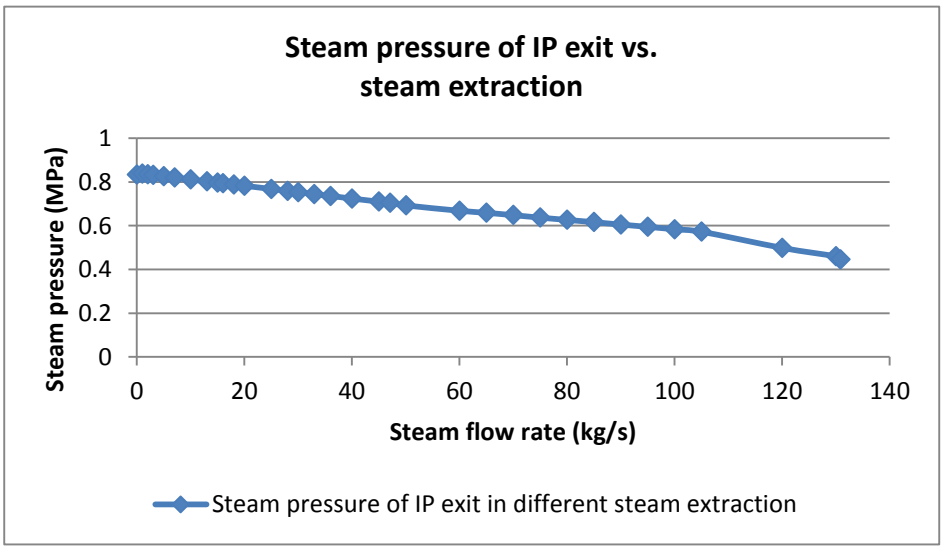

Figure 6-8: Steam pressure of intermediate pressure turbine under different steam extractions

One direct result of the lower steam pressure caused by the extraction is that the power plant is not able to deliver enough steam to the reboiler to fulfil the heat duty when the capture command is high. Simulation study shows that the power plant is able to provide the steam for a capture capacity of 10% to 20% when the power plant is working at level of 500MW output, depending on the CO_2 load and the concentration of the lean amine. Additionally an unstable steam pressure can also cause potential problems to the generation as it may cause unstable outputs of the turbines.

In order to stabilize the steam pressure at the exit of intermediate pressure turbine, a throttle valve is introduced to the simulator at the entrance of the low pressure turbine (node 19 in Figure 6-4). This valve is controlled together with the control valve IEV5. This throttle valve will be closed to a proper position consequently to maintain the steam pressure when the valve IEV5 is opening to satisfy the steam increase demand and vice versa.

A series of simulations have been carried out to study the dynamic responses of the power plant when both the penalty recovery and the steam pressure stabilization actions are brought in to the system. In these simulation tests, 15% to 70% of the carbon dioxide is captured and the important variables are recorded. As steam extraction is the main variable in the capture plant, which affects the power output, the simulation study will use a fixed concentration of the 30% lean amine with 0.29mol/mol CO_2 load.

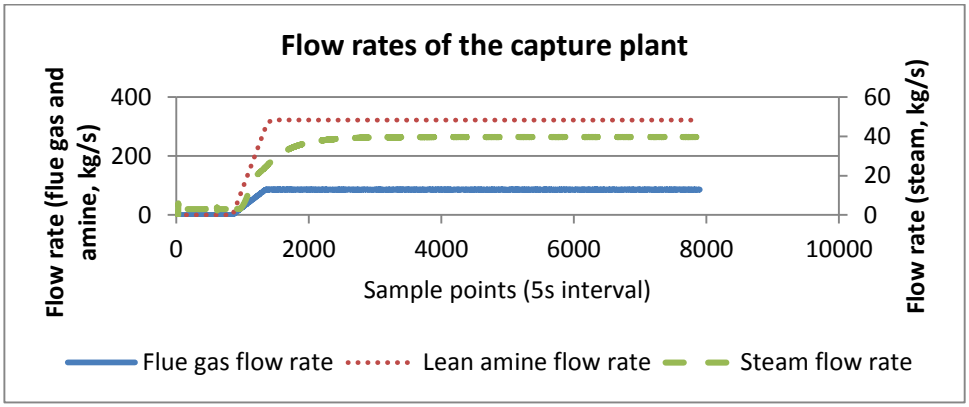

(a)

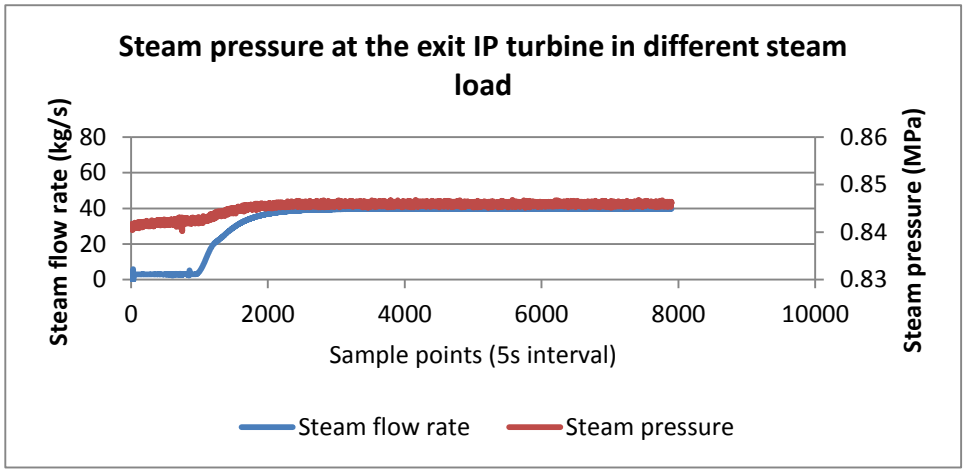

(b)

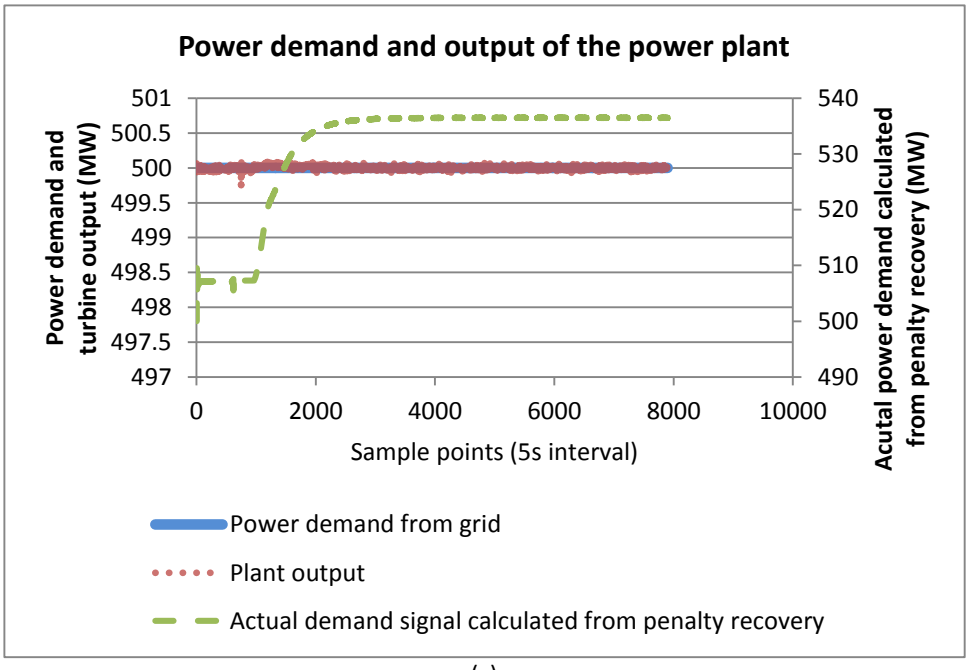

(c)

Figure 6-9: (a) flow rates of the capture plant for 15% capture rate on a supercritical power plant with 500MW power output (30%, 0.29mol/mol MEA); (b) Steam pressure at the exit of the intermediate pressure turbine in the starting up of capture plant ; (c) Power demand and plant output

The data shown in Figure 6-9 represents the flow rates of the flue gas, lean amine and steam of the capture plant, the power output and the steam pressure at the low pressure turbine entrance when the capture plant is starting up with 15% capture rate and the simulator is running with a 500MW power demand. Figure 6-9 (b) shows the dynamics of the steam pressure that enters the low pressure turbine and the reboiler, which illustrates much more stabilized responses. It is noticed that instead of being kept as a constant, the steam pressure is increased by 0.005MPa when the capture plant is started. The explanation to this change is that penalty recovery gives a positive variation to the actual demand signal (as shown in Figure 6-9 (c)) so the firing rate (including feed coal, feed water and primary/secondary air) is increased, in turn, the pressure of the whole network increases at different levels. Figure 6-9 (c) also gives the dynamic response on the plant output and the results show a much lower power turbulence comparing with the case of using the strategy without a throttle valve installed prior to the entrance to the low pressure turbine, which is approximately 1.5MW.

Similar results can be obtained in two other simulation cases on the simulator for 20% and 30% CO_2 capture rate for a 500MW power demand and the key variables are shown in Figure 6-10 and Figure 6-11.

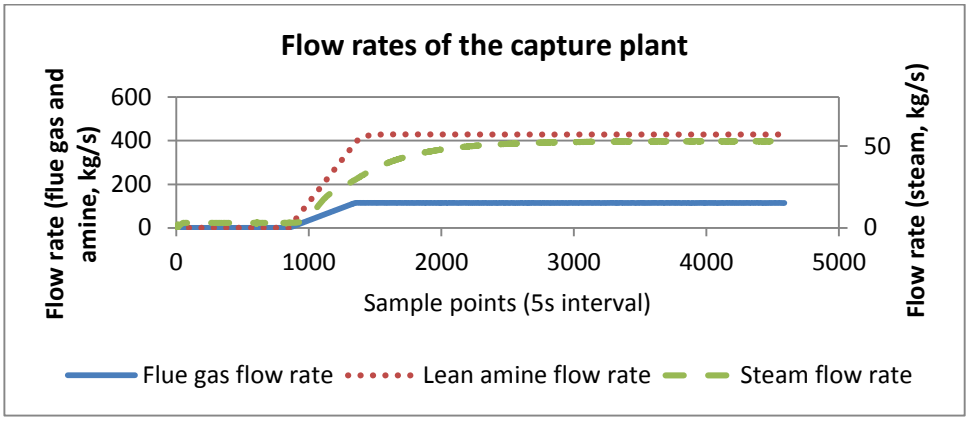

(a)

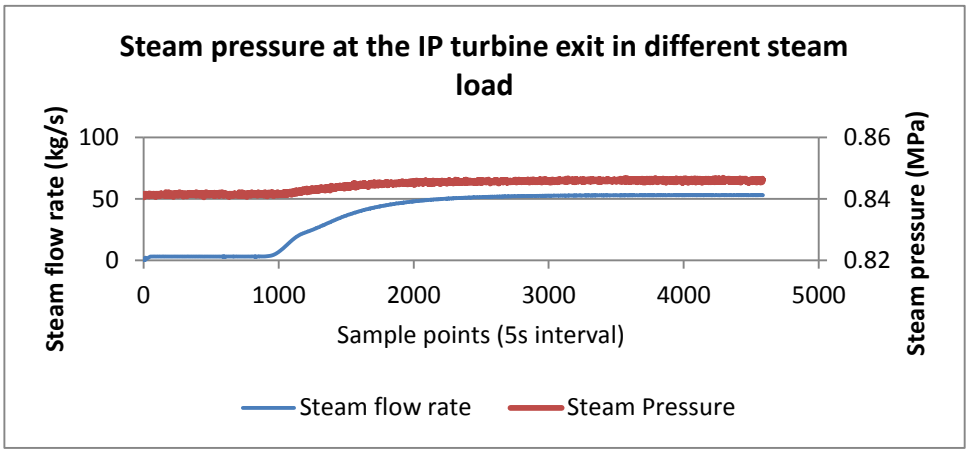

(b)

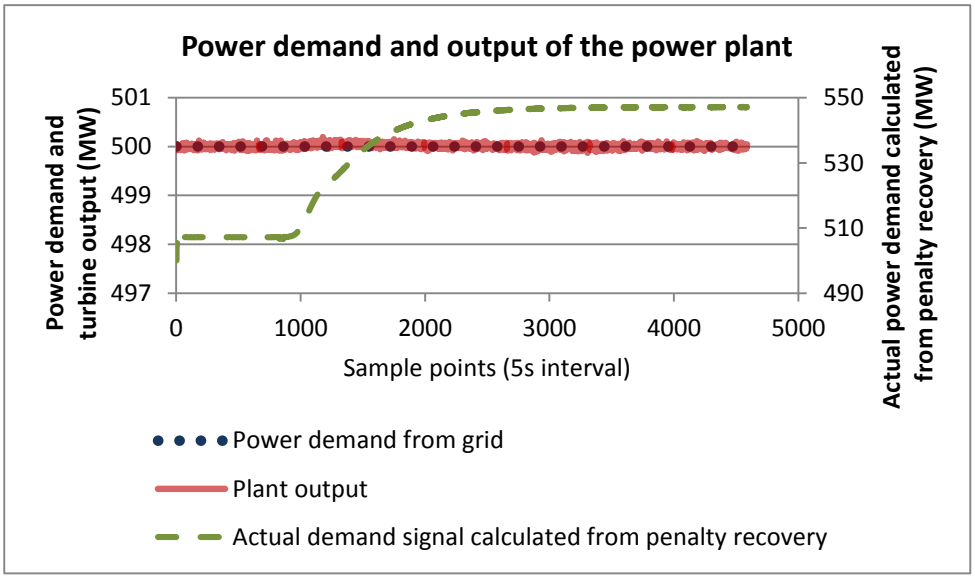

(c)

Figure 6-10: (a) flow rates of the capture plant for 20% capture rate on a supercritical power plant with 500MW power output (30%, 0.29mol/mol MEA); (b) Steam pressure at the exit of the intermediate pressure turbine in the starting up of capture plant; (c) Power demand and plant output

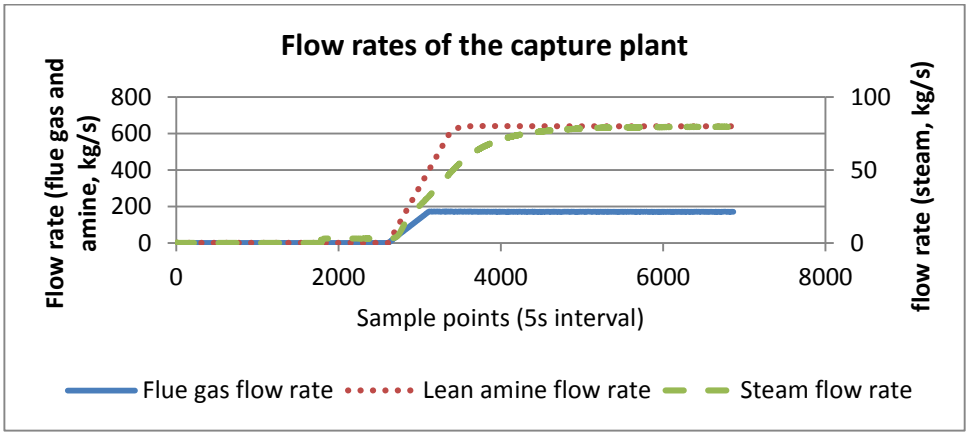

(a)

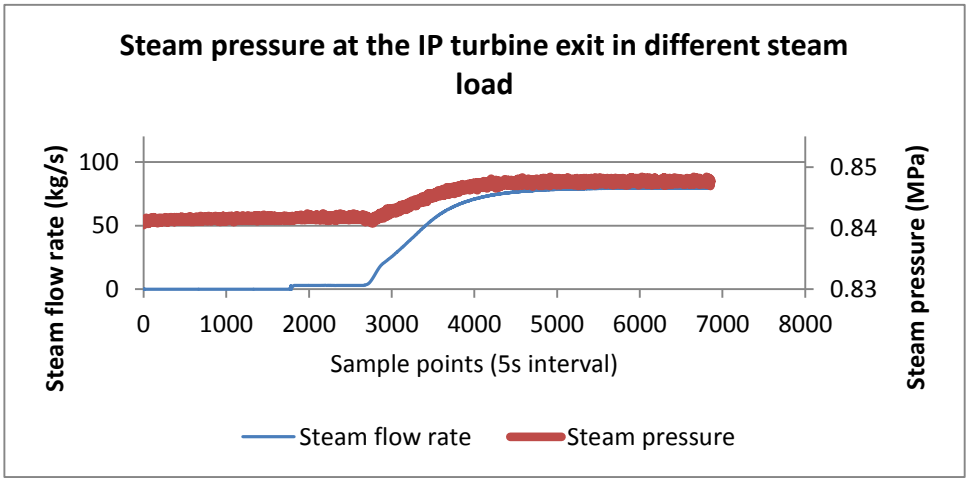

(b)

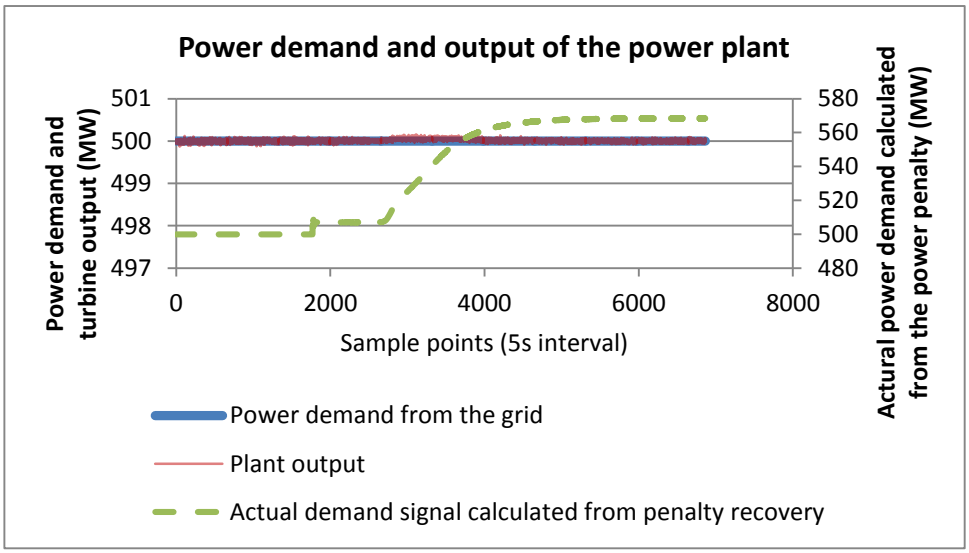

(c)

Figure 6-11: (a) flow rates of the capture plant for 30% capture rate on a supercritical power plant with 500MW power output (30%, 0.29mol/mol MEA); (b) Steam pressure at the exit of the intermediate pressure turbine in the starting up of capture plant; (c) Power demand and plant output

6.5 DYNAMICS OF CAPTURE PLANT AND POWER PLANT IN SWITCHING CAPTURE LOADS

The dynamic response of a power plant while the capture plant is engaged and in operation is reported in this section. As small variations of the steam temperature in the regenerator reboiler system exist after the normal working condition is successfully established, the relationship of variations between the flow rate of the flue gas, lean amine and steam demand are relatively linear at different capture levels therefore the dynamic response of the capture plant is relatively simple. Apart from the steady state study, simulation study that is switched from one capture load to another is carried out for the study of a capture plant dynamic process. The dynamic response of the capture plant and the power plant from starting up is illustrated in Figure 6-12. An initial capture load at 30% of the flue gas is given to an idle capture plant and then the target is increased to 40% and 50% after the system is stabilized.

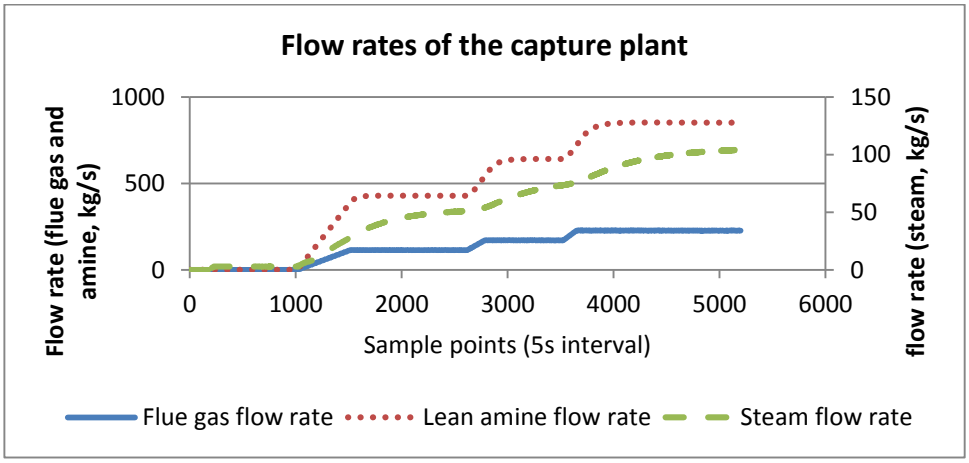

(a)

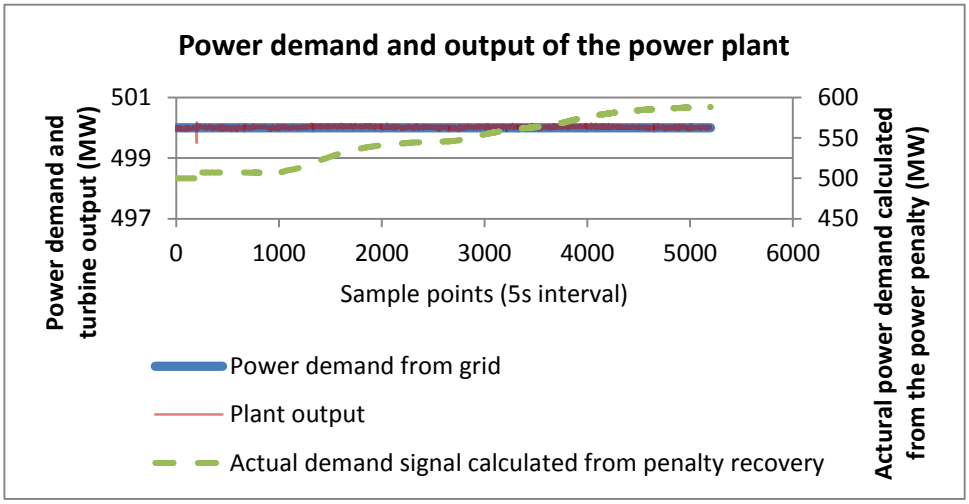

(b)

Figure 6-12: (a) Flow rates of the capture plant for 30% capture rate on a supercritical power plant with 500MW power output (30%, 0.29mol/mol MEA); (b) Power demand and plant output

Similar results can be obtained in Figure 6-13 that represents the increasing capture load from 60% to 70% of the CO_2 generated from the power plant. From the simulation result it can be proved that the power plant is capable to deliver a fast response to satisfy both the power demand and the heat required by the post combustion carbon capture with the penalty recovery strategy and the control of the steam pressure stabilization valve located at the entrance of the low pressure turbine.

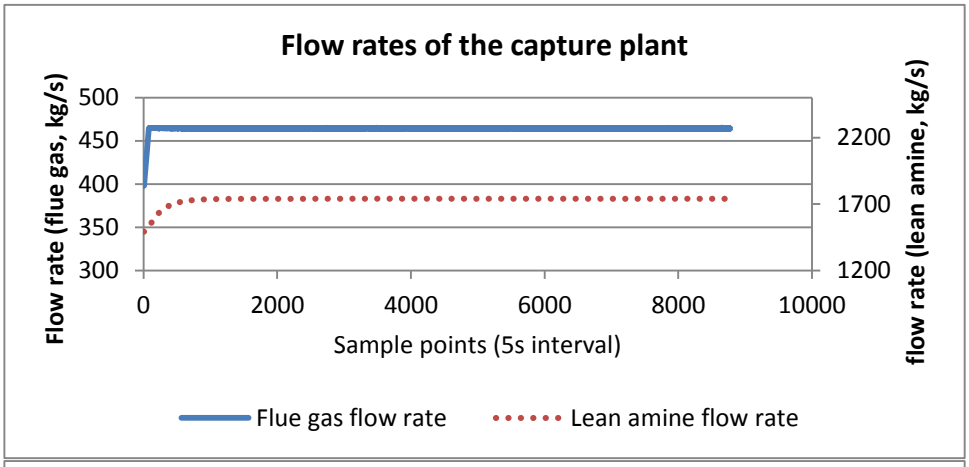

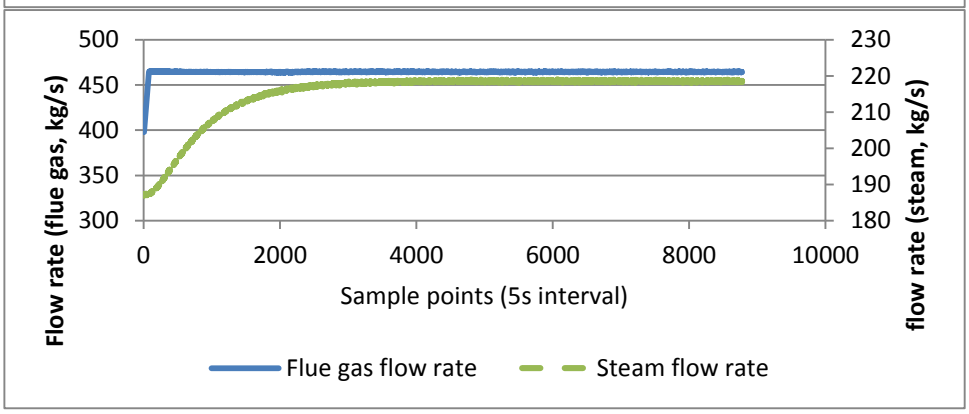

(a)

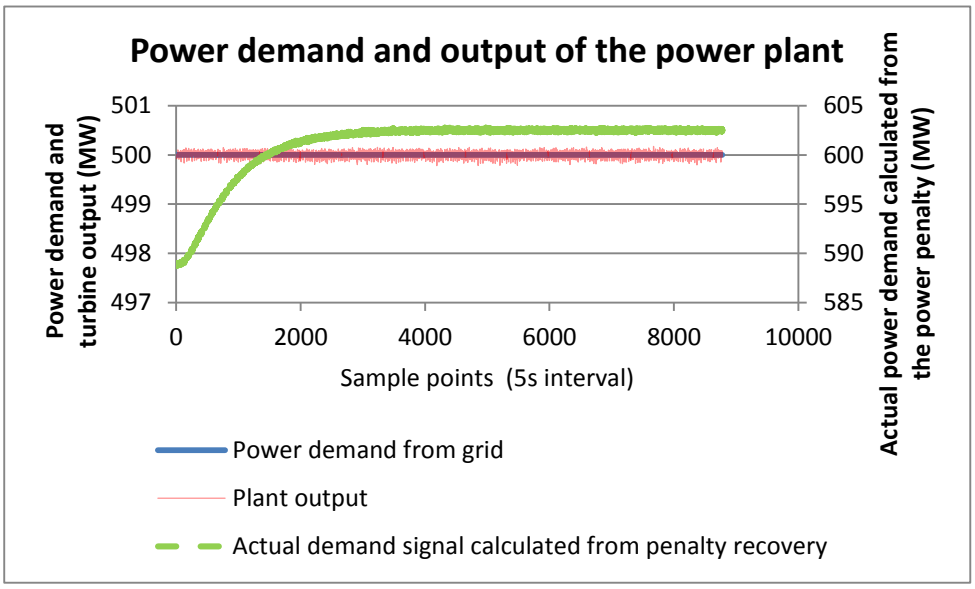

(b)

Figure 6-13: (a) flow rates of the capture plant for 30% capture rate on a supercritical power plant with 500MW power output (30%, 0.29mol/mol MEA); (b) Power demand and plant output

6.6 SUMMARY

A simplified starting up procedure of the capture plant was designed and implemented in a simulation environment to mimic the real power plant operation process. This provides a unique platform for initial test of different capture and control strategies before a real capture plant is built. Based on this procedure the steam demand and the dynamic response of the carbon capture process are studied. The steam is drawn from the steam turbine system to meet the steam demand therefore retrofit of channelling steam out for capture has been carried out on the simulator to study the impact of steam extraction on power plant dynamic responses. Simulation study shows that the output power will have a sudden drop when the steam is extracted to the capture plant, which has a very high agreement with the flow rate of the steam drawn out of the turbine system.

The power output of an industrial power plant must meet the power demand to maintain the stability of the grid which means that the power penalty caused by the steam loss must be compensated. In this project a power penalty recovery control strategy has been developed by adding a compensation value to the power penalty to the control signal of the power demand. Simulation results show that the capture load needs to be limited to 20% of the flue gas as the steam pressure becomes unstable when the limit is broken. To achieve capture over 20%, a throttle valve is introduced at the low pressure turbine for control purpose. With this throttle valve implemented, simulation results show that dynamic responses of the power plant can be greatly improved while the capture load

gradually increases and the dynamic response of the power plant with the penalty recovery strategy is fast enough to satisfy both the heat duty of the capture plant and the power demand.

Chapter 7.

CONCLUSIONS AND SUGGESTED FUTURE RESEARCH

Carbon capture and storage in coal fired power generation is recognised to be one of key technologies in reducing CO_2 emissions for the next few decades. The thesis aims to investigate the impact of carbon capture process on plant dynamic responses.

A power plant simulator is studied in this thesis and its functions are enhanced from the fuel preparation modelling. Simulation study of post combustion carbon capture has been carried out and a procedure that estimates the steam required to start a capture plant from idle is proposed in the thesis and the dynamic response of a power plant with the steam drawn from the turbine to satisfy this steam demand is studied.

This chapter is dedicated to summarize the completed work and the contribution made in the PhD research. Some suggestions for future research directions are given.

7.1 CONCLUSIONS

The main contributions reported in the thesis are summarized below:

1. Two simulation approaches of a power plant, including the first principle model and the fluidic network simulator, have been reviewed for simulation study of supercritical power generation process. Comparison of these two methods are carried out and the simulator employed to represent the reference plant in this project.
2. The process of coal preparation in the coal mill has been studied and a dynamic mathematical model of the mill has been developed based on first principle and empirical equations.
3. A software has been developed for on-line implementation of mill model, by which the adaptive parameter algorithms can be re-identified by the measured site data whenever necessary. Monitoring these parameters and the intermediate variables estimated in the model provides the capability to predict potential risks of incidents.
4. Different post combustion CO_2 capture techniques were reviewed in this thesis. The modular mathematical model of the post combustion capture plant is designed and implemented in the software platform of the simulator.

5. The mathematical model of the capture plant has been connected to the simulator. Steam from the the junction between the intermediate and the low pressure turbines are extracted to satisfy the heat demand of the reboiler.
6. A simplified starting up procedure of the capture plant has been proposed in this thesis which estimates the steam demand of the capture plant. The impact on plant dynamics from the integration of post combustion carbon capture has been studied from a series of experiments based on different steam loads.
7. The combination of the capture process and the generation quality has been studied. By retrofitting the plant design and introducing the power penalty recovery strategies, the simulator is able to start the capture plant without sacrificing the load and the system stability.

7.2 RECOMMENDATIONS OF FUTURE RESEARCH

Although a lot of simulation studies have been carried out on the dynamic response of power plant with post combustion capture, the thesis has not covered some challenging topics which can be studied in the future research and development in this area. From the research conducted, the following recommendations can be made:

1. The absorption capability of the lean amine in this thesis is supposed to work at the ideal condition which means the CO_2 load of the rich amine can reach up to 0.5 mol/mol. But this is not realistic in the real packing

progress and theoretically the faster the amine and flue gas flows, the lower capture load the amine can provide, which means the steam duty increases faster than the flow rate of flue gas when the capture load rises. As a result one possible research direction can be focused on the study of the packing efficiency in different the flow rate of fluid to achieve a more accurate estimation of the required steam.

2. The designed starting up procedure of capture plant introduced in this thesis only targets to establish normal working condition of regenerator so this procedure is simplified as much as possible. As a heat transfer problem the control of this process has a relatively long delay. Additionally neither the efficiency nor the safety is carefully considered therefore it cannot represent the actual control process as the industrial capture plant. Based on these considerations, another research direction that worth considering is to design better and proper starting up of capture plant.
3. The frequency regulation of the power plant to the power grid plays a very important role in the generation control. Frequency response is usually added to the demand command to maintain the rotate speed of the turbine shaft at 3000 rpm. Additionally decided by the customers, the power demand from the grid also changes from time to time. There is a potential that these two problems may affect the dynamic response of power plant therefore more research activities can be focused on this relationships.

As the studies of the dynamic response of the power plant and the capture plant is studied in the simulator environment prior to a plant being built, the work achieved in this project can also provide some guidance suggestions to the development and design of the capture plant, and additionally, can give some initial investigations of the power plant retrofit in the plant structure and the control strategies.

References:

ABDENNOUR, A. 2000. An intelligent supervisory system for drum type boilers during severe disturbances. *International Journal of Electrical Power & Energy Systems,* 22**,** 381-387.

AFKHAMIPOUR, M. & MOFARAHI, M. 2013. Comparison of rate-based and equilibrium-stage models of a packed column for post-combustion CO2 capture using 2-amino-2-methyl-1-propanol (AMP) solution. *International Journal of Greenhouse Gas Control,* 15**,** 186-199.

AHN, H., LUBERTI, M., LIU, Z. & BRANDANI, S. 2013. Process Simulation of Aqueous MEA Plants for Post-combustion Capture from Coal-fired Power Plants. *Energy Procedia.*

AL-BAGHLI, N. A., PRUESS, S. A., YESAVAGE, V. F. & SELIM, M. S. 2001. A rate-based model for the design of gas absorbers for the removal of CO2 and H2S using aqueous solutions of MEA and DEA. *Fluid Phase Equilibria,* 185**,** 31-43.

Anon 2008. Climate Change Act 2008. *In:* LEGISLATION.GOV.UK (ed.). The National Archives.

Anon 2010. U.S. Climate Action Report 2010. Washington: United States Department of State.

ARMITAGE, P. 1983. Methods of improving the performance of the John Thompson air swept suction tube ball mills and associated equipments. EDF Energy Internal Report.

ARTANTO, Y., JANSEN, J., PEARSON, P., DO, T., COTTRELL, A., MEULEMAN, E. & FERON, P. 2012. Performance of MEA and amine-blends in the CSIRO PCC pilot plant at Loy Yang Power in Australia. *Fuel.*

BEÉR, J. 2007. High Efficiency Electric Power Generation: The Environmental Role. *Progress in Energy and Combustion Science.*

BEN-ABDENNOUR, A., LEE, K. Y. & EDWARDS, R. M. 1993. Multivariable robust control of a power plant deaerator. *Energy Conversion, IEEE Transactions on,* 8**,** 123-129.

BHOWN, A. S. & FREEMAN, B. C. 2011. Analysis and Status of Post-Combustion Carbon Dioxide Capture Technologies. *Environmental Science & Technology.*

BILLC 2006. A coal-fired thermal power station.

BOND, G. M., STRINGER, J., BRANDVOLD, D. K., SIMSEK, F. A., MEDINA, M.-G. & EGELAND, G. 2001. Development of Integrated System for Biomimetic CO2 Sequestration Using the Enzyme Carbonic Anhydrase. *Energy & Fuels,* 15**,** 309-316.

BORGNAKKE, C. & SONNTAG, R. E. 2009. *Fundamentals of Thermodynamics*, John Wiley & Sons, Inc.

BP 2014. BP Statistical Review of World Energy 2014. BP.

BROWNE, A. 2014. *Technical and Economic Optimisation of Post Combustion Carbon Capture by Aqueous Amine Absorption.* Engineering Doctoral Degree, University of Nottingham.

CDIAC n.d. Carbon Dioxide emissions (CO2), thousand metric tons of CO2 (CDIAC). *Millennium Development GoalS Indicators.*

CHAIBAKHSH, A., GHAFFARI, A. & MOOSAVIAN, S. A. A. 2007. A simulated model for a once-through boiler by parameter adjustment based on genetic algorithms. *Simulation Modelling Practice and Theory,* 15**,** 1029-1051.

CHEN, Y.-J. & LI, M.-H. 2001. Heat Capacity of Aqueous Mixtures of Monoethanolamine with 2-Amino-2-methyl-l-propanol. *Journal of Chemical & Engineering Data.*

CHEN, Y.-J., SHIH, T.-W. & LI, M.-H. 2001. Heat Capacity of Aqueous Mixtures of Monoethanolamine with N-Methyldiethanolamine. *Journal of Chemical & Engineering Data.*

CHEN, Y., CAO, Y., SUN, X., YAN, C. & MU, T. 2013. New criteria combined of efficiency, greenness, and economy for screening ionic liquids for CO2 capture. *International Journal of Greenhouse Gas Control,* 16**,** 13-20.

CHENG, L., ZHANG, L., CHEN, H. & GAO, C. 2006. Carbon dioxide removal from air by microalgae cultured in a membrane-photobioreactor. *Separation and Purification Technology,* 50**,** 324-329.

CHISHOLM, D. 1980. *Developments in Heat Exchanger Technology,* Applied Science Publishers.

DILMORE, R., GRIFFITH, C., LIU, Z., SOONG, Y., HEDGES, S. W., KOEPSEL, R. & ATAAI, M. 2009. Carbonic anhydrase-facilitated CO2 absorption with polyacrylamide buffering bead capture. *International Journal of Greenhouse Gas Control,* 3**,** 401-410.

DUGAS, R. E. 2006. *Pilot plant study of carbon dioxide capture by aqueous monoethanolamine.* M.S.E, University of Texas at Austin.

EIA 2013. International Energy Outlook 2013. Washington, DC,: U.S. Department of Energy.

EITELBERG, E. & BOJE, E. 2004. Water circulation control during once-through boiler start-up. *Control Engineering Practice,* 12**,** 677-685.

EUROPEAN COMMISSION. 2014. *Summary of the impact assessment on energy and climate policy up to 2030* [Online]. EUR-Lex. Available: http://eur-lex.europa.eu/legal-content/EN/ALL/?uri=CELEX:52014SC0016.

FAN, Y., CHENG, F., SUI, Z. & LV, C. 2000. Study on the dynamic characteristics of a 600MW supercritical once-through boiler. *Journal of Tsinghua University,* Vol.40**,** 104-107.

FAN, Y. & LV, C. 1998. Research on modeling and simulation of steam generator of supercritical once-through boiler. *Proceedings of the Chinese Society for Electrical Engineering,* Vol.18.

FAUTH, D. J., FROMMELL, E. A., HOFFMAN, J. S., REASBECK, R. P. & PENNLINE, H. W. 2005. Eutectic salt promoted lithium zirconate: Novel high temperature sorbent for CO2 capture. *Fuel Processing Technology.*

GHAFFARI, A., CHAIBAKHSH, A. & LUCAS, C. 2007. Soft computing approach for modeling power plant with a once-through boiler. *Engineering Applications of Artificial Intelligence,* 20**,** 809-819.

GLASER, A. 2011. After Fukushima: Preparing for a More Uncertain Future of Nuclear Power. *The Electricity Journal,* 24**,** 27-35.

GREEN FACTS 2012. Facts on CO2 Capture and Storage: A Summary of a Special Report by the Intergovernmental Panel on Climate Change. GreenFacts.

GU, J.-J., ZHANG, L.-Y. & LI, J.-Q. Study on mathematical model of coordinated control system for supercritical units. Machine Learning and Cybernetics, 2009 International Conference on, 12-15 July 2009 2009. 2158-2163.

GUO, S., WANG, J., WEI, J. & ZACHARIADES, P. 2014. A new model-based approach for power plant Tube-ball mill condition monitoring and fault detection. *Energy Conversion and Management,* 80**,** 10-19.

HARUN, N., NITTAYA, T., DOUGLAS, P. L., CROISET, E. & RICARDEZ-SANDOVAL, L. A. 2012. Dynamic simulation of MEA absorption process for CO2 capture from power plants. *International Journal of Greenhouse Gas Control*, 10**,** 295-309.

HAYNES, W. M. 2013. *CRC Handbook of Chemistry and Physics*, CRC Press.

HERZOG, H., MELDON, J. & HATTON, A. 2009. Advanced Post-Combustion CO2 Capture. Paper für die USamerikanische „Clean Air Task Force: 1-39.

HERZOG, H., MELDON, J. & HATTON, A. April 2009. Advanced Post-Combustion CO2 Capture. Paper für die USamerikanische „Clean Air Task Force: 1-39.

HIGMAN, C. & VAN DER BURGT, M. 2008. *Gasification (Second Edition)*, Burlington, Gulf Professional Publishing.

HIKITA, H., ASAI, S., ISHIKAWA, H. & HONDA, M. 1977. The kinetics of reactions of carbon dioxide with monoethanolamine, diethanolamine and triethanolamine by a rapid mixing method. *The Chemical Engineering Journal.*

IDEM, R., WILSON, M., TONTIWACHWUTHIKUL, P., CHAKMA, A., VEAWAB, A., AROONWILAS, A. & GELOWITZ, D. 2006. Pilot Plant Studies of the CO2 Capture Performance of Aqueous MEA and Mixed MEA/MDEA Solvents at the University of Regina CO2 Capture Technology Development Plant and the Boundary Dam CO2 Capture Demonstration Plant. *Industrial & Engineering Chemistry Research.*

IEA 2012. *Energy Technology Perspectives 2012*, OECD Publishing.

IEA 2013a. *CO2 emissions from fuel combustion: Highlights.*, Luxembourg, International Energy Agency.

IEA 2013b. *Electricity in a Climate-Constrained World: Data and Analyses*, OECD Publishing.

IEA 2014. *Energy Technology Perspectives 2014*, IEA.

INOUE, T. & AMANO, H. A Thermal Power Plant Model for Dynamic Simulation of Load Frequency Control. Power Systems Conference and Exposition, 2006. PSCE '06. 2006 IEEE PES, Oct. 29 2006-Nov. 1 2006 2006. 1442-1447.

IPCC 2005. *Carbon Dioxide Capture and Storage*, Cambridge University Press, UK. pp 431.

IPCC 2007. *Climate Change 2007: The Physical Science Basis. Contribution of Working Group I to the Fourth Assessment Report of the Intergovernmental Panel on Climate Change,* Cambridge Cambridge University press.

JIAO, Z., SURDAM, R. C., ZHOU, L. & WANG, Y. 2013. A Feasibility Study of the Integration of Geologic CO2 Storage with Enhanced Oil Recovery (CO2 Flooding) in the Ordos Basin, China. *In:* SURDAM, R. C. (ed.) *Geological CO2 Storage Characterization2013: The Key to Deploying Clean Fossil Energy Technology.* Springer New York.

KARMARKAR, M. 2006. Impact of CO2 removal on coal gasification based fuel plants. Jacobs Consultancy,.

KENIG, E. Y., SCHNEIDER, R. & GÓRAK, A. 2001. Reactive absorption: Optimal process design via optimal modelling. *Chemical Engineering Science,* 56**,** 343-350.

KITTEL, J., IDEM, R., GELOWITZ, D., TONTIWACHWUTHIKUL, P., PARRAIN, G. & BONNEAU, A. 2009. Corrosion in MEA units for CO2 capture: Pilot plant studies. *Energy Procedia.*

KOLA, V., BOSE, A. & ANDERSON, P. M. 1989. Power plant models for operator training simulators. *Power Systems, IEEE Transactions on,* 4**,** 559-565.

KONDURU, N., LINDNER, P. & ASSAF-ANID, N. M. 2007. Curbing the greenhouse effect by carbon dioxide adsorption with Zeolite 13X. *AIChE Journal.*

KUKOSKI, A. E. 1992. Ball Mill Pulverizer Design. Beijing: Foster Wheeler Energy Corporation.

KVAMSDAL, H. M., JAKOBSEN, J. P. & HOFF, K. A. 2009. Dynamic modeling and simulation of a CO2 absorber column for post-combustion CO2 capture. *Chemical Engineering and Processing: Process Intensification,* 48**,** 135-144.

LATIN, M. 1980. *Enhanced Oil Recovery (Institut Francais Du Petrole Publications),* Editions Technip.

LAWAL, A., WANG, M., STEPHENSON, P. & YEUNG, H. 2009. Dynamic modelling of CO2 absorption for post combustion capture in coal-fired power plants. *Fuel,* 88**,** 2455-2462.

LI, Y. 2009. *Research on the Dynamic Characteristics of a 600MWe Supercritical Circulationg Fluidized Bed Boiler System.* PhD, Tsinghua University.

LIU, S. 2007. Research on object-oriented graphical modeling system based on DCOSE. *Science & Technology Review*.

LIU, X.-C., CAI, R.-Z. & LV, C.-D. 2002. Simulation investigation of large-scale steam heating network. *Acta Simulata Systematica Sinica*.

LIU, Y., ZHANG, L. & WATANASIRI, S. 1999. Representing Vapor−Liquid Equilibrium for an Aqueous MEA−CO2 System Using the Electrolyte Nonrandom-Two-Liquid Mode. *Industrial & Engineering Chemistry Research.*

LU, S. 1999. Dynamic modelling and simulation of power plant systems. *Proceedings of the Institution of Mechanical Engineers, Part A: Journal of Power and Energy,* 213**,** 7-22.

LU, S. & HOGG, B. W. 2000. Dynamic nonlinear modelling of power plant by physical principles and neural networks. *International Journal of Electrical Power & Energy Systems,* 22**,** 67-78.

LUCQUIAUD, M. & GIBBINS, J. 2009. Retrofitting CO2 capture ready fossil plants with post-combustion capture. Part 1: Requirements for supercritical pulverized coal plants using solvent-based flue gas scrubbing. *Proceedings of the Institution of Mechanical Engineers, Part A: Journal of Power and Energy,* 223**,** 213-226.

LUO, Z. 1988. *Fluid network* China Machine Press.

MELZER, L. S. 2012. Carbon Dioxide Enhanced Oil Recovery (CO2-EOR): Factors Involved in Adding Carbon Capture, Utilization and Storage (CCUS) to Enhanced Oil Recovery The National Enhanced Oil Recovery Initiative (NEORI): Melzer Consulting.

MERSMANN, A., KIND, M. & STICHLMAIR, J. 2011. *Thermal separation technology: principles, methods, process design*.

MITSUI BABCOCK LTD 2002. Introduction to China of supercritical boilers and emerging CCTs. *In:* KINGDOM), D. O. T. A. I. C. C. T. P. U. (ed.). London: Department of Trade and Industry.

MOHAMED, O., WANG, J., AL-DURI, B. & GUO, S. Modeling Study of Supercritical Power Plant and Parameter Identification Using Genetic Algorithm. the World Congress on Engineering 2010, June 30 - July 2 2010 London. Newswood Limited, pp973-978.

MOHAMED, O., WANG, J., GUO, S., WEI, J., AL-DURI, B., LV, J. & GAO, Q. 2011. Mathematical Modelling for Coal Fired Supercritical Power Plants and Model Parameter Identification Using Genetic Algorithms. *In:*

AO, S.-I. & GELMAN, L. (eds.) *Electrical Engineering and Applied Computing*. Springer Netherlands.

MOHAMED, O. R. I. 2012. *Study of energy efficient supercritical coal-fired power plant dynamic responses and control strategies*. Ph.D., University of Birmingham.

MORES, P., SCENNA, N. & MUSSATI, S. 2011. Post-combustion CO2 capture process: Equilibrium stage mathematical model of the chemical absorption of CO2 into monoethanolamine (MEA) aqueous solution. *Chemical Engineering Research and Design.*

MOSER, P., SCHMIDT, S., SIEDER, G., GARCIA, H. & STOFFREGEN, T. 2011. Performance of MEA in a long-term test at the post-combustion capture pilot plant in Niederaussem. *International Journal of Greenhouse Gas Control.*

NOOA 2013. In-situ CO2 monthly averages. Maunaloa, Hawaii: US. Department of Commerce, National Oceanic and Atmospheric Administration

NORDLANDER, S. 2003. TRNSYS model for Type 210 Pellet stove with liquid heat exchanger. Borlänge: Solar Energy Research Centre, Dalarna University.

NOTZ, R., MANGALAPALLY, H. P. & HASSE, H. 2012. Post combustion CO2 capture by reactive absorption: Pilot plant description and results of systematic studies with MEA. *International Journal of Greenhouse Gas Control.*

OECD 2013. *OECD Factbook 2013: Economic, Environmental and Social Statistics*, OECD Publishing.

PACHECO, M. A. & ROCHELLE, G. T. 1998. Rate-Based Modeling of Reactive Absorption of CO2 and H2S into Aqueous Methyldiethanolamine. *Industrial & Engineering Chemistry Research,* 37**,** 4107-4117.

PERSSON, T., FIEDLER, F. & NORDLANDER, S. 2006. Methodology for identifying parameters for the TRNSYS model Type 210 -wood pellet stoves and boilers. Borlänge: Solar Energy Research Centre, Dalarna University.

RAMDIN, M., DE LOOS, T. W. & VLUGT, T. J. H. 2012. State-of-the-Art of CO2 Capture with Ionic Liquids. *Industrial & Engineering Chemistry Research,* 51**,** 8149-8177.

RAMEZAN, M. & SKONE, T. J. 2007. Carbon dioxide capture from existing coal-fired power plants.: National Energy Technology Laboratory (NETL).

RAO, A. B. 2002. Details of A Technical, Economic and Environmental Assessment of Amine - based CO 2 Capture Technology for Power Plant Greenhouse Gas Control: Appendix to Annual Technical Progress Report. Center for Energy and Environmental Studies, Carnegie Mellon University.

RAYAPROLU, K. 2009. Pulverized Fuel Firing. *Boilers for Power and Process.* CRC Press.

REN, T. & GAO, Q. 1999. Fluid network calculation in thermodynamics. Institute of Simulation & Control of Power System, Tsinghua University.

RESNIK, K. P., YEH, J. T. & PENNLINE, H. W. 2004. Aqua ammonia process for simultaneous removal of CO2, SO2 and NOx. *Int. J. Environmental Technology and Management,*.

ROCHON, E. K., JO; BJUREBY, ERIKA; JOHNSTON, PAUL; OAKLEY, ROBIN; SANTILLO, DAVID; SCHULZ, NINA; GOERNE, GABRIELA VON 2008. False Hope: Why carbon capture and storage won't save the climate Greenpeace. Amsterdam: Greenpeace International.

RUSSELL, J. 2011. *Duke CEO about plant: 'Yes, it's expensive'* [Online]. Indianapolis Star. Available: http://archive.indystar.com/article/20111027/NEWS14/110270360/star-watch-duke-energy-Edwardsport-iurc.

RWE INNOGY PLC 2000. Pulverised Fuel Mills. *Power Plant Handbook, Innogy Plc Internal Documents.* RWE Innogy Plc.

SALISBURY, J. K. 1950. *Steam Turbines and Their Cycles,* New York, John Wiley & Sons.

SEADER, J. D. & HENLEY, E. J. 2006. *Separation process principles*

SHINOHARA, W. & KODITSHEK, D. E. 1996. A simplified model based supercritical power plant controller. *35th IEEE Conference on Decision and Control.*

SKJÅNES, K., LINDBLAD, P. & MULLER, J. 2007. BioCO2 – A multidisciplinary, biological approach using solar energy to capture CO2 while producing H2 and high value products. *Biomolecular Engineering,* 24**,** 405-413.

SRINIVASAN, T. N. & GOPI RETHINARAJ, T. S. 2013. Fukushima and thereafter: Reassessment of risks of nuclear power. *Energy Policy,* 52**,** 726-736.

SYMON, C. 2013. Climate - Everyone's Business: Action, Trends and Implications for Business. European Climate Foundation.

THOMAS, G. B. & FINNEY, R. L. 1979. *Calculus and analytic geometry* Addison-Wesley.

USORO, P. B., ROUHANI, R., MEHRA, R. K. & VARAIYA, P. 1983. Power system modelling for emergency state simulation. *Mathematical Modelling,* 4**,** 143-165.

VANDEWEIJER, V., VAN DER MEER, B., HOFSTEE, C., MULDERS, F., D'HOORE, D. & GRAVEN, H. 2011. Monitoring the CO2 injection site: K12-B. *Energy Procedia,* 4**,** 5471-5478.

VOCKE, C. Supercritical Boiler Control & Operational Experience. 2007 Birmingham. Power Generation Control, 2007 IET Seminar on 29-35.

WANG, J. 2011. Can Coal Fired Generation be Cleaner? Coventry: University of Warwick.

WANG, J. & GUO, S. 2009. Study of Supercritical Coal Fired Power Plant Dynamic Responses - Start-up Funding for UK-China Collaboration Research. Birmingham: School of Electronic, Electrical and Computer Engineering, University of Birmingham.

WANG, M., LAWAL, A., STEPHENSON, P., SIDDERS, J. & RAMSHAW, C. 2011. Post-combustion CO2 capture with chemical absorption: A state-of-the-art review. *Chemical Engineering Research and Design.*

WEI, J. 2007. *Development of Coal Mill and Aggregate Load Area Models in Power System using Genetic Algorithms.* Doctor of Philosophy, The University of Liverpool.

WEI, J., WANG, J. & GUO, S. Mathematic modeling and condition monitoring of power station tube-ball mill systems. American Control Conference, 2009. ACC '09., 10-12 June 2009 2009. 4699-4704.

WEI, J., WANG, J. & WU, Q. H. 2007. Development of a Multisegment Coal Mill Model Using an Evolutionary Computation Technique. *Energy Conversion, IEEE Transactions on,* 22**,** 718-727.

WEILAND, R. H., DINGMAN, J. C. & CRONIN, D. B. 1997. Heat Capacity of Aqueous Monoethanolamine, Diethanolamine, N-

Methyldiethanolamine, and N-Methyldiethanolamine-Based Blends with Carbon Dioxide. *Journal of Chemical & Engineering Data.*

WYLEN, G. J. V., SONNTAG, R. E. & BORGNAKKE, C. 1994. *Fundamentals of Classical Thermodynamics*, John Wileys & Sons, Inc.

XIAO, D. 2006. *Coal-fired Supercritical power generation: Control systems*, China Electric Power Press.

YANG, H., XU, Z., FAN, M., GUPTA, R., SLIMANE, R. B., BLAND, A. E. & WRIGHT, I. 2008. Progress in carbon dioxide separation and capture: A review. *Journal of Environmental Sciences.*

YEH, A. C. & BAI, H. 1999. Comparison of ammonia and monoethanolamine solvents to reduce CO2 greenhouse gas emissions. *Science of The Total Environment.*

YEH, J. T., RESNIK, K. P., RYGLE, K. & PENNLINE, H. W. 2005. Semi-batch absorption and regeneration studies for CO2 capture by aqueous ammonia. *Fuel Processing Technology.*

ZHANG, Y., QUE, H. & CHEN, C.-C. 2011. Thermodynamic modeling for CO2 absorption in aqueous MEA solution with electrolyte NRTL model. *Fluid Phase Equilibria.*

ZHAO, Z., DONG, H. & ZHANG, X. 2012. The Research Progress of CO2 Capture with Ionic Liquids. *Chinese Journal of Chemical Engineering,* 20**,** 120-129.

ZIAII, S., ROCHELLE, G. T. & EDGAR, T. F. 2009. Dynamic Modeling to Minimize Energy Use for CO2 Capture in Power Plants by Aqueous Monoethanolamine. *Industrial & Engineering Chemistry Research,* 48**,** 6105-6111.

APPENDIX

SIMULATOR FLUID NETWORK FIGURES

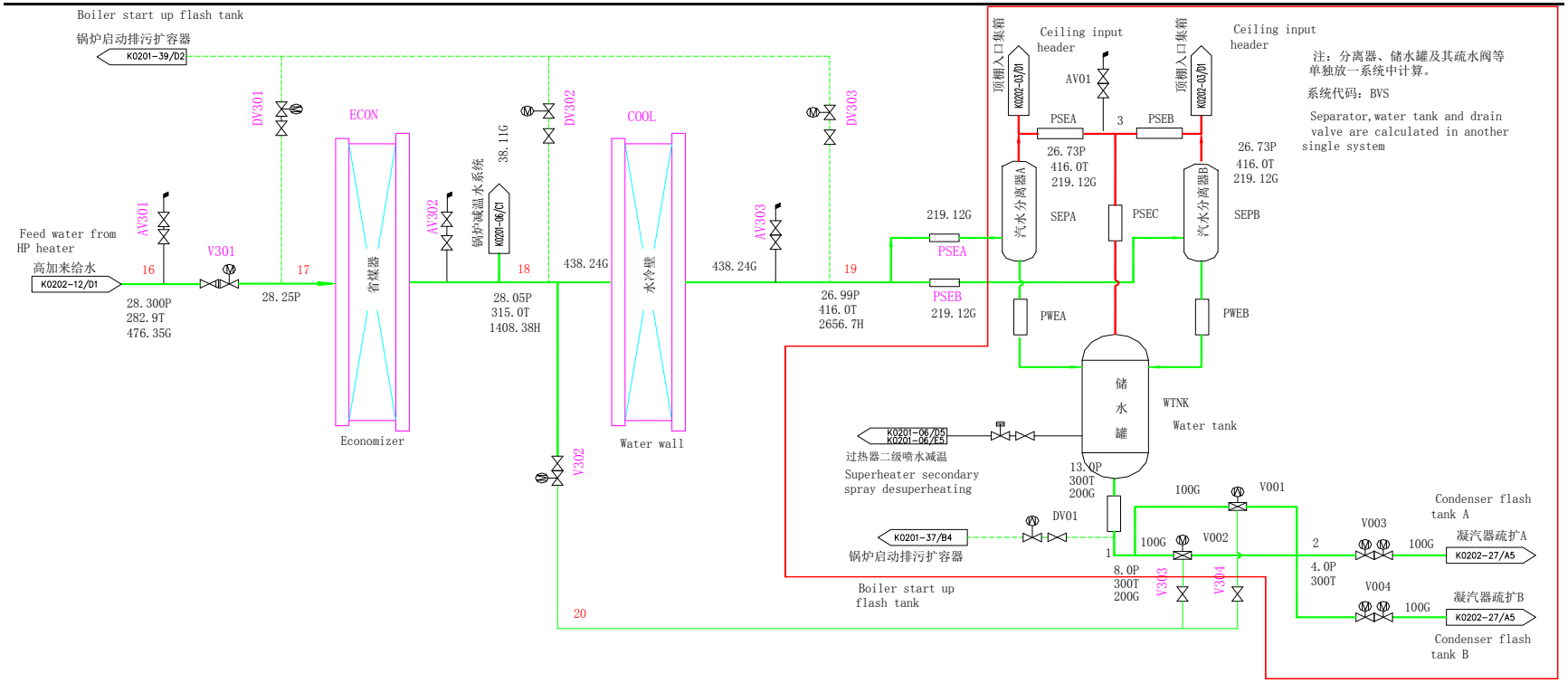

Boiler evaporation system flownet decives surrounded by red line is evaporation system

锅炉蒸发系统流体网络图
图中红线框内包含的设备为蒸发系统

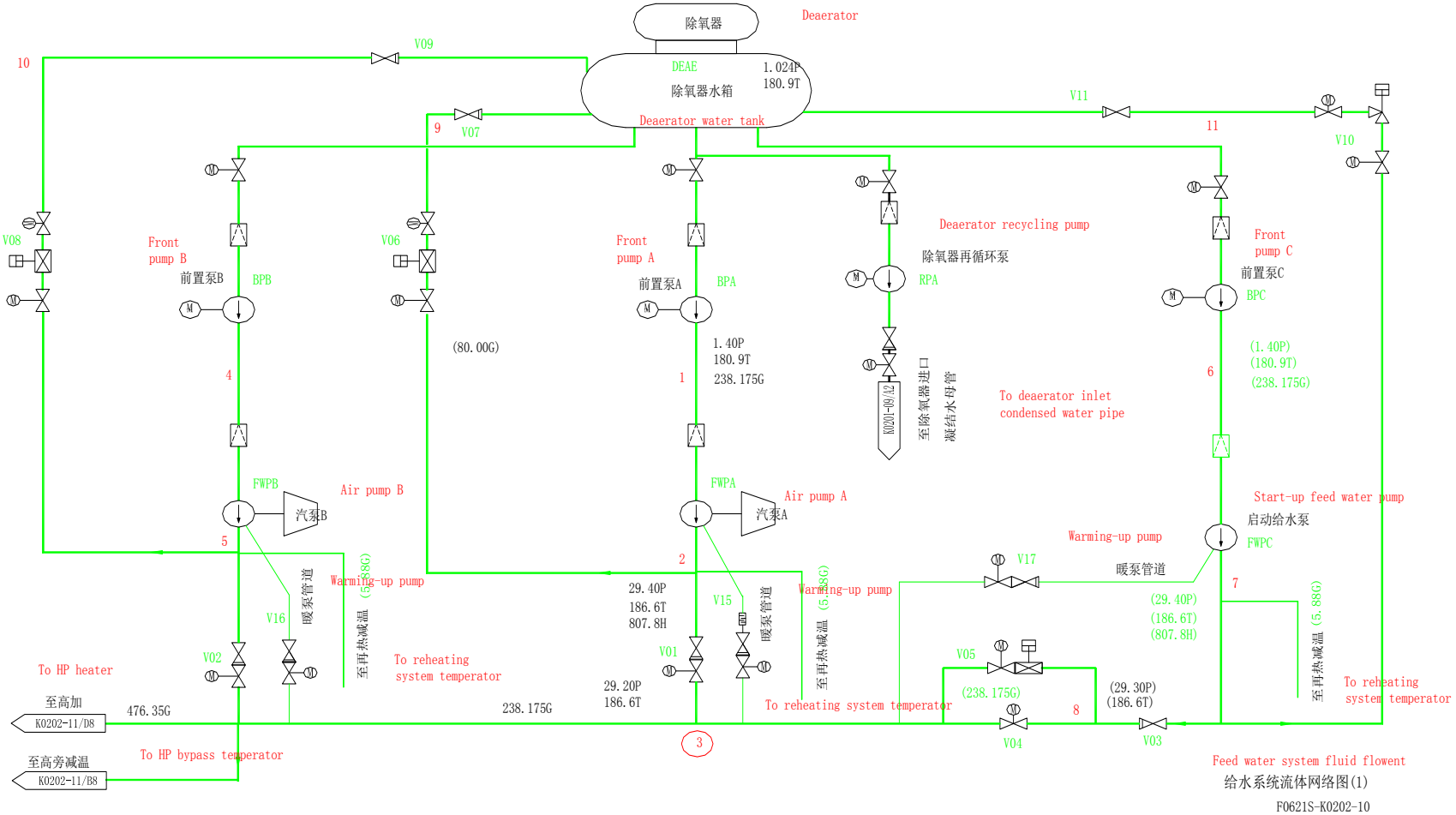

给水系统流体网络图(1)

F0621S-K0202-10

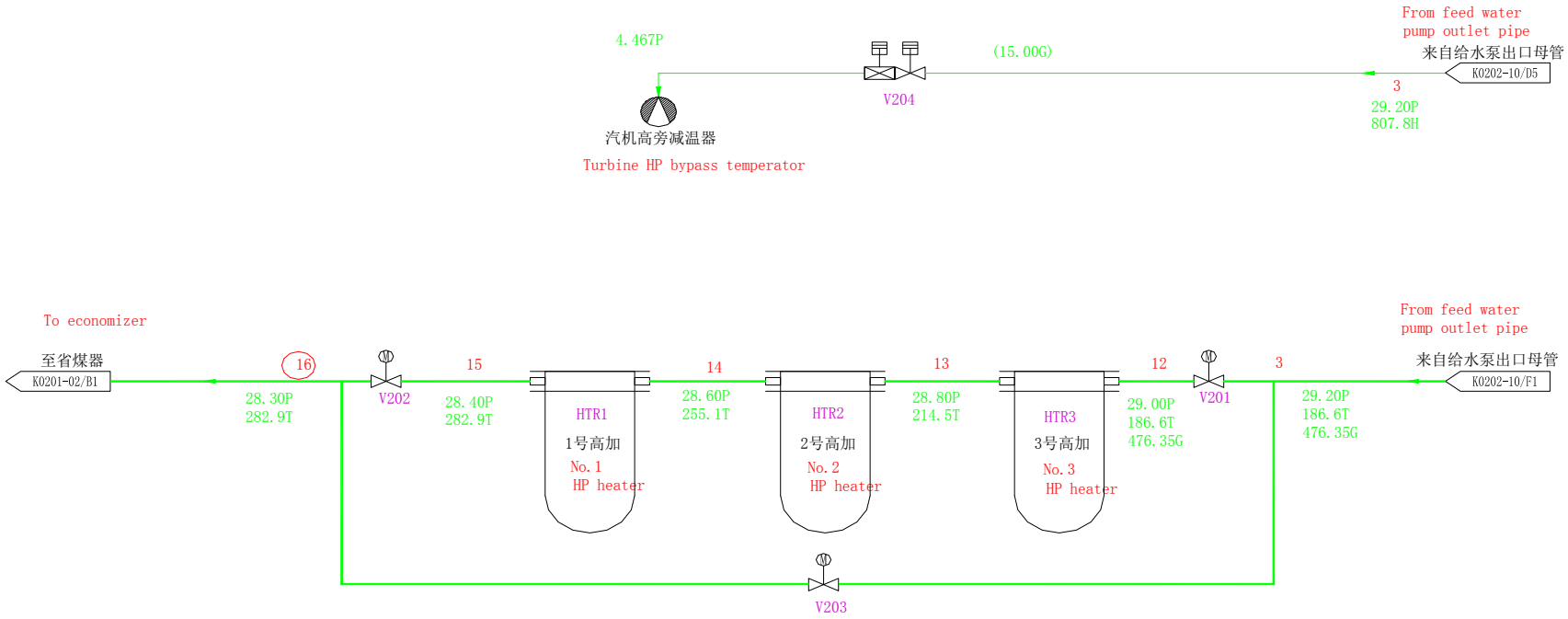

Feed water system fluid flownet

给水系统流体网络图(2)

F0621S-K0202-11

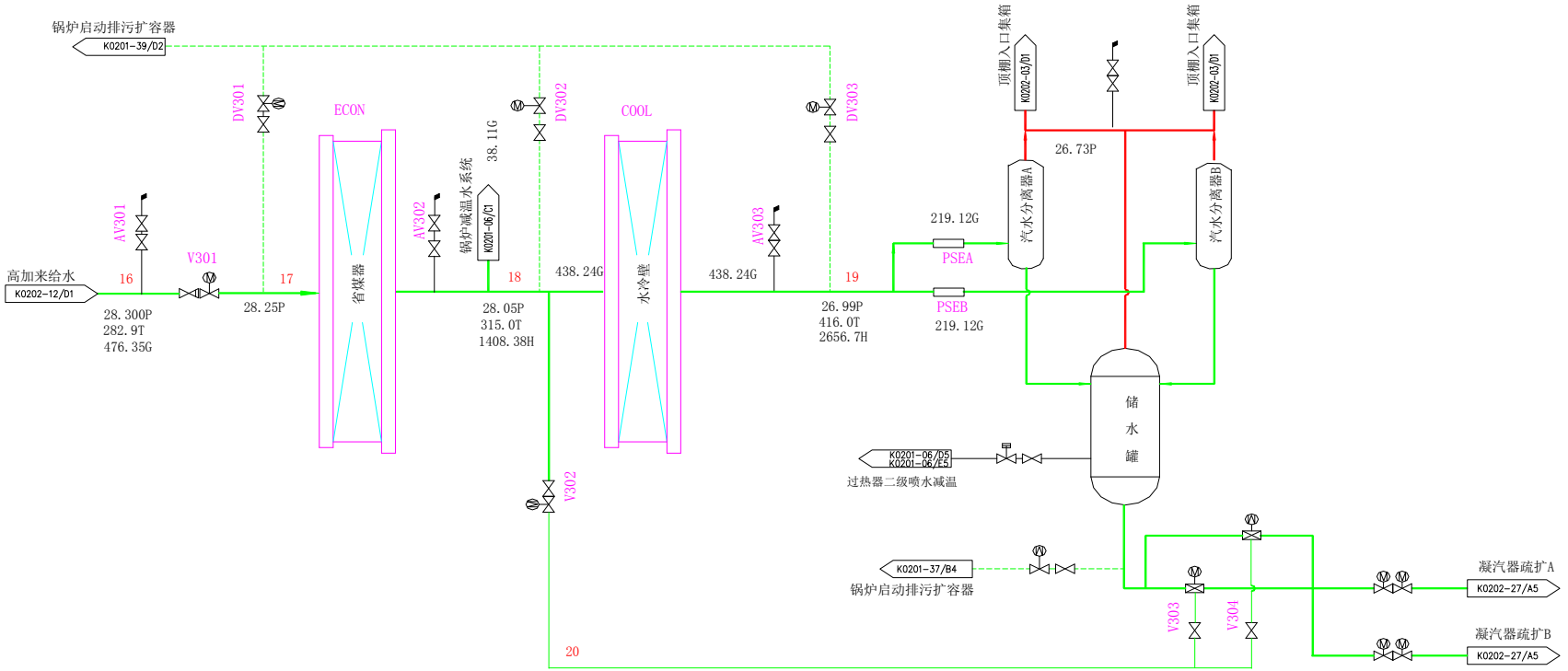

Feedwater system (3)
F0621S-K0201-02

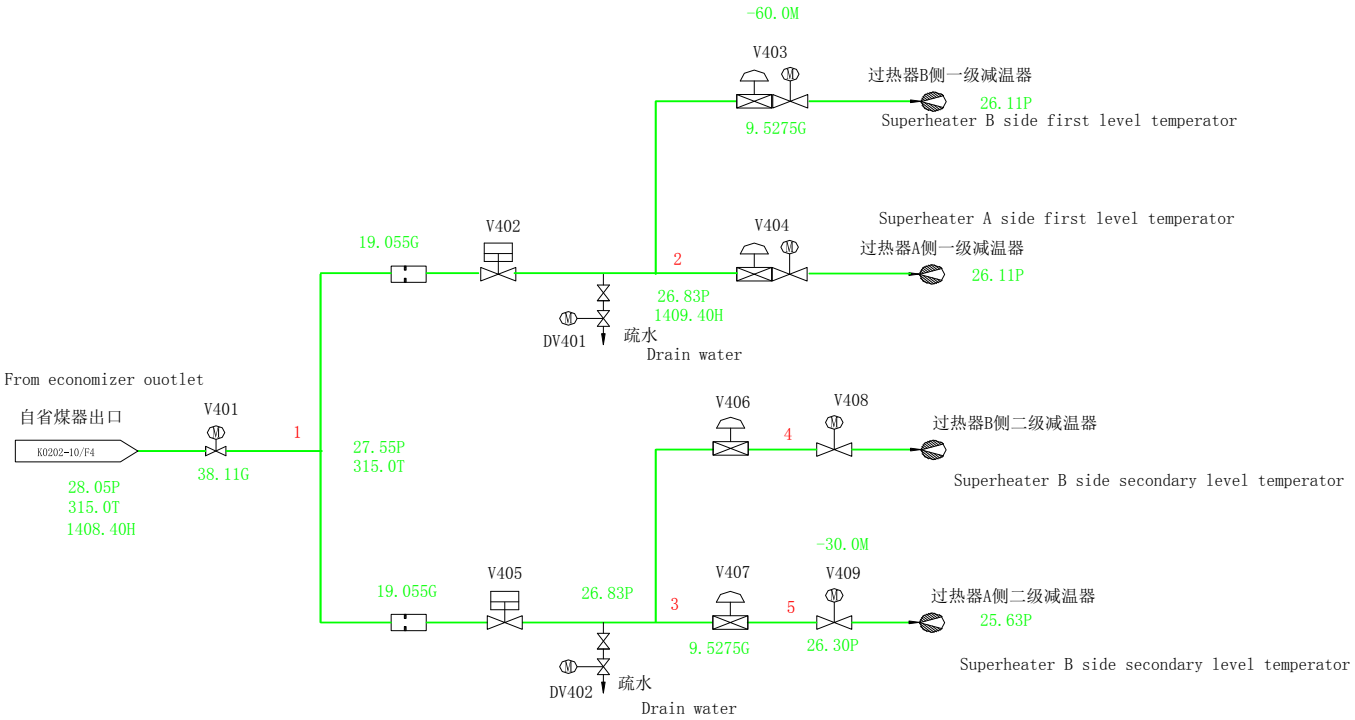

过热器减温水系统,计算时流量放大10倍
主程序：TFW2.F
Superheater cooling water system
enlarge flow rate 10 times during calculation
Main subroutine: TFW2.F

Feed water superheater
cooling water flownet
给水过热器减温水流网图（4）
F0621S-K0201-06

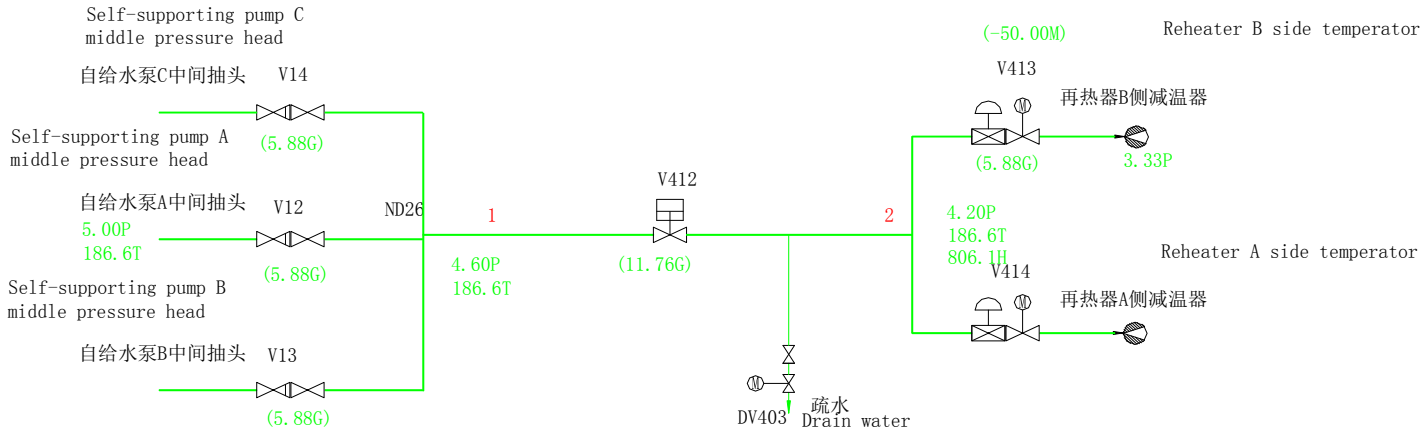

This is the reheating cooling water system,input pressure is 1/6 of the pump output pressure and calculate pressure and flowrate.
In the main programe this part is treated as leakage.
Main program name:tfw3.f, flownet preogram: tfw_net3.f
Enlarge flowrate 100 times in calculation.

注：此为再热减温水系统，进口压力取给水泵出口压力的六分之一

单独计算压力流量，在主程序中此部分流量计入泄漏处理。

主程序名：tfw3.f，流网程序：tfw_net3.f

计算时流量放大100倍

Feed water reheater
desuperheating water flownet

给水再热减温水流网图（5）

F0621S-K0201-06

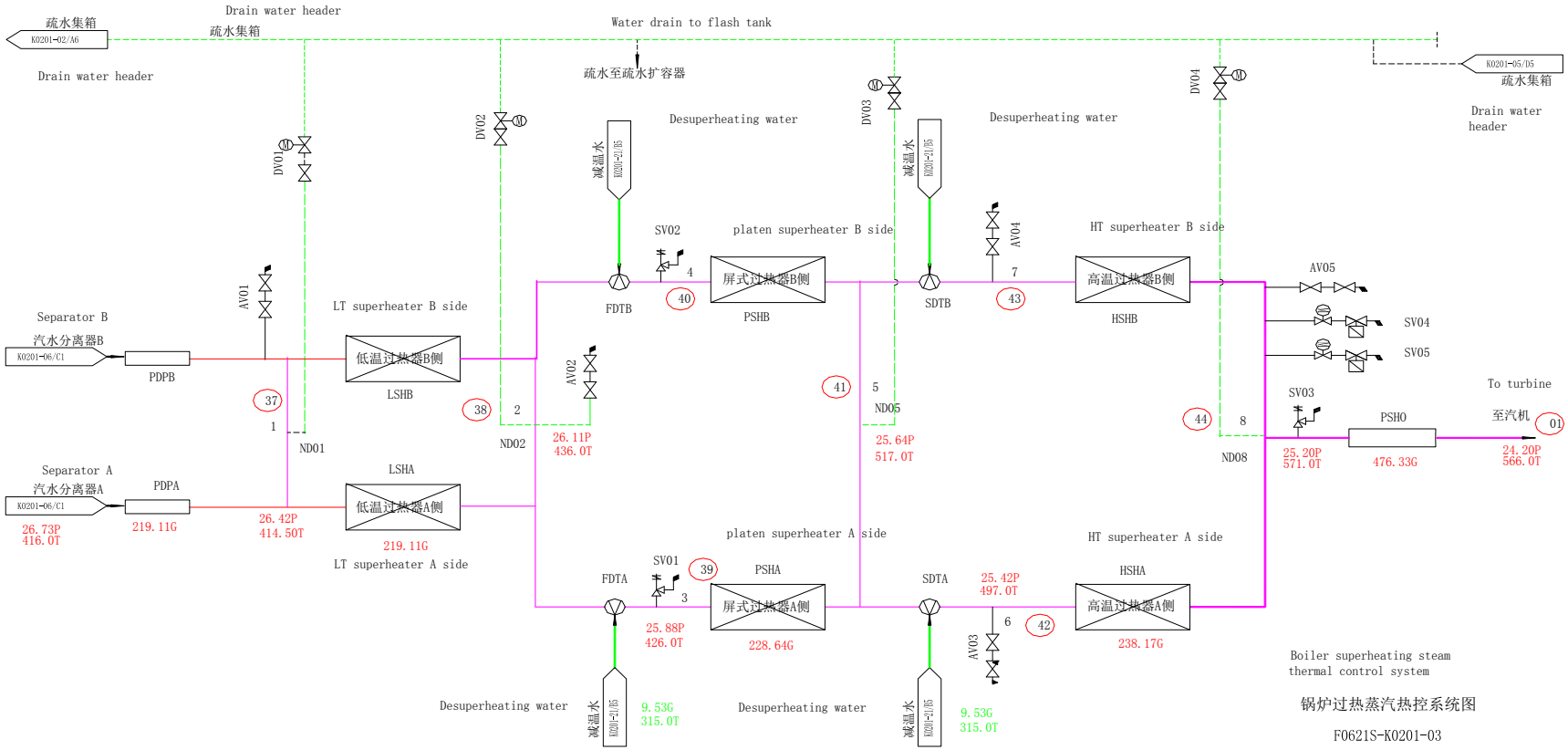
疏水集箱
K0201-02/A6
Drain water header
疏水集箱
Drain water header
Water drain to flash tank
疏水至疏水扩容器
K0201-05/D5
疏水集箱
Drain water header
DV01
DV02
DV03
DV04
减温水
K0201-21/D5
Desuperheating water
Desuperheating water
SV02
platen superheater B side
HT superheater B side
AV01
AV04
AV05
Separator B
汽水分离器B
K0201-06/C1
PDPB
LT superheater B side
低温过热器B侧
LSHB
FDTB
屏式过热器B侧
PSHB
SDTB
高温过热器B侧
HSHB
SV04
SV05
37
38
40
41
43
44
1
2
4
5
7
8
AV02
ND01
ND02
ND05
ND08
26.11P
436.0T
25.64P
517.0T
SV03
PSHO
To turbine
至汽机
01
25.20P
571.0T
476.33G
24.20P
566.0T
Separator A
汽水分离器A
K0201-06/C1
PDPA
LSHA
低温过热器A侧
LT superheater A side
26.73P
416.0T
219.11G
26.42P
414.50T
219.11G
platen superheater A side
HT superheater A side
FDTA
SV01
PSHA
屏式过热器A侧
SDTA
HSHA
高温过热器A侧
39
3
6
42
25.88P
426.0T
228.64G
25.42P
497.0T
238.17G
AV03
Desuperheating water
Desuperheating water
9.53G
315.0T
9.53G
315.0T
Boiler superheating steam
thermal control system
锅炉过热蒸汽热控系统图
F0621S-K0201-03

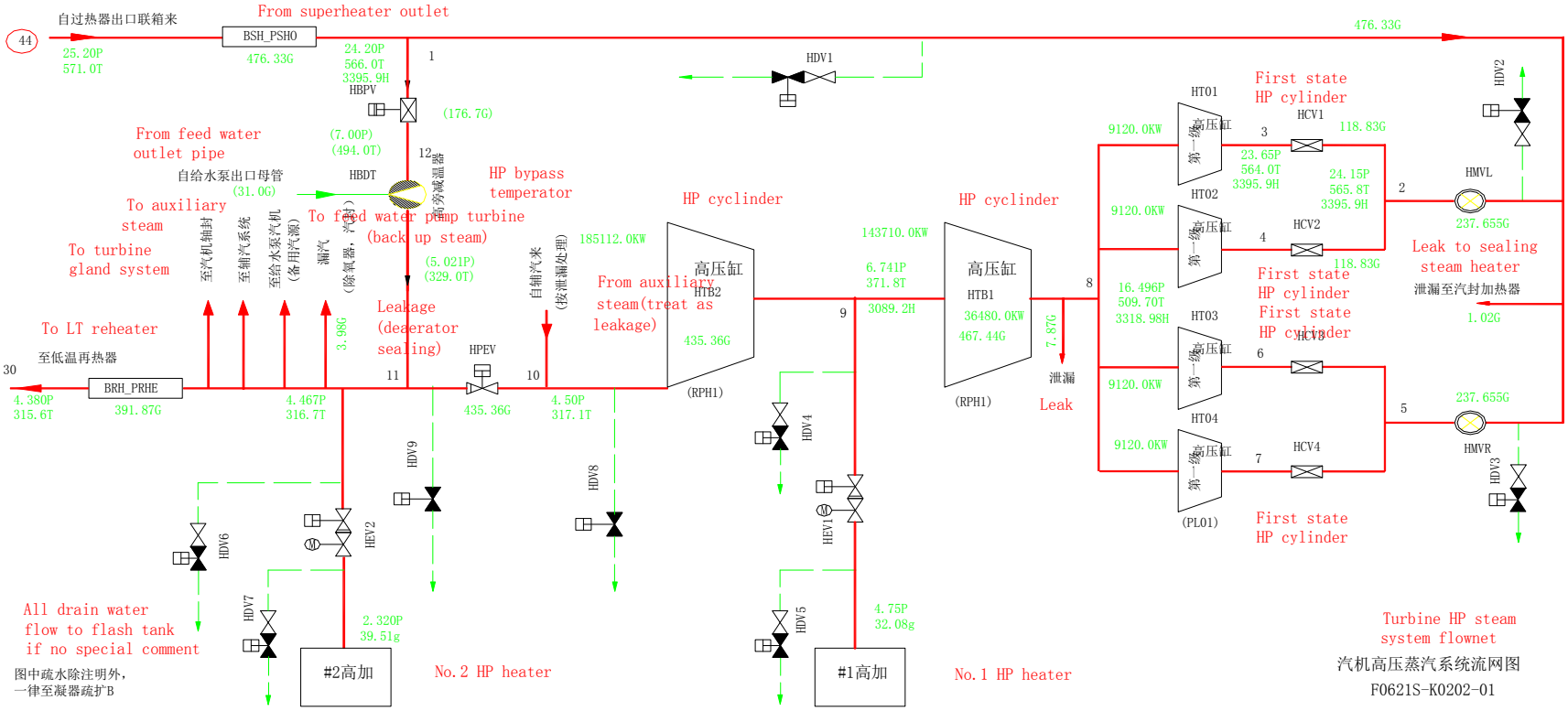
自过热器出口联箱来
From superheater outlet
44
BSH_PSH0
25.20P
571.0T
476.33G
24.20P
566.0T
3395.9H
1
HBPV
(176.7G)
HDV1
476.33G
From feed water
outlet pipe
(7.00P)
(494.0T)
12
自给水泵出口母管
(31.0G)
HBDT
HP bypass
temperator
旁路减温器
To auxiliary
steam
To feed water pump turbine
(back up steam)
To turbine
gland system
至汽机轴封
至辅汽系统
至给水泵汽机
(备用汽源)
漏汽
(除氧器，汽封)
(5.021P)
(329.0T)
自辅汽来
(按泄漏处理)
185112.0KW
HP cyclinder
From auxiliary
steam(treat as
leakage)
高压缸
HTB2
435.36G
(RPH1)
143710.0KW
6.741P
371.8T
HP cyclinder
高压缸
HTB1
36480.0KW
467.44G
(RPH1)
7.87G
泄漏
Leak
8
9
3089.2H
Leakage
(deaerator
sealing)
3.98G
To LT reheater
至低温再热器
30
BRH_PRHE
4.380P
315.6T
391.87G
4.467P
316.7T
11
HPEV
435.36G
10
4.50P
317.1T
HDV9
HDV8
HDV4
HEV1
HDV6
HEV2
HDV7
2.320P
39.51g
#2高加
No.2 HP heater
4.75P
32.08g
HDV5
#1高加
No.1 HP heater
All drain water
flow to flash tank
if no special comment
图中疏水除注明外，
一律至凝器疏扩B
HT01
HT02
HT03
HT04
第一级高压缸
(PL01)
9120.0KW
16.496P
509.70T
3318.98H
First state
HP cylinder
HCV1
HCV2
HCV3
HCV4
3
4
6
7
23.65P
564.0T
3395.9H
118.83G
24.15P
565.8T
3395.9H
118.83G
First state
HP cylinder
First state
HP cylinder
First state
HP cylinder
2
5
HMVL
HMVR
237.655G
237.655G
HDV2
HDV3
Leak to sealing
steam heater
泄漏至汽封加热器
1.02G
Turbine HP steam
system flownet
汽机高压蒸汽系统流网图
F0621S-K0202-01

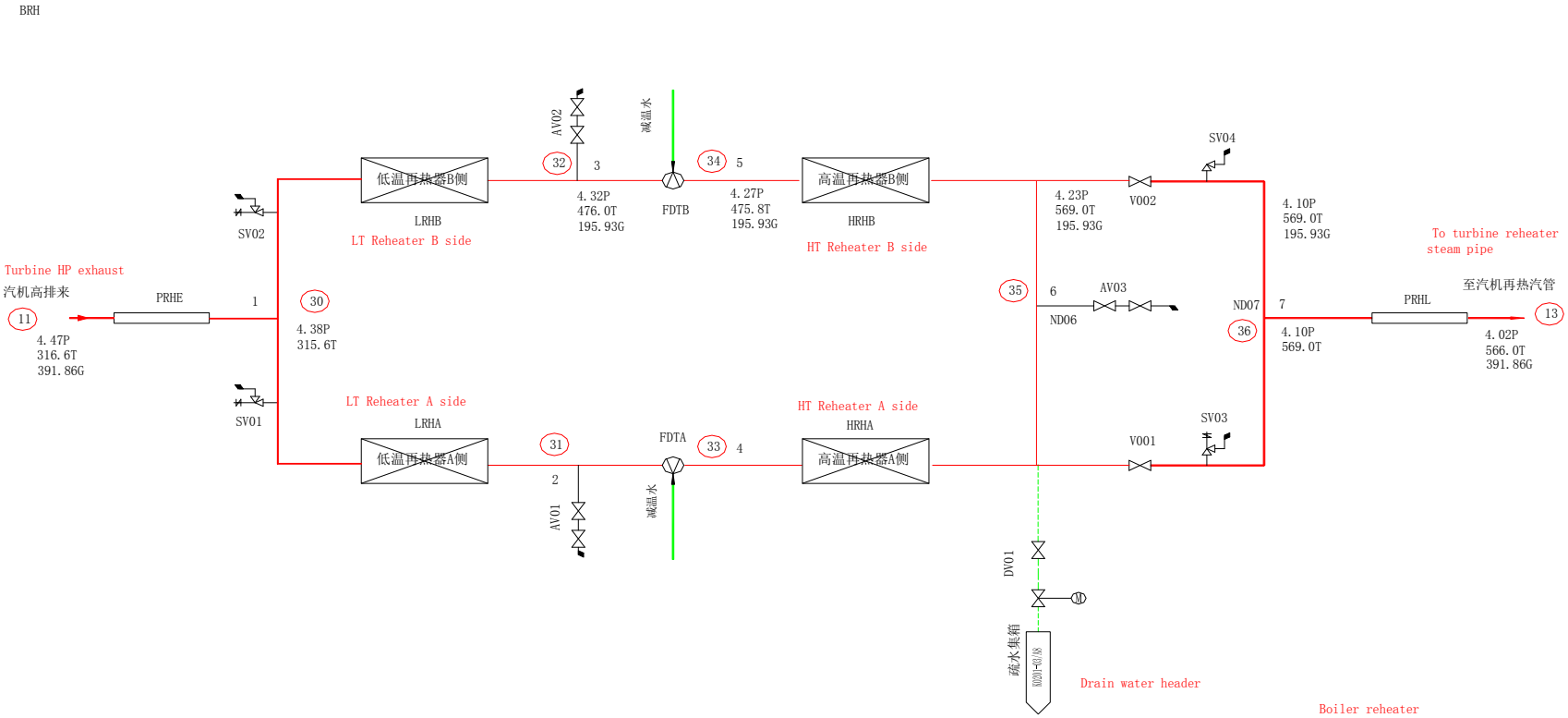
BRH
Turbine HP exhaust
汽机高排来
11
4.47P
316.6T
391.86G
PRHE
1
30
4.38P
315.6T
SV02
SV01
LT Reheater B side
低温再热器B侧
LRHB
LT Reheater A side
LRHA
低温再热器A侧
AV02
32
3
4.32P
476.0T
195.93G
AV01
31
2
减温水
FDTB
FDTA
34
5
33
4
4.27P
475.8T
195.93G
HT Reheater B side
高温再热器B侧
HRHB
HT Reheater A side
HRHA
高温再热器A侧
35
6
ND06
AV03
4.23P
569.0T
195.93G
VO02
VO01
SV04
SV03
ND07
7
36
4.10P
569.0T
195.93G
PRHL
4.10P
569.0T
195.93G
To turbine reheater
steam pipe
至汽机再热汽管
13
4.02P
566.0T
391.86G
DV01
疏水集箱
Drain water header
Boiler reheater
steam system flownet
锅炉再热蒸汽系统流网图

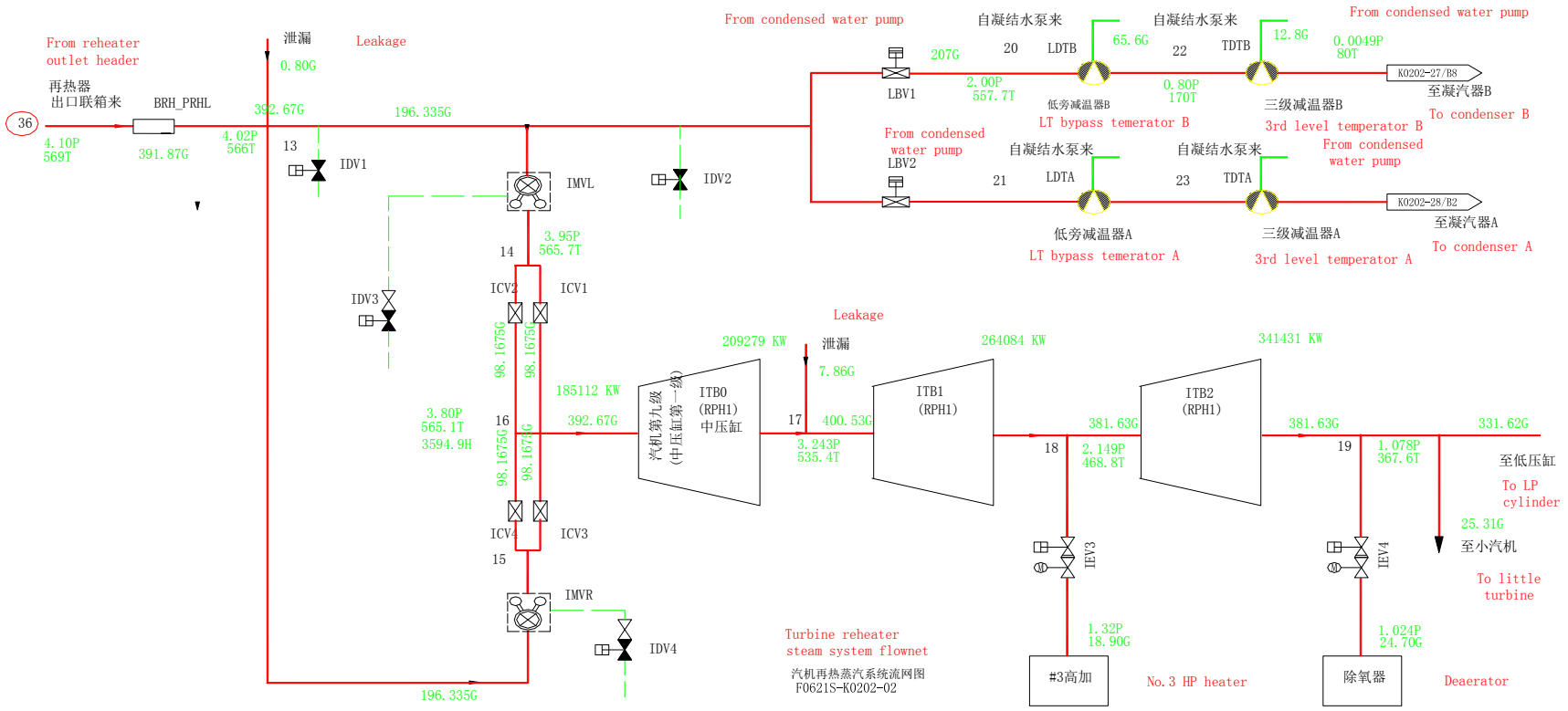
From reheater
outlet header
再热器
出口联箱来
BRH_PRHL
36
4.10P
569T
391.87G
4.02P
566T
392.67G
泄漏
0.80G
Leakage
196.335G
13
IDV1
IMVL
IDV2
3.95P
565.7T
14
ICV2
ICV1
IDV3
98.1675G
98.1675G
185112 KW
3.80P
565.1T
3594.9H
16
392.67G
98.1675G
98.1675G
ICV4
ICV3
15
IMVR
IDV4
196.335G
汽机第九级
(中压缸第一级)
ITB0
(RPH1)
中压缸
209279 KW
泄漏
7.86G
17
400.53G
3.243P
535.4T
ITB1
(RPH1)
264084 KW
381.63G
18
2.149P
468.8T
ITB2
(RPH1)
341431 KW
381.63G
19
1.078P
367.6T
331.62G
至低压缸
To LP
cylinder
25.31G
至小汽机
To little
turbine
IEV3
IEV4
1.32P
18.90G
1.024P
24.70G
#3高加
No.3 HP heater
除氧器
Deaerator
Turbine reheater
steam system flownet
汽机再热蒸汽系统流网图
F0621S-K0202-02
From condensed water pump
自凝结水泵来
207G
20
LDTB
65.6G
22
TDTB
12.8G
0.0049P
80T
K0202-27/B8
至凝汽器B
To condenser B
LBV1
2.00P
557.7T
低旁减温器B
LT bypass temerator B
0.80P
170T
三级减温器B
3rd level temperator B
From condensed
water pump
自凝结水泵来
LBV2
21
LDTA
23
TDTA
From condensed
water pump
K0202-28/B2
至凝汽器A
To condenser A
低旁减温器A
LT bypass temerator A
三级减温器A
3rd level temperator A

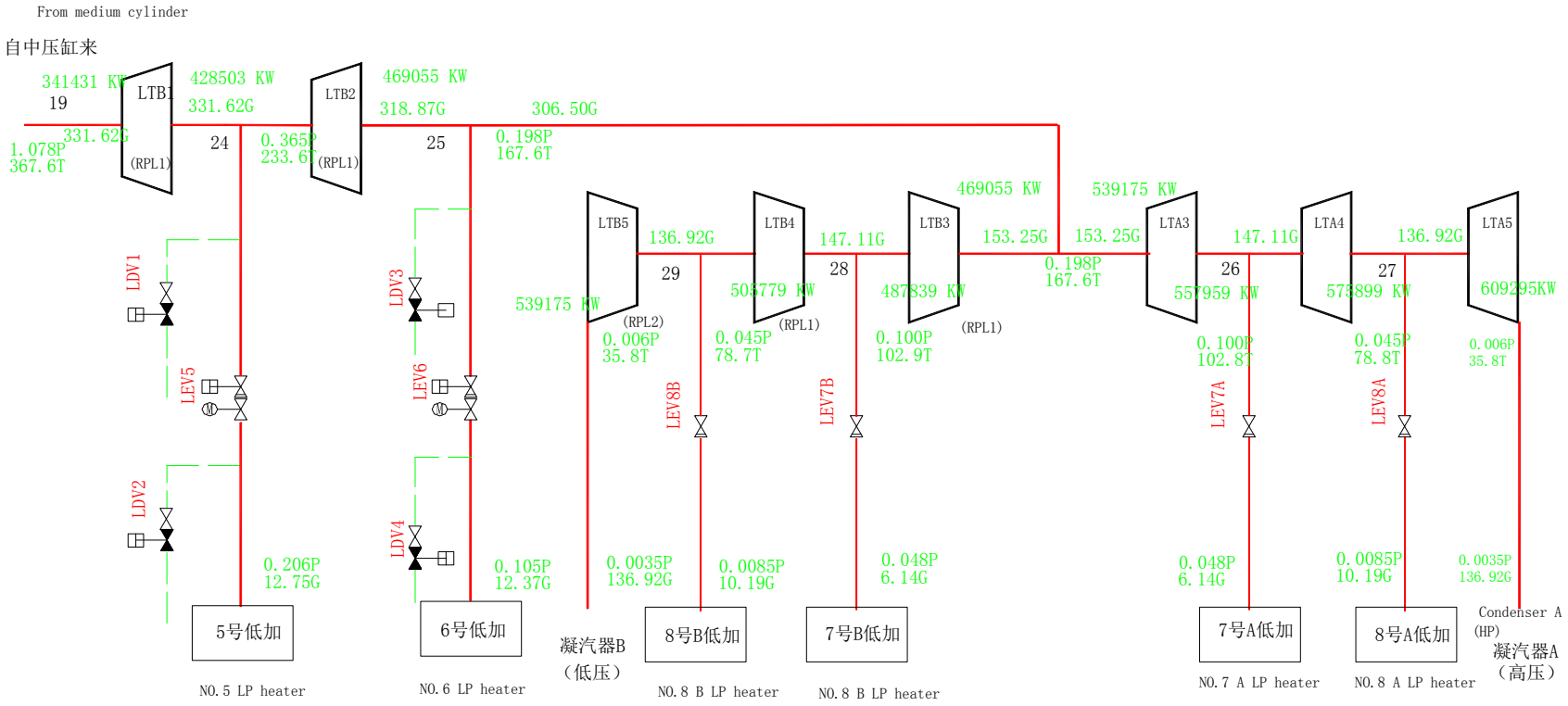

汽机主蒸汽系统流网图3

Turbine main steam system flownet

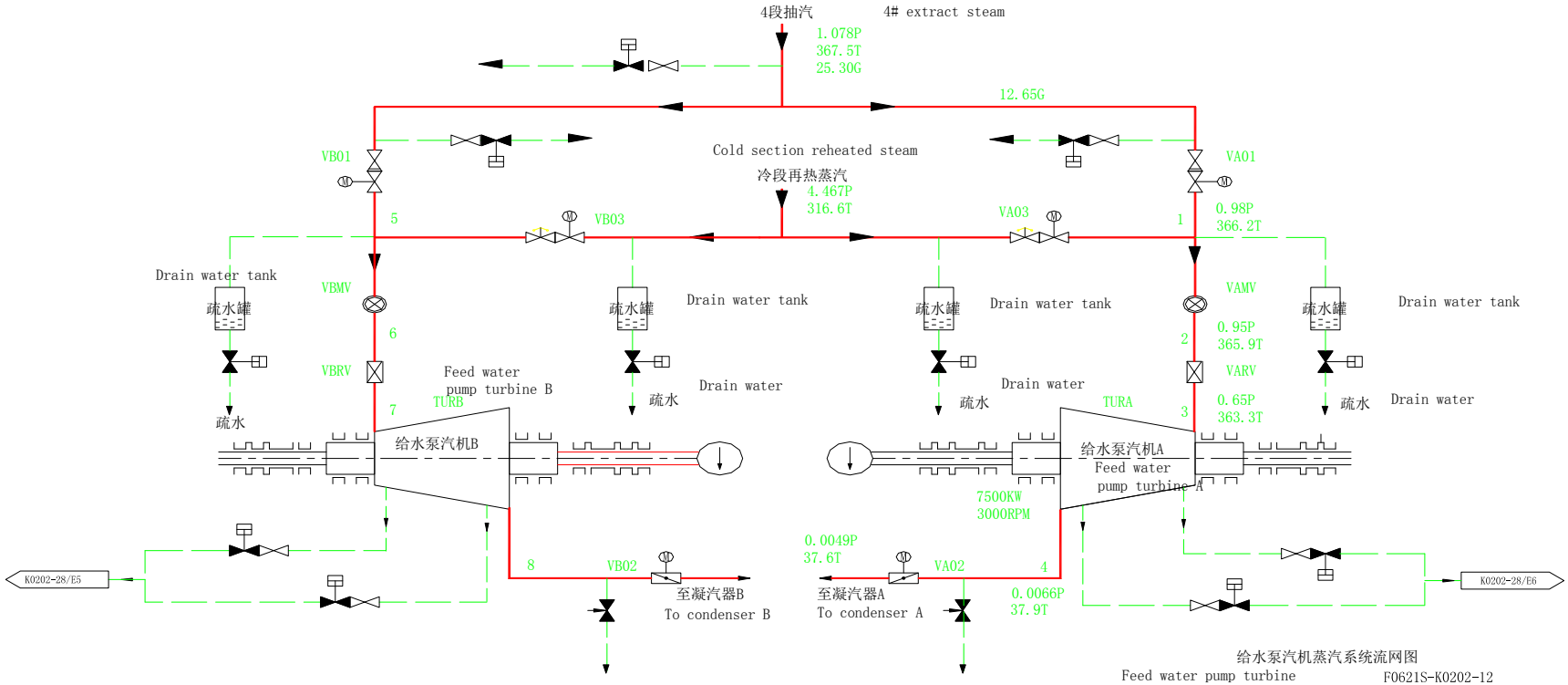
4段抽汽
4# extract steam
1.078P
367.5T
25.30G
12.65G
Cold section reheated steam
冷段再热蒸汽
4.467P
316.6T
VB01
VB03
VA01
VA03
0.98P
366.2T
5
1
Drain water tank
疏水罐
VBMV
VAMV
6
2
0.95P
365.9T
VBRV
VARV
Feed water
pump turbine B
TURB
Drain water
疏水
7
0.65P
363.3T
3
给水泵汽机B
给水泵汽机A
Feed water
pump turbine A
TURA
7500KW
3000RPM
0.0049P
37.6T
VA02
4
0.0066P
37.9T
8
VB02
至凝汽器B
To condenser B
至凝汽器A
To condenser A
K0202-28/E5
K0202-28/E6
给水泵汽机蒸汽系统流网图
Feed water pump turbine
steam system flownet
F0621S-K0202-12

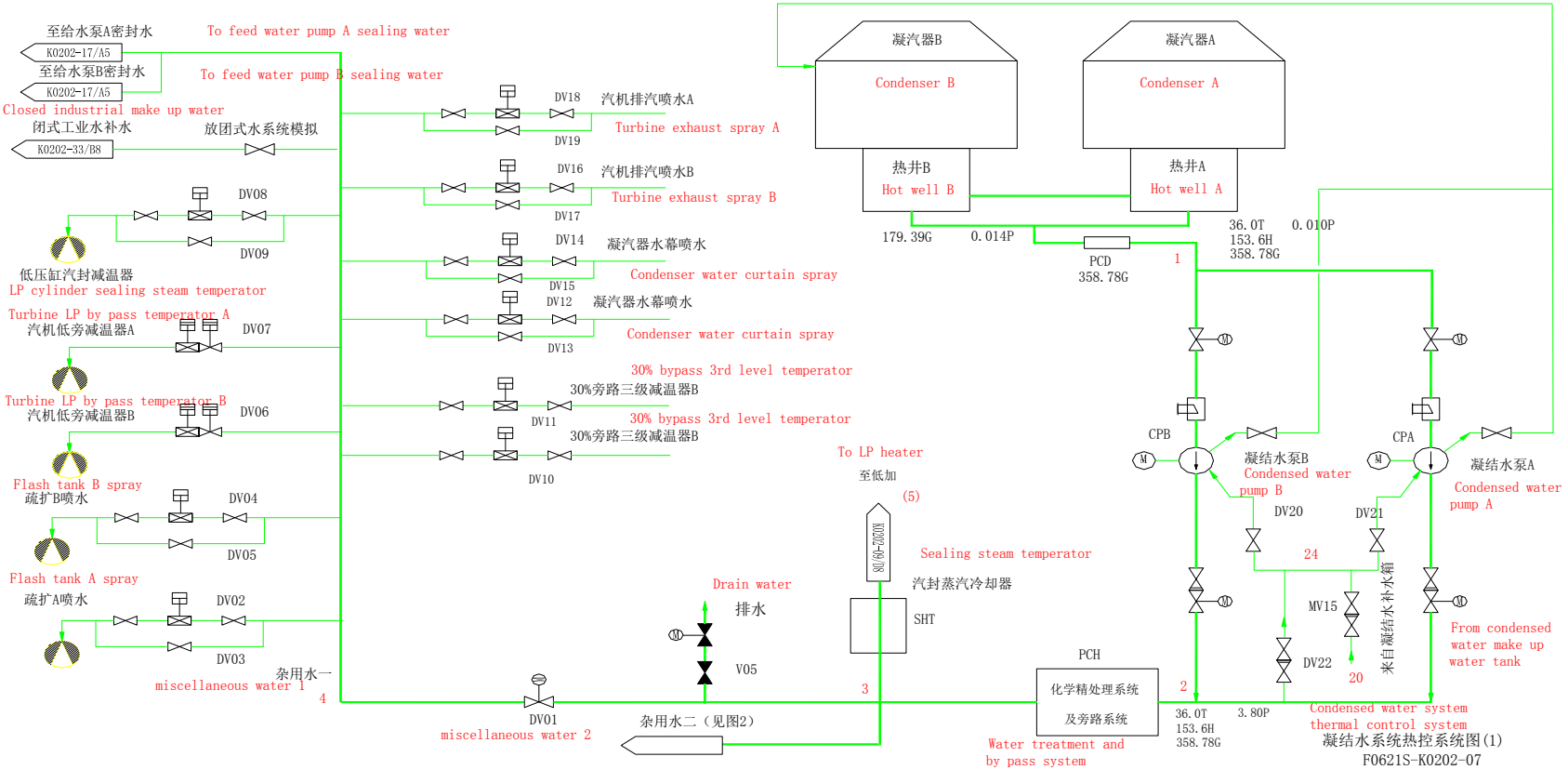
至给水泵A密封水
To feed water pump A sealing water
K0202-17/A5
至给水泵B密封水
To feed water pump B sealing water
K0202-17/A5
Closed industrial make up water
闭式工业水补水
放团式水系统模拟
K0202-33/B8
DV08
DV09
低压缸汽封减温器
LP cylinder sealing steam temperator
Turbine LP by pass temperator A
汽机低旁减温器A
DV07
Turbine LP by pass temperator B
汽机低旁减温器B
DV06
Flash tank B spray
疏扩B喷水
DV04
DV05
Flash tank A spray
疏扩A喷水
DV02
DV03
杂用水一
miscellaneous water 1
4
DV18
汽机排汽喷水A
Turbine exhaust spray A
DV19
DV16
汽机排汽喷水B
Turbine exhaust spray B
DV17
DV14
凝汽器水幕喷水
Condenser water curtain spray
DV15
DV12
凝汽器水幕喷水
Condenser water curtain spray
DV13
30% bypass 3rd level temperator
30%旁路三级减温器B
DV11
30% bypass 3rd level temperator
30%旁路三级减温器B
DV10
DV01
miscellaneous water 2
杂用水二（见图2）
Drain water
排水
V05
To LP heater
至低加
(5)
Sealing steam temperator
汽封蒸汽冷却器
SHT
3
凝汽器B
Condenser B
凝汽器A
Condenser A
热井B
Hot well B
热井A
Hot well A
179.39G
0.014P
PCD
358.78G
1
36.0T
153.6H
358.78G
0.010P
CPB
CPA
凝结水泵B
Condensed water pump B
凝结水泵A
Condensed water pump A
DV20
DV21
24
MV15
DV22
20
来自凝结水补水箱
From condensed water make up water tank
PCH
化学精处理系统
及旁路系统
Water treatment and by pass system
2
36.0T
153.6H
358.78G
3.80P
Condensed water system thermal control system
凝结水系统热控系统图(1)
F0621S-K0202-07

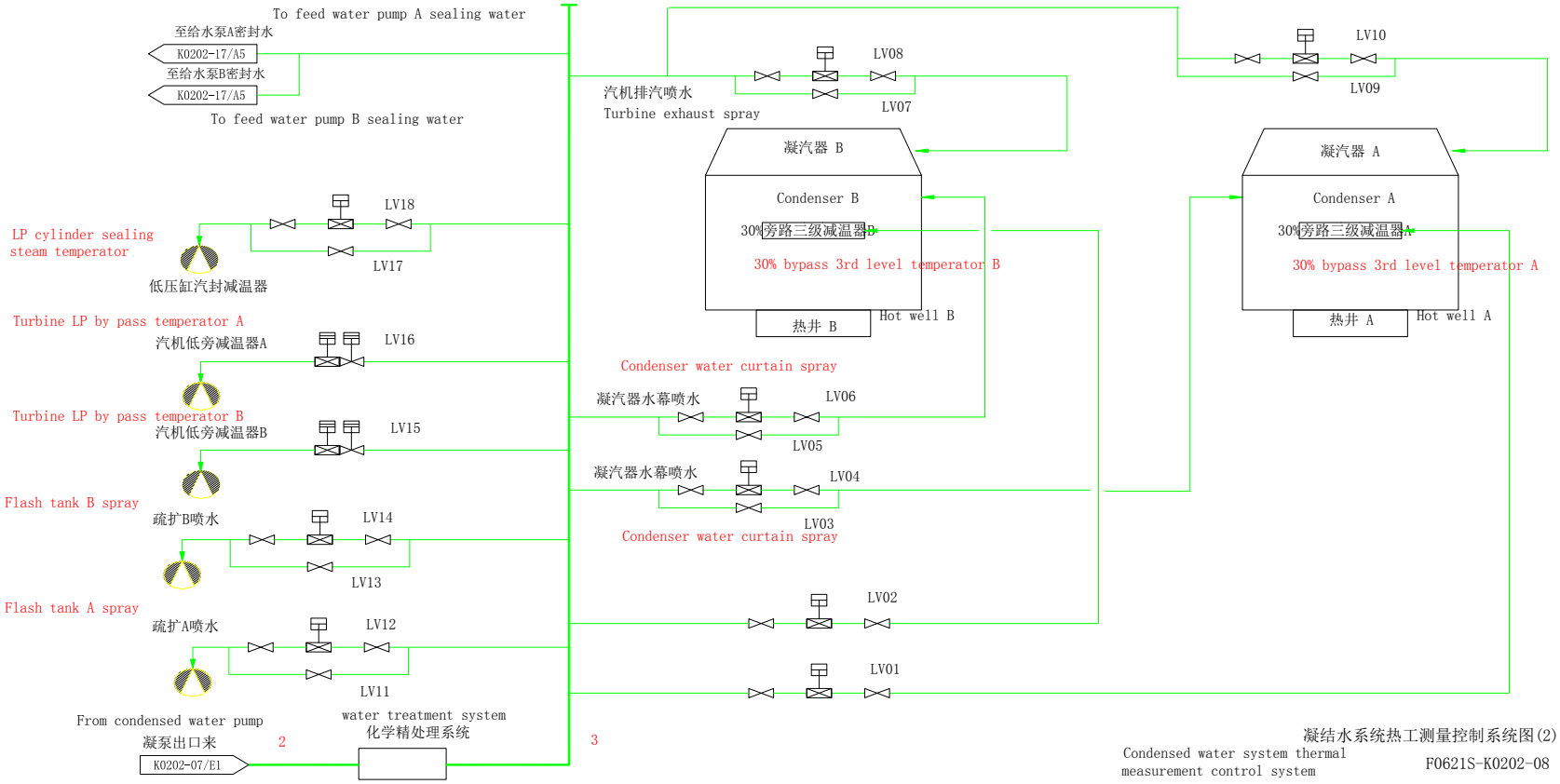
To feed water pump A sealing water
至给水泵A密封水
K0202-17/A5
至给水泵B密封水
K0202-17/A5
To feed water pump B sealing water
LV18
LP cylinder sealing steam temperator
LV17
低压缸汽封减温器
Turbine LP by pass temperator A
汽机低旁减温器A
LV16
Turbine LP by pass temperator B
汽机低旁减温器B
LV15
Flash tank B spray
疏扩B喷水
LV14
LV13
Flash tank A spray
疏扩A喷水
LV12
LV11
From condensed water pump
凝泵出口来
K0202-07/E1
2
water treatment system
化学精处理系统
3
汽机排汽喷水
Turbine exhaust spray
LV08
LV07
凝汽器 B
Condenser B
30%旁路三级减温器B
30% bypass 3rd level temperator B
热井 B
Hot well B
Condenser water curtain spray
凝汽器水幕喷水
LV06
LV05
凝汽器水幕喷水
LV04
LV03
Condenser water curtain spray
LV02
LV01
LV10
LV09
凝汽器 A
Condenser A
30%旁路三级减温器A
30% bypass 3rd level temperator A
热井 A
Hot well A
凝结水系统热工测量控制系统图(2)
Condensed water system thermal measurement control system
F0621S-K0202-08

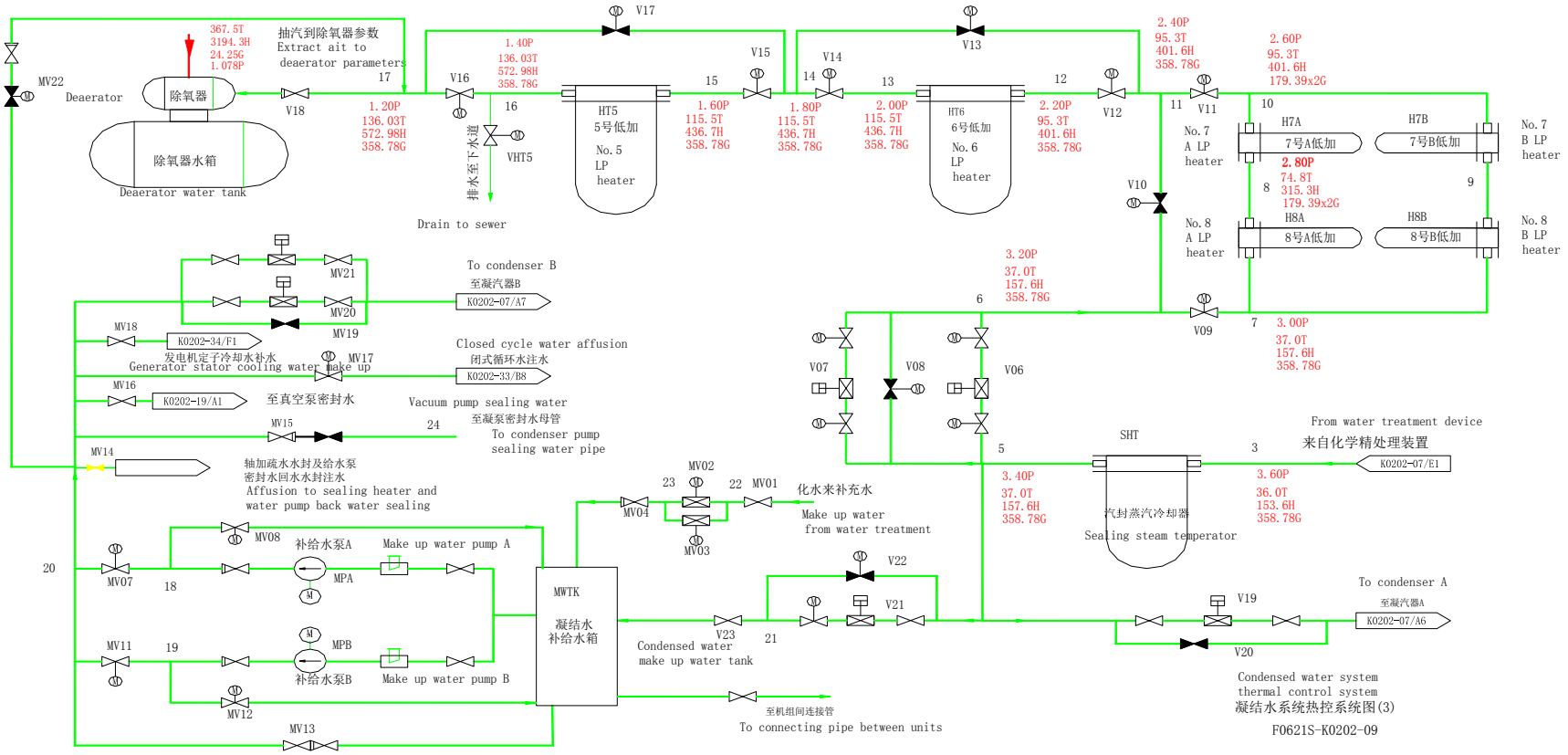
抽汽到除氧器参数
Extract ait to deaerator parameters
367.5T
3194.3H
24.25G
1.078P
MV22
Deaerator
除氧器
除氧器水箱
Deaerator water tank
V18
17
1.20P
136.03T
572.98H
358.78G
V16
16
排水至下水道
VHT5
Drain to sewer
1.40P
136.03T
572.98H
358.78G
V17
HT5
5号低加
No.5 LP heater
15
1.60P
115.5T
436.7H
358.78G
V15
14
1.80P
115.5T
436.7H
358.78G
V14
13
2.00P
115.5T
436.7H
358.78G
V13
HT6
6号低加
No.6 LP heater
12
2.20P
95.3T
401.6H
358.78G
V12
2.40P
95.3T
401.6H
358.78G
11
V11
2.60P
95.3T
401.6H
179.39x2G
10
No.7 A LP heater
H7A
7号A低加
H7B
7号B低加
No.7 B LP heater
2.80P
74.8T
315.3H
179.39x2G
8
9
V10
No.8 A LP heater
H8A
8号A低加
H8B
8号B低加
No.8 B LP heater
3.20P
37.0T
157.6H
358.78G
6
V09
7
3.00P
37.0T
157.6H
358.78G
To condenser B
至凝汽器B
K0202-07/A7
MV21
MV20
MV19
MV18
K0202-34/F1
发电机定子冷却水补水
Generator stator cooling water make up
MV17
Closed cycle water affusion
闭式循环水注水
K0202-33/B8
MV16
K0202-19/A1
至真空泵密封水
Vacuum pump sealing water
至凝泵密封水母管
To condenser pump sealing water pipe
MV15
24
V07
V08
V06
5
SHT
汽封蒸汽冷却器
Sealing steam temperator
3.40P
37.0T
157.6H
358.78G
3
3.60P
36.0T
153.6H
358.78G
From water treatment device
来自化学精处理装置
K0202-07/E1
MV14
轴加疏水水封及给水泵密封水回水水封注水
Affusion to sealing heater and water pump back water sealing
MV02
23
22
MV01
化水来补充水
Make up water from water treatment
MV04
MV03
V22
V21
V23
21
Condensed water make up water tank
MWTK
凝结水补给水箱
20
MV07
18
MV08
补给水泵A
MPA
Make up water pump A
MV11
19
MV12
MPB
补给水泵B
Make up water pump B
MV13
至机组间连接管
To connecting pipe between units
V19
V20
To condenser A
至凝汽器A
K0202-07/A6
Condensed water system thermal control system
凝结水系统热控系统图(3)
F0621S-K0202-09